Tropical forest conversion to rubber and oil palm plantations: landscape-scale and inter-annual variability of soil greenhouse gas (GHG) fluxes and the contribution of tree-stem emissions to the soil GHG budget in Jambi province, Sumatra, Indonesia

Dissertation

to attain the doctoral degree (Dr. rer. Nat.) of the Faculty of Forest Sciences and Forest Ecology,

Georg-August University Göttingen

Submitted by

Josephus Adrianus Koks

Born on 14-07-1990 in Eindhoven

Göttingen, 30-09-2019

Table of contents

Summary

Deforestation rates have rapidly increased over the last two decades in Sumatra, Indonesia, where large areas of lowland rainforest have now been converted into the monoculture plantation types of oil palm (*Elaeis guineensis*) and rubber (*Hevea brasiliensis*). The high global demand for palm oil and latex is continuously pushing expansion of this forest-to-plantation conversion and might even increase in the next decades. Land-use conversion is known to influence the soil-atmosphere exchange of the climate-relevant greenhouse gases (GHG) nitrous oxide (N_2O), methane (CH_4) and carbon dioxide (CO_2). Despite the extensive land-use conversion in Sumatra, long-term studies quantifying soil GHG fluxes from these land-use types are sparse. The few studies on soil GHG fluxes with year-round measurements from oil palm and rubber plantations on mineral soils in Sumatra have limitations for spatial and temporal extrapolations, as they were mainly conducted on well-drained sites of the landscape and did not cover the spatial heterogeneity (e.g. topography-driven redistribution of water and solutes) that influences soil GHG emission and uptake processes, and neither accounted for inter-annual variation in GHG fluxes related to different precipitation quantities. Furthermore, recent studies have revealed plant-mediated transport of GHG can contribute substantially to the total (soil + plant) GHG fluxes from an ecosystem. Stem-emitted GHG are currently largely unquantified in a majority of ecosystems and have never been measured in Sumatra. The present thesis tries to fill these gaps by accounting for 1) landscape-heterogeneity-driven variability in soil GHG fluxes by including riparian areas: zones between well-drained sites and lower located positions, under strong influence of water, known to be hotspots of biogeochemical processes; 2) temporal variability in soil GHG fluxes by measuring another annual cycle of GHG fluxes from the same plots measured four years ago; and 3) the contributions of stem GHG emissions to total (soil + stem) GHG fluxes. We conducted our study in Jambi province, Sumatra, Indonesia, a region subject to large forest conversion. We have measured N_2O, CH_4 and CO_2 fluxes from soils and stems in lowland forest (reference land use), as well as in smallholder oil palm and rubber plantations (conversion land uses). Fluxes were measured with soil and stem chambers between March 2017 – March 2018.

The first study aimed to quantify N_2O and CH_4 fluxes from stems and N_2O, CH_4 and CO_2 fluxes from soils in oil palm plantations located on riparian areas, and to assess their controlling factors. Annual stem N_2O and CH_4 fluxes were (g ha^{-1} yr^{-1}; mean ± SE) 12 ± 4 and 99 ± 46, respectively, and soil N_2O, CH_4 and CO_2 fluxes (kg ha^{-1} yr^{-1}; mean ± SE) were 3.4 ±

0.3, 0.7 ± 0.1 and 11092 ± 264, respectively. Stems contributed 3.0 – 14.7 % of the total (soil + stem) GHG fluxes. Stem GHG fluxes correlated with water-filled pore space (WFPS), soil-air GHG concentrations and vapor pressure deficit, which suggested stem-emitted GHG were soil-borne. Soil N_2O fluxes correlated with NO_3^- content, whereas soil CH_4 fluxes correlated with soil moisture content, and soil CO_2 fluxes displayed an exponential relationship with soil moisture content. This study showed that at riparian areas, the combination of high mineral N content and high WFPS can lead to relatively high stem and soil N_2O emissions, whereas a high WFPS can lead to net soil CH_4 emissions.

The second study aimed to quantify N_2O, CH_4 and CO_2 fluxes of soils and N_2O and CH_4 fluxes from stems from forest and rubber plantations located on riparian areas, to assess their controlling factors and to determine the effect of land-use change. Net soil N_2O, CH_4 and CO_2 fluxes (kg ha^{-1} yr^{-1}; mean ± SE) in forest were 1.1 ± 0.5, 1.7 ± 1.2 and 11700 ± 500, respectively, and in rubber plantations 0.8 ± 0.3, -0.5 ± 0.1 and 12700 ± 1300, respectively, and net fluxes did not differ between land uses (P ≥ 0.12). Annual stem N_2O and CH_4 fluxes in the forest were (g ha^{-1} yr^{-1}; mean ± SE) 4 ± 1 and 150 ± 8, respectively, and 5 ± 1 and 110 ± 4 in the rubber plantations, respectively, and did not differ between land uses either (P ≥ 0.24). The WFPS was the most important factor controlling N_2O, CH_4 and CO_2 fluxes from forest and rubber plantations on riparian sites, which might have overruled the influence of variability in soil characteristics due to land-use change, and that stems contributed significantly to the total (soil + stem) GHG fluxes.

The third study aimed to quantify inter-annual variation in soil N_2O, CH_4, and CO_2 fluxes as a result of inter-annual changes in precipitation and management practices. In 2017/2018, we measured one year of soil N_2O, CH_4 and CO_2 fluxes from forest, oil palm and rubber plantations across two landscapes (clay and loam Acrisol soils) by soil chambers and compared these with measurements at the same locations in 2012/2013. In general, annual soil N_2O and CH_4 fluxes did not show differences between years, whereas annual soil CO_2 fluxes were lower in 2017 than in 2013 for most land uses across both landscapes. A decreased WFPS in 2017 as a result of a decrease in precipitation of 30 % was the main driver of these differences, showing that changes in annual precipitation can lead to changes in soil-emitted GHG.

Our studies showed 1) that neglecting increased soil GHG fluxes from riparian areas, as well as contributions of stems, might lead to significant underestimation in GHG fluxes, 2) that soil GHG fluxes might vary inter-annually, and 3) that the effects of land-use change on GHG fluxes can be more pronounced at riparian areas. Therefore, it is important to include

the effect of spatial and temporal variation of GHG-flux controlling factors on soil and stem GHG fluxes, as well as to cover the different components involved on ecosystem-level (soils and stems) in future GHG flux studies, as it would provide us more specific information for improved predictions in global atmospheric GHG concentrations.

Zusammenfassung

Die Entwaldung hat sich über die letzten Jahrzehnte auf Sumatra (Indonesien) weit verbreitet – große Flächen von Tieflandregenwald wurden dort in Palmöl (*Elaeis guineensis*)- und Kautschuk (*Hevea brasiliensis*)-Monokulturplantagen umgewandelt. Die hohe globale Nachfrage nach Palmöl und Kautschuk wird in den nächsten Jahrzehnten zur Fortsetzung und möglicherweise sogar zur Zunahme dieser Umwandlung führen. Landnutzungsänderungen beeinflussen den Boden-Atmosphäre-Austausch der klimarelevanten Spurengase Distickstoffmonoxid (N_2O), Methan (CH_4) und Kohlenstoffdioxid (CO_2). Trotz der umfangreichen Landnutzungsänderungen auf Sumatra gibt es kaum Langzeitstudien, welche die Boden-Spurengasflüsse quantifizieren. Die wenigen ganzjährigen Studien zu Spurengasflüssen von Palmöl- und Kautschukplantagen auf mineralischen Böden in Sumatra haben ihre Grenzen, da sie nur auf gut entwässerten Böden stattfanden und keine jährlichen Variationen in Betracht ziehen. Sowohl räumliche Heterogenität (z.B. topografiegesteuerte Umverteilung von Wasser und gelösten Stoffen), die die Boden-Spurengas-Emissionen und -Aufnahme beeinflussen, als auch jährliche Variationen, aufgrund von Änderungen in der Quantität des Niederschlags, können signifikanten Einfluss auf Spurengasflüsse nehmen. Außerdem haben neuere Studien gezeigt, dass der pflanzengeleitete Transport von Spurengasen substanziell zu den Gesamt (Boden und Stamm)-Spurengasflüssen eines Ökosystems beitragen kann. Stammemittierte Spurengasflüsse sind derzeit nur wenig quantifiziert und wurden bisher nicht auf Sumatra gemessen. Diese Doktorarbeit versucht diese Lücke zu schließen. Dies geschieht durch 1) Messungen von Spurengasflüssen von sowohl gut entwässerten Böden als auch Uferflächen [„riparian sites"], Zonen zwischen gut entwässerten und niedrig positionierten Flächen, die stark von Wasser beeinflusst sind und deswegen bekannte Hotspots biogeochemischer Prozesse sind; 2) Messungen temporärer und zwischenjährlicher Variabilität von Spurengasflüssen, indem bereits 2013 gemessene Probeflächen nochmal ein Jahr gemessen wurden; und 3) Messungen der Gesamt-Spurengasflüsse von Stämmen. Wir haben unsere Studien in der Provinz Jambi, Sumatra, Indonesien durchgeführt, einer Region, die für ihre große Entwaldung bekannt ist. Wir haben N_2O-, CH_4- und CO_2-Flüsse von Böden und Stämmen im Tieflandregenwald

(Referenzlandnutzung), sowie auf Palmöl- und Kautschuk-Plantagen von Kleinbauern (umgewandelte Landnutzung) gemessen. Die Flüsse wurden mit Boden- und Stammhauben zwischen März 2017 und März 2018 gemessen.

Das Ziel der ersten Studie war die Quantifizierung von N_2O-, CH_4- und CO_2-Flüssen von Stämmen und Böden in Ölpalmplantagen auf Uferflächen, sowie die Bewertung der beeinflussenden Faktoren. Jährliche Stamm-N_2O- und CH_4-Flüsse umfassten (g ha^{-1} yr^{-1}; Mittelwert ± Standard Fehler) jeweils 12 ± 4 und 99 ± 46 und Boden-N_2O-, CH_4- und CO_2-Flüsse (kg ha^{-1} yr^{-1}; MW ± SF) waren jeweils 3.4 ± 0.3, 0.7 ± 0.1 und 11092 ± 264. Stämme trugen mit 3.0 – 14.7 % zu den Gesamtspurengasflüssen bei. Sie korrelierten mit Bodenfeuchte, Boden-Luft-Konzentration und Dampfdruckdefizit, was darauf hinweist, dass der Boden Ursprung der stammemittierten Spurengasflüsse war. Boden-N_2O korrelierte mit NO_3^- Gehalt, während Boden-CH_4-Flüsse mit Bodenfeuchte korrelierten und CO_2-Flüsse zeigten ein exponentielles Verhältnis zu Bodenfeuchte. Diese Studie zeigte, dass die Kombination von hohem mineralischem N-Gehalt und höherer Bodenfeuchte zu relativ hohen Stamm- und Boden-N_2O-Emissionen führten, sowie hohe Bodenfeuchte zu Netto-Boden-CH_4-Emission führte.

Das Ziel der zweiten Studie war die Quantifizierung von N_2O-, CH_4- und CO_2-Flüssen von Böden und Stämmen in Wald- und Kautschukplantagen auf Uferflächen, sowie die Bewertung der bestimmenden Faktoren und die Bestimmung des Effekts der Landnutzungsänderung. Netto-Boden-N_2O-, CH_4- und CO_2-Flüsse (kg ha^{-1} yr^{-1}; MW ± SF) in Waldflächen waren jeweils 1.1 ± 0.5, 1.7 ± 1.2 und 11700 ± 500 und in Kautschukplantagen jeweils 0.8 ± 0.3, -0.5 ± 0.1 und 12700 ± 1300. Nettoflüsse waren vergleichbar zwischen beiden Landnutzungssystemen (P ≥ 0.12). Netto-Stamm-N_2O- und CH_4-Flüsse im Wald betrugen (g ha^{-1} yr^{-1}; MW ± SF) jeweils 4 ± 1 und 150 ± 8, sowie jeweils 5 ± 1 und 110 ± 4 in den Kautschukplantagen und waren vergleichbar zwischen beiden Landnutzungssystemen (P ≥ 0.24). Diese Studie zeigte, 1) dass Bodenfeuchte der wichtigste bestimmende Faktor für N_2O-, CH_4- und CO_2-Flüsse auf Uferflächen in Wald und Kautschukplantagen war und damit potenziell den Einfluss der Variabilität der Bodencharakteristika nach der Landnutzungsänderung ausschließt, sowie, 2) dass Stämme signifikant zu den Gesamt (Boden + Stamm)-Spurengasflüssen beitragen.

Das Ziel der dritten Studie war die Quantifizierung der jährlichen Variation in Boden-N_2O-, CH_4- und CO_2-Flüsse durch jährliche Änderungen in der Quantität von Niederschlag und Managementpraktiken. In 2017/2018, haben wir Boden N_2O-, CH_4- und

CO$_2$-Flüsse von Wald, Palmöl- und Kautschukplantagen in zwei Landschaften (mit ton- bzw. lehmhaltigem Acrisol-Böden) mit Bodenhauben gemessen und diese mit Messungen von 2012/2013 verglichen. Im Allgemeinen zeigten Boden N$_2$O- und CH$_4$-Flüsse keine Unterschiede zwischen beiden Jahren, wobei Boden CO$_2$-Flüsse in den meisten Landnutzungssystemen beider Landschaften 2017 geringer waren als 2013. Eine Reduktion der Bodenfeuchte von circa 30 %, auf Grund von vermindertem Niederschlag 2017, war Haupttreiber dieser Unterschiede, was uns zeigte, dass Änderungen in der jährlichen Quantität des Niederschlags zu einer jährlichen Änderung in Spurengasflüssen führen kann.

Unsere Studien zeigten zusammenfassend, dass 1) die Vernachlässigung von sowohl erhöhten Spurengasflüssen von Uferflächen, als auch der Beiträge der Stämme zu einer signifikanten Unterschätzung von Spurengasflüssen führen kann, dass 2) Spurengasflüsse jährlich unterschiedlich sein können und, dass 3) auf Uferflächen die Effekte der Landnutzungsänderungen verstärkt auf Spurengasflüsse Einfluss nehmen können. Daher ist es wichtig, dass die räumliche und zeitliche Variabilität von spurengasbeeinflussender Faktoren, sowie Stammspurengasflüsse in zukünftige Studien aufgenommen werden, damit spezifischere Informationen zur Verfügung stehen, um globale atmosphärische Spurengaskonzentrationen besser vorhersagen zu können.

1 General introduction

1.1 Land-use change in Sumatra

Since the 1950s, large-scale land-use conversion from forest (Fig. 1a) to agriculture is taking place in Indonesia (Food and Agricultural Organization, 2019). Especially in the last two decades, the country's total oil palm (*Elaeis guineensis*; Fig. 1b) and rubber (*Hevea brasiliensis*; Fig. 1c) plantation areas increased drastically (BPS, 2017), as Indonesia became the world's largest producer of oil palm and the second-largest producer of rubber. The country's current total oil palm and rubber plantation areas are approximately eight and four million ha, respectively, from which 66 % of the oil palm and 70 % of the rubber plantations are located on the island of Sumatra (BPS, 2017). Land-use conversion from forest to plantation systems in Sumatra is known to affect a broad range of biogeochemical and ecological functions (Clough et al., 2016), such as greenhouse gas fluxes coming from the soil (e.g. Aini et al., 2015; Hassler et al., 2017; Ishizuka et al., 2005). Land-use conversion to oil palm plantations in Sumatra alone is projected to increase with roughly 200 % in the next decade (Sung, 2016), which is putting pressure on available land. Easily-accessible and well-drained sites are getting sparser, and the expansion of oil palm and rubber is increasingly affecting lower-located, wet landscape components, known as riparian areas (Gregory et al., 1991). It is estimated that 7 - 15 % of Sumatra's total land cover qualifies as riparian area.

Figure 1 Three common land-use types in Sumatra: (a) low land rainforest, (b) smallholder palm oil (*Elaeis guineensis*) monoculture plantation and (c) smallholder rubber (*Hevea brasiliensis)* monoculture plantation.

1.2 Landscape-scale variability in greenhouse gasses: influence of riparian areas

Landscape variability exerts considerable effects on the spatial variability of soil properties and water redistribution, and consequently on biogeochemical processes and greenhouse gas fluxes (Arias-Navarro et al., 2017; Pennock & Corre, 2001; Premke et al., 2016). Therefore, landscape-scale variability is an important factor to take into account while conducting GHG flux measurements (e.g. Jacinthe et al., 2012; Vidon et al., 2015). Riparian sites, compared to well-drained sites, are known for their large temporal variability in soil water level, as they

experience occasional large drainage impediments and subsequent intermittent inundation after prolonged precipitation events. As a result, they are known to be hotspots for biogeochemical processes, characterized by strong retention of nutrients and high organic matter contents in the soil (Haag & Kaupenjohann, 2002; Pennock & Corre, 2001). Important ecological functions of riparian areas, therefore, include trapping of eroded sediment (Cooper et al., 2010; Lee et al., 2000), storage of soil organic carbon (SOC) and dissolved organic matter (DOM) (Masese et al., 2016; Wantzen et al., 2012) and removal of non-point source pollutants, including nitrate, through denitrification and plant uptake (Dosskey et al., 2010; Lowrance, 1985). Such important functions may be lost when natural riparian areas are converted to agriculture (Décamps et al., 2009). In the tropics, N_2O fluxes from reforestation area and fertilized maize farms on riparian area in Thailand (Kachenchart et al., 2012) were found to be approximately 1.3 times higher at riparian areas than at well-drained sites, whereas N_2O fluxes from a rainforest in Puerto Rico (Bowden et al., 1992), were found to be higher at topographical breaks in the landscape, compared to hillslope area. Also, numerous studies in the temperate and subtropical zones report increased N_2O, CH_4 and CO_2 fluxes coming from riparian sites compared to sites with well-drained soils (e.g. Corre et al., 1996; Zhu et al., 2013, Vidon et al., 2015).

1.3 Inter-annual variation in greenhouse gas fluxes

Next to spatial variation in GHG fluxes (section 1.2), temporal variation also plays an important role for the soil GHG production and uptake and thus the quantity of soil-emitted GHG. Multiple studies in the tropics show that there can be considerable inter-annual variation in GHG fluxes because of inter-annual differences in their drivers (e.g. Basso et al., 2016). GHG fluxes are known to strongly interact with soil moisture content and soil temperature, which can vary seasonally or inter-annually as a result of differences in rainfall quantity and cloud cover, as well as with mineral nitrogen (N) content, which can change because of varying quantities of litter input or management practices (e.g. Corre et al., 2014; Hashimoto et al., 2016; Veldkamp et al., 2013).

1.4 GHG contributions from tree stems

Plant-mediated transport (e.g. Pangala et al., 2017; Pangala et al., 2013; Welch et al., 2019) and within-plant production (e.g. Yip et al., 2018) of N_2O and CH_4 can contribute substantially to the total (soil + stem) N_2O and CH_4 fluxes from an ecosystem. These sources are currently unquantified in a majority of tropical ecosystems and are gaining scientific

attention because of the prevailing discrepancy in global budget of these gases between top-down and bottom-up approaches (e.g. Pangala et al., 2017). Annual stem N_2O and CH_4 fluxes and their contributions to the total GHG flux largely differ among reported studies. Presently, long-term and large-scale quantification of stem GHG fluxes is needed in order to understand their temporal and spatial drivers, which will help constrain the magnitude of these fluxes for future upscaling using a process-based model (Barba et al., 2019). So far, the only study on stem N_2O fluxes from an upland, mineral soil was conducted in Panama, where they reported much larger N_2O emissions from tree stems than soils (Welch et al., 2019). A study in the wetlands of the Amazon basin area reported that stem CH_4 emissions accounted for up to 65 % of the total CH_4 fluxes (Pangala et al., 2017), whereas another study in peatlands of Borneo showed that stem CH_4 emissions can contribute up to 83 % of the total CH_4 fluxes (Pangala et al., 2013), indicating the importance of often neglected stem contributions. Seasonal and spatial controlling factors on stem GHG fluxes were not explored so far in studies conducted in tropical upland (Welch et al., 2019) and wetland soils (Pangala et al., 2013, Pangala et al., 2017), but studies in the temperate zone showed variability in stem GHG fluxes is largely attributed to spatial variability and difference in tree species (e.g. Barba et al., 2019). Wood density, lenticel density, presence of aerenchyma tissue, transpiration rates and sap flow rates may contribute to these species-level differences (Barba et al., 2019; Covey et al., 2012; Machacova et al., 2013; Pihlatie et al., 2005; Warner et al., 2017). Contrary to a lot of tropical forest species, the oil palm does not have cambium, secondary growth, growth rings and heartwood (Corley & Tinker, 2015), which might have a significant influence on the amount of stem-emitted GHG fluxes. Until now, no attempts have been made to quantify stem GHG fluxes from tree cash-crop plantations like oil palm and rubber.

1.5 Effect of land-use conversion on GHG fluxes from riparian areas

In natural ecosystems, the vegetation on riparian areas is adapted to the strong influence of water (e.g. Dosskey et al., 2010), which is one of the main reasons these landscape components show strong nutrient retention. However, studies in the temperate zone have shown the conversion of natural riparian area to agricultural area leads to loss of important ecological functions, as the crop vegetation might not be efficient in terms of nutrient usage (e.g. Haag & Kaupenjohann, 2002). Some important ecological functions which may be reduced are the storage of organic carbon in the soil and the supply of labile organic carbon. Conversion of tropical forests to oil palm and rubber plantations on well-drained sites has shown to alter multiple soil characteristics, known to influence GHG production and uptake.

Reported changes in soil characteristics, on which forest conversion in Sumatra and Borneo, Indonesia showed the highest impact, include: decreased soil organic carbon storage (Allen et al., 2015; Kotowska et al., 2015; Kusin et al., 2017; Rahman et al., 2018; van Straaten et al., 2011), changes in nitrogen availability (Allen et al., 2015; Hassler et al., 2017; Kurniawan et al., 2018) and soil compaction (Guillaume et al., 2016). The alteration of soil characteristics due to land-use conversion may have a different effect on soil GHG fluxes under the strong influence of water, as found at riparian sites.

1.6 Current limitations in GHG flux quantifications from Sumatra

Despite the extensive land-use conversion to oil palm and rubber plantations in Sumatra, long-term studies quantifying soil GHG fluxes from these land-use types are sparse. The few studies on soil GHG fluxes with year-round measurements from oil palm and rubber plantations on mineral soils in Sumatra (Aini et al., 2015; Hassler et al., 2015; Hassler et al., 2017) have limitations for full ecosystem-scale GHG flux quantifications, because 1) they lack spatial extrapolation, as these were mainly conducted on well-drained areas of the landscape, and did not cover a wide spatial heterogeneity (e.g. topography-driven redistribution of water and solutes) that influences soil GHG emission and uptake processes (Pennock & Corre, 2001); 2) they did not include contributions of stem-emitted GHG to the GHG fluxes; and 3) they covered a maximum measurement period of 13 months and, thus, do not account for inter-annual variation. Presently, it remains unclear how spatial variability in landscape affects soil GHG flux quantities, how stems contribute to ecosystem-scale soil GHG fluxes, whether inter-annual variation in precipitation or soil mineral N content leads to distinct differences in soil GHG fluxes and how land-use conversion from forest to oil palm and rubber plantations on riparian areas affects soil GHG fluxes.

1.7 Soil greenhouse gasses and their potential controlling factors

Nitrous oxide (N_2O) is produced in soils largely by the microbial processes of denitrification and nitrification (Firestone & Davidson, 1989). There are two main levels of controls on soil N_2O fluxes, as depicted by the conceptual hole-in-the-pipe (HIP) model (Davidson et al., 2000): N availability, which regulates the process rates; and soil water content, which influences the proportion of N_2O on the gaseous N (Corre et al., 2014; Hassler et al., 2017; Koehler et al., 2009; Matson et al., 2017). Therefore, by altering soil moisture levels, frequent inundations in riparian areas could lead to the evolution of an active denitrifying community in riparian buffers, ultimately resulting in increased N_2O production. In the oil palm

plantations, the common smallholder management practices by smallholders create distinct spatial structures: fertilized areas around the palm trees (~ 4 % of plantation area), inter-rows (~86 % of plantation area), and frond piles (~ 10 % of plantation area) where senesced fronds are piled (Corley & Tinker, 2015). These *management zones* distinctly differ in mineral N (Hassler et al., 2017) and dissolved organic C (Kurniawan et al., 2018), and thus may regulate the spatial pattern of N_2O fluxes from oil palm plantations. The fertilized area, where nitrogen (N), phosphorus (P), and potassium (K), as well as lime are applied, has high mineral N but low dissolved organic C (Hassler et al., 2017; Kurniawan et al., 2018), which could lead to high soil N_2O fluxes. As rubber plantations lack management practices like fertilization and litter collection, site-specific differences in soil mineral N are not expected. Inter-annual variation in rainfall and thus soil moisture content, being the second level of control in the HIP model, might result in varying annual N_2O fluxes. A wetter year, with increased precipitation, could, therefore, lead to significantly larger soil N_2O emissions. Stem N_2O emissions could be subject to the same spatial, seasonal and inter-annual variation, as they can act as a conduit for transport of soil air, where it is ultimately released at the stem surface. In riparian areas with increased soil N_2O production, stem N_2O emissions might, therefore, be high. The decrease in soil organic carbon after land-use change from forest to oil palm and rubber plantations can lead to reduced soil N_2O emissions, through reduced substrate availability (Senbayram et al., 2012). Increased N availability in fertilized agricultural systems like oil palm plantations, might lead to increased N_2O emissions (Hassler et al., 2017), whereas decreased N availability in unfertilized agricultural systems like rubber plantations, can result in decreased N_2O emissions (Verchot et al., 1999; Weitz et al., 2001; Weitz et al., 1998). Soil compaction, in turn, can result in reduced gas diffusivity and can enhance anaerobic soil conditions (Skiba et al., 1992). This might stimulate further reduction of N_2O to N_2 by denitrifying bacteria (Davidson et al., 2000) and thus reduce N_2O emissions.

Methane (CH_4) is produced in soils during anaerobic decomposition by methanogenic archaea as well as consumed in soils as a source of energy by methanotrophic bacteria (Smith et al., 2018). Hence, the soil CH_4 flux at the soil-atmosphere interface is the net result of both processes. Year-round measurements showed that the seasonal variation in soil CH_4 fluxes across sites in the tropics is positively correlated to soil moisture content (Hassler et al., 2015) and microbial activity (Wolf et al., 2012). Spatial patterns in soil CH_4 fluxes across sites of tropical land uses were reported to be related to soil texture, mainly through its control on gas diffusivity (Wolf et al., 2012; Veldkamp 2013), soil N availability (Veldkamp et al., 2013) and aluminium toxicity to methanotrophs (Hassler et al., 2015). Tropical lowland rainforests,

as well as oil palm and rubber plantations, on upland mineral soils are usually sinks for CH_4 (e.g. Hassler et al., 2015; Ishizuka et al., 2005), whereas forests on wetlands are known to be sources of CH_4. Riparian areas, with intermittent drainage impediment, may act as a net CH_4 source during the wet season or large rainfall events and as a net CH_4 sink during the dry days (Itoh et al., 2007). Inter-annual variation in rainfall and thus soil moisture content might also result in changes in annual CH_4 fluxes, where wetter years could show significantly lower soil CH_4 uptake or might even result in soil CH_4 emissions. Concurrent to soil CH_4 uptake, stem CH_4 emissions have been measured in a tropical forest in Panama (Welch et al., 2019). A possible mechanism behind stem CH_4 emission is the transport of soil-air CH_4 from lower anaerobic soil horizons via aerenchyma tissue through stems, where it bypasses the oxygenated surface horizons where the majority of CH_4 oxidation takes place (Teh et al., 2005). This is a process likely to occur in riparian areas, known for their occasional large quantities of water and thus temporary high groundwater tables. The decrease in soil organic carbon after land-use change from forest to oil palm and rubber plantations can lead to reduced CH_4 uptake or CH_4 emissions (e.g. Veldkamp et al., 2008). Increased N availability might lead to reduction in soil CH_4 uptake (Hassler et al., 2015), whereas decreased N availability can result in increased CH_4 consumption and/or reduced CH_4 production (Veldkamp et al., 2013). Reduced gas diffusivity after soil compaction can limit aerobic CH_4 oxidation, while at the same time enhancing anaerobic CH_4 production (Keller & Reiners, 1994; Veldkamp et al., 2008).

Soil respiration refers to the production of carbon dioxide (CO_2) when soil organisms respire and includes respiration of plant roots, the rhizosphere, microbes and fauna (Prentice et al, 2001). It has a central role in the biosphere-atmosphere exchange. Even though it is the second-largest flux in the C cycle, it is less quantified in converted agricultural systems in the tropics. The few studies conducted in Indonesia with year-round measurements showed that the seasonal patterns of soil CO_2 emissions are controlled by soil moisture content (Swails et al., 2019; van Straaten et al., 2011) and temperature (Hassler et al., 2015), whereas spatial patterns in soil CO_2 emissions from oil palm and rubber plantations were reported to be controlled by soil organic-matter quality and quantity, e.g. ^{15}N abundance (Hassler et al., 2015). Riparian areas may have lower CO_2 emissions compared to well-drained sites, due to permanently high soil moisture content, especially during the wet season. Moreover, the conversion of natural riparian areas to oil palm and rubber plantations with reduced organic material input (Kotowska et al., 2015), might enhance reduction of CO_2 emissions (Hassler et al., 2015; Nelson et al., 2006). Increased N availability might lead to reduced soil respiration

16

(Hassler et al., 2015), whereas decreased N availability can result in increased soil respiration. Reduced gas diffusivity after soil compaction is known to reduce soil respiration (Jensen et al., 1996).

1.8 Study area

Our study area is located in the lowlands (11 − 29 m above sea level) of Jambi province, Sumatra, Indonesia (Fig. 2). Here, a humid, tropical climate with a mean annual air temperature of 26.7 ± 1.0 ℃ and mean annual precipitation of 2235 ± 385 mm (data from meteorological station at the Jambi Sultan Thaha Airport) is found. The rainfall in the region was 2772 mm in the year we measured (2017-2018), and the dry season (< 100 mm rainfall month^{-1}) lasted from July to October 2017.
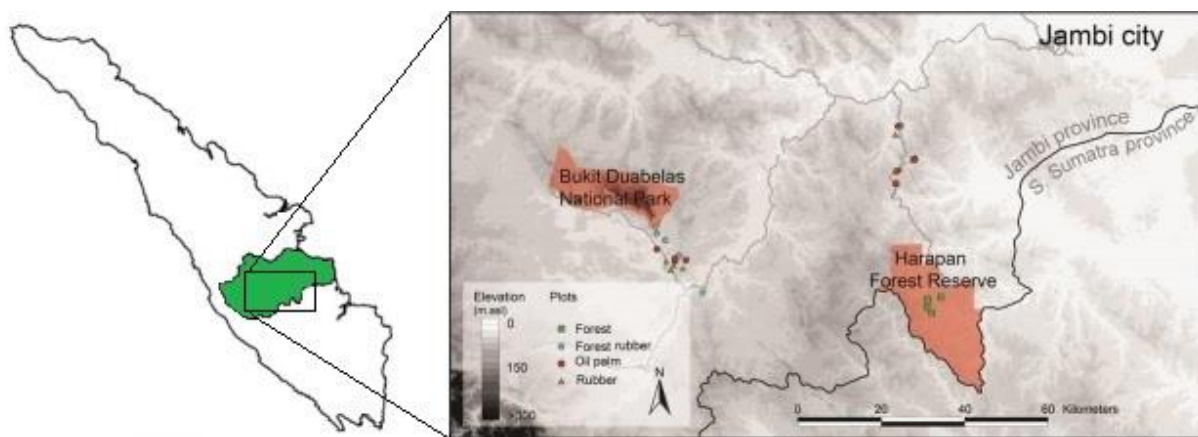
Figure 2 Map of Sumatra, with Jambi province highlighted in green (left) and the study area with the different selected research plots (right). The well-drained plots on clay Acrisol soils are located close to the Bukit Duabelas National Park, whereas the well-drained and riparian plots on clay or clay loam Stagnosols are located near the Harapan Forest Reserve (both protected areas highlighted in orange). Map adapted after design by Drescher et al. (2016) and Hassler et al. (2017).

In forest and smallholder oil palm and rubber plantations, we selected study sites on both well-drained and riparian soils. Soils in the well-drained sites were classified as either clay or loam Acrisol soils (32 ± 2 to 45 ± 4 % clay in the top 1-m depth), whereas in the riparian sites we found clay or clay-loam Stagnosols (29 ± 2 to 58 ± 4 % clay in the top 1-m depth).

1.9 Aims and objectives

The overall aim of this study was to obtain a better insight into soil GHG fluxes coming from oil palm and rubber plantations after conversion from forest, by accounting for (1) landscape-scale-driven variability in soil GHG fluxes by including riparian areas, (2) temporal variability in soil GHG fluxes by measuring another annual cycle of GHG fluxes

from the same plots measured four years ago, and (3) contributions of stem GHG emissions to total (soil + stem) GHG fluxes. We hypothesized (1) that riparian areas, serving as hotspots of biogeochemical processes, will have high N_2O, CH_4 and CO_2 fluxes, (2) that conversion of forest to oil palm plantations leads to enhanced soil GHG production in the oil palm plantations, as a consequence of high nutrient availability from fertilizer application and liming, but to reduced soil GHG production or increased GHG uptake in the rubber plantations, due to lower nutrient availability as a consequence of reduced organic matter input, (3) that stems are large contributors to the total N_2O and CH_4 emissions and (4) that GHG emissions can vary inter-annually as a result of changes in precipitation. The results will help us better understand the soil GHG fluxes coming from these two plantation systems.

The aim of the first study was (1) to quantify soil N_2O, CH_4, and CO_2 fluxes, as well as stem N_2O and CH_4 fluxes from smallholder oil palm plantations on mineral soils in riparian areas of Jambi, Indonesia, and (2) to assess their seasonal and spatial controlling factors. In a year-round, monthly measurement, including a more intensive measurement following fertilization, (fertilizer-induced) soil and stem GHG fluxes were measured. We hypothesized that (1) riparian areas, serving as hotspots of biogeochemical processes, will have high N_2O, CH_4 and CO_2 fluxes as a consequence of high nutrient availability from fertilizer application and liming, and (2) stems are large contributors to the total N_2O and CH_4 emissions.

The aim of the second study was (1) to quantify soil N_2O, CH_4, and CO_2 fluxes, as well as stem N_2O and CH_4 fluxes from both forest and smallholder rubber plantations on mineral soils in riparian areas of Jambi, Indonesia, and (2) to assess their seasonal and spatial controlling factors during a year-long, monthly-measurement campaign. We hypothesized (1) that riparian areas, serving as hotspots of biogeochemical processes, will have high N_2O, CH_4 and CO_2 fluxes, (2) that tree stems are contributing to the total N_2O and CH_4 fluxes, and (3) that conversion of forest to rubber plantations leads to reduced soil GHG production/increased GHG uptake.

The aim of the third study was (1) to quantify the inter-annual variability of atmospheric GHG exchange of smallholder oil palm and rubber after conversion from forest, between 2012 and 2017, in Sumatra, Indonesia, and (2) to assess the relative importance of the various climatic and site management factors that controlled the reported variability. We hypothesized that inter-annual differences in precipitation quantities and management practices might lead to differences in annual GHG fluxes.

1.10 EFForTS CRC-990 framework

This study was conducted within the EFForTS (Ecological and Socio-economic Functions of Tropical Lowland Rainforest Transformation Systems) project, which is a Collaborative Research Center (CRC-990) funded by the German Research Association (DFG).

References

Aini, F. K., Hergoualc'h, K., Smith, J. U., & Verchot, L. (2015). Nitrous oxide emissions along a gradient of tropical forest disturbance on mineral soils in Sumatra. *Agriculture, Ecosystems and Environment*, *214*, 107–117. https://doi.org/10.1016/j.agee.2015.08.022

Allen, K., Corre, Ma. D., Tjoa, A., & Veldkamp, E. (2015). Soil Nitrogen-Cycling Responses to Conversion of Lowland Forests to Oil Palm and Rubber Plantations in Sumatra, Indonesia. *PLOS ONE*, *10*(7), e0133325. https://doi.org/10.1371/journal.pone.0133325

Arias-Navarro, C., Díaz-Pinés, E., Klatt, S., Brandt, P., Rufino, M. C., Butterbach-Bahl, K., & Verchot, L. V. (2017). Spatial variability of soil N 2 O and CO 2 fluxes in different topographic positions in a tropical montane forest in Kenya. *Journal of Geophysical Research: Biogeosciences*, *122*(3), 514–527. https://doi.org/10.1002/2016JG003667

Barba, J., Bradford, M. A., Brewer, P. E., Bruhn, D., Covey, K., Haren, J., … Vargas, R. (2019). Methane emissions from tree stems: a new frontier in the global carbon cycle. *New Phytologist*, *222*(1), 18–28. https://doi.org/10.1111/nph.15582

Barba, J., Poyatos, R., & Vargas, R. (2019). Automated measurements of greenhouse gases fluxes from tree stems and soils: magnitudes, patterns and drivers. *Scientific Reports*, *9*(1). https://doi.org/10.1038/s41598-019-39663-8

Bowden, W. B., McDowell, W. H., Asbury, C. E., & Finley, A. M. (1992). Riparian nitrogen dynamics in two geomorphologically distinct tropical rain forest watersheds: subsurface solute patterns. *Biogeochemistry*, *18*(2), 53–75. https://doi.org/10.1007/BF00002703

BPS (Badan Pusak Statistik): Statistical Oce of Jambi Province, available via https://jambi.bps.go.id/ (last access 01.04.2019), 2017. (n.d.).

Clough, Y., Krishna, V. V., Corre, M. D., Darras, K., Denmead, L. H., Meijide, A., … Scheu, S. (2016). Land-use choices follow profitability at the expense of ecological functions in Indonesian smallholder landscapes. *Nature Communications*, *7*(1), 13137. https://doi.org/10.1038/ncomms13137

Cooper, J. R., Gilliam, J. W., Daniels, R. B., & Robarge, W. P. (2010). Riparian Areas as Filters for Agricultural Sediment. *Soil Science Society of America Journal*, *51*(2), 416. https://doi.org/10.2136/sssaj1987.03615995005100020029x

Corley, R., & Tinker, P. (2015). *The Oil Palm*. https://doi.org/10.1002/9781118953297

Corre, M. D., Van Kessel, C., & Pennock, D. J. (1996). Landscape and seasonal patterns of nitrous oxide emissions in a semiarid region. *Soil Science Society of America Journal*, *60*(6), 1806–1815. https://doi.org/10.2136/sssaj1996.03615995006000060028x

Corre, Marife D., Sueta, J. P., & Veldkamp, E. (2014). Nitrogen-oxide emissions from

tropical forest soils exposed to elevated nitrogen input strongly interact with rainfall quantity and seasonality. *Biogeochemistry*, *118*(1–3), 103–120. https://doi.org/10.1007/s10533-013-9908-3

Davidson, E. A., Keller, M., Erickson, H. E., Verchot, L. V., & Veldkamp, E. (2000). Testing a Conceptual Model of Soil Emissions of Nitrous and Nitric Oxides. *BioScience*, *50*(8), 667. https://doi.org/10.1641/0006-3568(2000)050

Décamps, H., Naiman, R. J., & McClain, M. E. (2009). Riparian Zones. In *Encyclopedia of Inland Waters* (pp. 396–403). https://doi.org/10.1016/B978-012370626-3.00053-3

Dosskey, M. G., Vidon, P., Gurwick, N. P., Allan, C. J., Duval, T. P., & Lowrance, R. (2010). The Role of Riparian Vegetation in Protecting and Improving Chemical Water Quality in Streams 1. *JAWRA Journal of the American Water Resources Association*, *46*(2), 261–277. https://doi.org/10.1111/j.1752-1688.2010.00419.x

Drescher, J., Rembold, K., Allen, K., Beckschäfer, P., Buchori, D., Clough, Y., Faust, H., Fauzi, A.M., Gunawan, D., Irawan, B. et al.: Ecological and socio-economic functions across tropical land use systems after rainforest conversion, *Philos. T. Roy. Soc. B.*, 371, 20150275, 2016

Firestone, M. K., & Davidson, E. A. (1989). Microbiological Basis of NO and N2O Production and Consumption in Soil. *Exchange of Trace Gases between Terrestrial Ecosystems and the Atmosphere*, 7–21.

Food and Agricultural Organization, *FAOSTAT Database*. Retrieved from http://faostat.fao.org *(last access 01.04.2019),* 2019

Gregory, S. V, Swanson, F. J., McKee, W. A., & Cummins, K. W. (1991). An ecosystem perspective of riparian zones. *BioScience*, *41*(8), 540–550.

Guillaume, T., Holtkamp, A. M., Damris, M., Brümmer, B., & Kuzyakov, Y. (2016). Soil degradation in oil palm and rubber plantations under land resource scarcity. *Agriculture, Ecosystems & Environment*, *232*, 110–118. https://doi.org/10.1016/j.agee.2016.07.002

Haag, D., & Kaupenjohann, M. (2002). Landscape fate of nitrate fluxes and emissions in Central Europe. *Agriculture, Ecosystems & Environment*, *86*(1), 1–21. https://doi.org/10.1016/s0167-8809(00)00266-8

Hassler, E., Corre, M. D., Tjoa, A., Damris, M., Utami, S. R., & Veldkamp, E. (2015). Soil fertility controls soil-atmosphere carbon dioxide and methane fluxes in a tropical landscape converted from lowland forest to rubber and oil palm plantations. *Biogeosciences Discussions*, *12*(12), 9163–9207. https://doi.org/10.5194/bgd-12-9163-2015

Hassler, E., Corre, M. D., Kurniawan, S., & Veldkamp, E. (2017). Soil nitrogen oxide fluxes from lowland forests converted to smallholder rubber and oil palm plantations in Sumatra, Indonesia. *Biogeosciences*, *14*(11), 2781–2798. https://doi.org/10.5194/bg-14-2781-2017

Ishizuka, S., Iswandi, A., Nakajima, Y., Yonemura, S., Sudo, S., Tsuruta, H., & Murdiyarso, D. (2005). The variation of greenhouse gas emissions from soils of various land-use/cover types in Jambi province, Indonesia. *Nutrient Cycling in Agroecosystems*, *71*(1), 17–32. https://doi.org/10.1007/s10705-004-0382-0

Itoh, M., Ohte, N., Koba, K., Katsuyama, M., Hayamizu, K., & Tani, M. (2007). Hydrologic effects on methane dynamics in riparian wetlands in a temperate forest catchment. *Journal of Geophysical Research: Biogeosciences*, *112*(1), 1–14. https://doi.org/10.1029/2006JG000240

Jacinthe, P. A., Bills, J. S., Tedesco, L. P., & Barr, R. C. (2012). Nitrous Oxide Emission from Riparian Buffers in Relation to Vegetation and Flood Frequency. *Journal of Environment Quality*, *41*(1), 95. https://doi.org/10.2134/jeq2011.0308

Jensen, L. S., McQueen, D. J., & Shepherd, T. G. (1996). Effects of soil compaction on N-mineralization and microbial-C and -N. I. Field measurements. *Soil and Tillage Research*, *38*(3–4), 175–188. https://doi.org/10.1016/S0167-1987(96)01033-1

Kachenchart, B., Jones, D. L., Gajaseni, N., Edwards-Jones, G., & Limsakul, A. (2012). Seasonal nitrous oxide emissions from different land uses and their controlling factors in a tropical riparian ecosystem. *Agriculture, Ecosystems and Environment*, *158*(3), 15–30. https://doi.org/10.1016/j.agee.2012.05.008

Keller, M., & Reiners, W. A. (1994). Soil-atmosphere exchange of nitrous oxide, nitric oxide, and methane under secondary succession of pasture to forest in the Atlantic lowlands of Costa Rica. *Global Biogeochemical Cycles*, *8*(4), 399–409. https://doi.org/10.1029/94GB01660

Koehler, B., Corre, M. D., Veldkamp, E., Wullaert, H., & Wright, S. J. (2009). Immediate and long-term nitrogen oxide emissions from tropical forest soils exposed to elevated nitrogen input. *Global Change Biology*, *15*(8), 2049–2066. https://doi.org/10.1111/j.1365-2486.2008.01826.x

Kotowska, M. M., Leuschner, C., Triadiati, T., Meriem, S., & Hertel, D. (2015). Quantifying above- and belowground biomass carbon loss with forest conversion in tropical lowlands of Sumatra (Indonesia). *Global Change Biology*, *21*(10), 3620–3634. https://doi.org/10.1111/gcb.12979

Kurniawan, S., Corre, M. D., Schulte-Bisping, H., van Straaten, O., Matson, A. L., Utami, S. R., & Veldkamp, E. (2018). Conversion of tropical forests to smallholder rubber and oil palm plantations impacts nutrient leaching losses and nutrient retention efficiency in highly weathered soils. *Biogeosciences*, *15*(16), 5131–5154. https://doi.org/10.5194/bg-15-5131-2018

Kusin, F. M., Akhir, N. I. M., Mohamat-Yusuff, F., & Awang, M. (2017). Greenhouse gas emissions during plantation stage of palm oil-based biofuel production addressing different land conversion scenarios in Malaysia. *Environmental Science and Pollution Research*, *24*(6), 5293–5304. https://doi.org/10.1007/s11356-016-8270-0

Lee, K., Isenhart, T. M., Schultz, R. C., & Mickelson, S. K. (2000). Multispecies Riparian Buffers Trap Sediment and Nutrients during Rainfall Simulations. *Surface Water Quality*, *29*, 1200–1205. https://doi.org/10.2134/jeq2000.00472425002900040025x

Lenhart, K., Behrendt, T., Greiner, S., Steinkamp, J., Well, R., Giesemann, A., & Keppler, F. (2019). Nitrous oxide effluxes from plants as a potentially important source to the atmosphere. *New Phytologist*, *221*(3), 1398–1408. https://doi.org/10.1111/nph.15455

Lowrance, R. (1985). Managing riparian ecosystems to control nonpoint pollution. *Journal of Soil and Water Conservation*, *40*(1), 87–91.

Masese, F. O., Salcedo-Borda, J. S., Gettel, G. M., Irvine, K., & McClain, M. E. (2016). Influence of catchment land use and seasonality on dissolved organic matter composition and ecosystem metabolism in headwater streams of a Kenyan river. *Biogeochemistry*, *132*(1–2), 1–22. https://doi.org/10.1007/s10533-016-0269-6

Matson, A. L., Corre, M. D., Langs, K., & Veldkamp, E. (2017). Soil trace gas fluxes along orthogonal precipitation and soil fertility gradients in tropical lowland forests of Panama. *Biogeosciences*, *14*(14), 3509–3524. https://doi.org/10.5194/bg-14-3509-2017

Nelson, P. N., Banabas, M., Scotter, D. R., & Webb, M. J. (2006). Using soil water depletion to measure spatial distribution of root activity in oil palm (Elaeis guineensis Jacq.) plantations. *Plant and Soil*, *286*(1–2), 109–121. https://doi.org/10.1007/s11104-006-9030-6

Pangala, S. R., Enrich-Prast, A., Basso, L. S., Peixoto, R. B., Bastviken, D., Hornibrook, E. R. C., … Gauci, V. (2017). Large emissions from floodplain trees close the Amazon methane budget. *Nature*, *552*(7684), 230–234. https://doi.org/10.1038/nature24639

Pangala, S. R., Moore, S., Hornibrook, E. R. C., & Gauci, V. (2013). Trees are major conduits for methane egress from tropical forested wetlands. *New Phytologist*, *197*(2), 524–531. https://doi.org/10.1111/nph.12031

Pennock, D. ., & Corre, M. . (2001). Development and application of landform segmentation procedures. *Soil and Tillage Research*, *58*(3–4), 151–162. https://doi.org/10.1016/S0167-1987(00)00165-3

Premke, K., Attermeyer, K., Augustin, J., Cabezas, A., Casper, P., Deumlich, D., … Zak, D. (2016). The importance of landscape diversity for carbon fluxes at the landscape level: small-scale heterogeneity matters. *Wiley Interdisciplinary Reviews: Water*, *3*(4), 601–617. https://doi.org/10.1002/wat2.1147

Rahman, N., De Neergaard, A., Magid, J., Van De Ven, G. W. J., Giller, K. E., & Bruun, T. B. (2018). Changes in soil organic carbon stocks after conversion from forest to oil palm plantations in Malaysian Borneo. *Environmental Research Letters*, *13*(10). https://doi.org/10.1088/1748-9326/aade0f

Senbayram, M., Chen, R., Budai, A., Bakken, L., & Dittert, K. (2012). N2O emission and the N2O/(N2O+N2) product ratio of denitrification as controlled by available carbon substrates and nitrate concentrations. *Agriculture, Ecosystems & Environment*, *147*, 4–12. https://doi.org/10.1016/j.agee.2011.06.022

Skiba, U., Hargreaves, K. J., Fowler, D., & Smith, K. A. (1992). Fluxes of nitric and nitrous oxides from agricultural soils in a cool temperate climate. *Atmospheric Environment. Part A. General Topics*, *26*(14), 2477–2488. https://doi.org/10.1016/0960-1686(92)90100-Y

Smith, K. A., Ball, T., Conen, F., Dobbie, K. E., Massheder, J., & Rey, A. (2018). Exchange of greenhouse gases between soil and atmosphere: interactions of soil physical factors and biological processes. *European Journal of Soil Science*, *69*(1), 10–20. https://doi.org/10.1111/ejss.12539

Sung, C. T. B. (2016). Availability, use, and removal of oil palm biomass in Indonesia. *International Council on Clean Transportation*, 1–39. https://doi.org/10.13140/RG.2.1.4697.4485

Swails, E., Hertanti, D., Hergoualc'h, K., Verchot, L., & Lawrence, D. (2019). The response of soil respiration to climatic drivers in undrained forest and drained oil palm plantations in an Indonesian peatland. *Biogeochemistry*, *142*(1), 37–51. https://doi.org/10.1007/s10533-018-0519-x

Teh, Y. A., Silver, W. L., & Conrad, M. E. (2005). Oxygen effects on methane production and oxidation in humid tropical forest soils. *Global Change Biology*, *11*(8), 1283–1297. https://doi.org/10.1111/j.1365-2486.2005.00983.x

van Straaten, O., Veldkamp, E., & Corre, M. D. (2011). Simulated drought reduces soil CO 2 efflux and production in a tropical forest in Sulawesi, Indonesia. *Ecosphere*, *2*(10), art119. https://doi.org/10.1890/es11-00079.1

Veldkamp, E., Koehler, B., & Corre, M. D. (2013). Indications of nitrogen-limited methane uptake in tropical forest soils. *Biogeosciences*, *10*(8), 5367–5379. https://doi.org/10.5194/bg-10-5367-2013

Veldkamp, Edzo, Purbopuspito, J., Corre, M. D., Brumme, R., & Murdiyarso, D. (2008). Land use change effects on trace gas fluxes in the forest margins of Central Sulawesi, Indonesia. *Journal of Geophysical Research: Biogeosciences*, *113*(G2), n/a-n/a. https://doi.org/10.1029/2007JG000522

Verchot, L. V, Davidson, E. a, Cattfinio, J. H., Ackerman, T. M. I. L., Erickson, H. E., & Keller, M. (1999). Land use change and biogeochemical controls of nitrogen oxide emissions from soils in eastern Amazonia. *Global*, *13*(1), 31–46.

Vidon, P., Marchese, S., Welsh, M., & McMillan, S. (2015). Short-term spatial and temporal variability in greenhouse gas fluxes in riparian zones. *Environmental Monitoring and Assessment*, *187*(8). https://doi.org/10.1007/s10661-015-4717-x

Wantzen, K. M., Couto, E. G., Mund, E. E., Amorim, R. S. S., Siqueira, A., Tielbörger, K., & Seifan, M. (2012). Soil carbon stocks in stream-valley-ecosystems in the Brazilian Cerrado agroscape. *Agriculture, Ecosystems and Environment*, *151*, 70–79. https://doi.org/10.1016/j.agee.2012.01.030

Weitz, A. M., Linder, E., Frolking, S., Crill, P. M., & Keller, M. (2001). N2O emissions from humid tropical agricultural soils: Effects of soil moisture, texture and nitrogen availability. *Soil Biology and Biochemistry*, *33*(7–8), 1077–1093. https://doi.org/10.1016/S0038-0717(01)00013-X

Weitz, A. M., Veldkamp, E., Keller, M., Neff, J., & Crill, P. M. (1998). Nitrous oxide, nitric oxide, and methane fluxes from soils following clearing and burning of tropical secondary forest. *Journal of Geophysical Research Atmospheres*, *103*(D21), 28047–28058. https://doi.org/10.1029/98JD02144

Welch, B., Gauci, V., & Sayer, E. J. (2019). Tree stem bases are sources of CH4 and N2O in a tropical forest on upland soil during the dry to wet season transition. *Global Change Biology*, *25*(1), 361–372. https://doi.org/10.1111/gcb.14498

Wolf, K., Flessa, H., & Veldkamp, E. (2012). Atmospheric methane uptake by tropical montane forest soils and the contribution of organic layers. *Biogeochemistry*, *111*(1–3), 469–483. https://doi.org/10.1007/s10533-011-9681-0

Yip, D. Z., Veach, A. M., Yang, Z. K., Cregger, M. A., & Schadt, C. W. (2018).

Methanogenic Archaea dominate mature heartwood habitats of Eastern Cottonwood (Populus deltoides). *New Phytologist*. https://doi.org/10.1111/nph.15346

Zhu, J., Mulder, J., Wu, L. P., Meng, X. X., Wang, Y. H., & Dörsch, P. (2013). Spatial and temporal variability of N2O emissions in a subtropical forest catchment in China. *Biogeosciences*, *10*(3), 1309–1321. https://doi.org/10.5194/bg-10-1309-2013

2 Smallholder oil palm plantations on mineral soils in riparian areas emit large quantities of nitrous oxide, methane and carbon dioxide in Sumatra, Indonesia

Josephus Koks, Marife Corre, Olivier van Straaten, Alexander Knohl, Greta Formaglio, Aiyen Tjoa, Edzo Veldkamp

Abstract

Large-scale conversion from forest to oil palm plantations in Sumatra, Indonesia is increasingly affecting less-accessible landscape components such as riparian areas. Riparian areas are lower landscape positions, under a strong influence of water, known for enhanced greenhouse gas (GHG) production. We quantified stem and soil GHG fluxes from oil palm plantations on mineral soils in riparian areas in Jambi province, Indonesia, and assessed their controlling factors.

On four replicate plots, we selected 5 oil palms and installed 6 chamber bases to measure the GHG fluxes with stem and soil chambers respectively.

Annual stem N_2O and CH_4 fluxes were (g ha^{-1} yr^{-1}; mean $\pm$ SE) 12 ± 4 and 99 ± 46, respectively, and soil N_2O, CH_4 and CO_2 fluxes (kg ha^{-1} yr^{-1}; mean $\pm$ SE) were 3.4 ± 0.3, 0.7 ± 0.1 and 11092 ± 264 respectively. Stems contributed to 3.0 and 14.7 % of the total (soil + stem) N_2O and CH_4 fluxes respectively. The amount of applied N-fertilizer translated into gaseous N_2O emissions, known as emission factor (EF), was 3.9 ± 0.2 %.

Stem GHG fluxes correlated with soil moisture content ($\rho = 0.47 - 0.69$; $p \leq 0.09$; $n = 13$), soil-air GHG concentrations ($\rho \leq 0.46 - 0.93$; $p \leq 0.07$; $n = 13$) and vapor pressure deficit ($\rho \leq 0.44 - 0.55$; $p \leq 0.09$; $n = 15 - 30$), suggesting stem-emitted GHG were soil-borne. Soil N_2O fluxes correlated with NO_3^- content ($\rho \leq 0.82$; $p \leq 0.01$; $n = 13$); soil CH_4 fluxes correlated with soil moisture content ($\rho = 0.71 - 0.78$; $p \leq 0.01$; $n = 13$); soil CO_2 fluxes displayed an exponential relationship with soil moisture content ($R^2 = 0.27$, $n = 78$, $p > 0.01$).

The measured net N_2O emissions and the EF were higher than those reported from oil palm plantations on well-drained sites, and the measured net CH_4 emissions contradicted with net CH_4 uptake reported from oil palm plantations on well-drained sites. These findings suggested that soil GHG production is enhanced and soil GHG uptake might be reduced at riparian sites compared to well-drained sites.

Our study underlines that coverage of spatial variability in a certain landscape, as well as the incorporation of the different GHG-emitting components on an ecosystem scale (stem +

soil fluxes), can improve landscape-scale GHG flux estimates and that exclusion of these factors can result in a significant underestimation of GHG fluxes.

Keywords

Nitrous oxide, methane, carbon dioxide, soil, riparian, greenhouse gas fluxes, tree stem emissions, Sumatra, Indonesia

2.1 Introduction

The production area of oil palm (*Elaeis guineensis*) is rapidly expanding as a result of the high global demand for palm oil (Carlson et al., 2013). Indonesia currently produces 42% of the global crude palm oil (Food and Agricultural Organization, 2019), with the island of Sumatra contributing to 66 % of Indonesia's production (BPS, 2017). The country's total plantation area is projected to double by 2025 (Sung, 2016). The expansion of oil palm is increasingly affecting less-accessible landscape components like riparian areas: zones between well-drained areas and lower-located positions bordering streams and rivers (Gregory, Swanson, McKee, & Cummins, 1991). Riparian areas are known to be hotspots for biogeochemical processes, characterized by large temporal variability in soil water level, as they are subject to occasional drainage impediments and intermittent inundation after high precipitation events (Figure S1), and are characterized by strong retention of nutrients and high organic matter contents in the soil (Haag & Kaupenjohann, 2002). These processes can lead to increased amounts of greenhouse gas (GHG) emissions (e.g. Vidon et al., 2015). In the tropics, N_2O fluxes from reforestation area and fertilized maize farms on riparian area in Thailand (Kachenchart, Jones, Gajaseni, Edwards-Jones, & Limsakul, 2012), as well as from a rainforest in Puerto Rico (Bowden, McDowell, Asbury, & Finley, 1992), were found to be higher at lower-located, riparian areas than at well-drained, higher-located sites.

Plant-mediated transport (e.g. Pangala et al., 2017; Pangala et al., 2013; Welch et al., 2019) and within-plant production (e.g. Yip et al., 2018) of N_2O and CH_4 can contribute substantially to the total (soil + plant) N_2O and CH_4 fluxes from an ecosystem. Annual stem N_2O and CH_4 fluxes and their contributions to the total GHG flux largely differ among reported studies and long-term and large-scale quantification of stem GHG fluxes is needed to understand their temporal and spatial drivers (Barba et al., 2019). The only study conducted on stem N_2O fluxes from forest on upland mineral soil in the tropics reported larger N_2O emissions from tree stems than from soils (Welch et al., 2019). In wetlands in the Amazon basin, forest stem CH_4 emissions contributed for up to 65 % of the total CH_4 flux budget

(Pangala et al., 2017), whereas in peatland on Borneo forest stem CH_4 emissions contributed up to 83 % of the total CH_4 flux budget (Pangala et al., 2013).

Despite the extensive increase in oil palm plantation area in Sumatra, long-term studies quantifying soil greenhouse gas (GHG) fluxes from this land use type are sparse. The few studies on soil GHG fluxes with year-round measurements from oil palm plantations on mineral soils in Sumatra (Aini et al., 2015; Hassler et al., 2015; Hassler et al., 2017) have limitations for spatial extrapolations because these were mainly conducted on well-drained areas of the landscape, and did not cover spatial heterogeneity (e.g. topography-driven redistribution of water and solutes) that influences soil GHG emission and uptake processes (Pennock & Corre, 2001). Furthermore, contributions of stem GHG emissions in oil palm plantations have never been taken into account. Presently, it remains unclear how the land use of oil palm plantation on riparian areas affects the soil GHG fluxes, and no attempts have been made to quantify stem GHG fluxes from tree cash-crop plantations like oil palm.

Soil nitrous oxide (N_2O) fluxes know two main levels of control, as depicted by the conceptual hole-in-the-pipe (HIP) model (Davidson, Keller, Erickson, Verchot, & Veldkamp, 2000): N availability, which regulates the process rates, and soil water content, which influences the proportion of N_2O of the gaseous N (Corre et al., 2014; Hassler et al., 2017; Koehler et al., 2009; Matson et al., 2017). High levels of available mineral N, due to fertilization (44 – 88 kg ha^{-1} yr^{-1} in smallholder oil palm plantations), and high soil moisture content, due to frequent inundations, could lead to the evolution of an active denitrifying community in riparian buffers, ultimately resulting in increased N_2O production. Stems might act as a conduit for transport of this soil air with increased N_2O concentrations, where it is ultimately released at the stem surface.

Methane (CH_4) is produced in soils during anaerobic decomposition by methanogenic archaea as well as consumed during aerobic conditions in soils as a source of energy by methanotrophic bacteria (Smith et al., 2018). The soil CH_4 flux at the soil-atmosphere interface is the net result of both processes. Oil palm plantations on well-drained soils in upland areas of Sumatra are usually net sinks of CH_4 (e.g. Hassler et al., 2015; Ishizuka et al., 2005). However, riparian areas with intermittent drainage impediment may act as a net CH_4 source during wet phases (Itoh et al., 2007). Seasonal variation in soil CH_4 fluxes across sites in the tropics is positively correlated to soil moisture content (Hassler et al., 2015) and microbial activity (Wolf et al., 2012). Concurrent to soil CH_4 uptake, stem CH_4 emissions have been measured in a tropical forest in Panama (Welch et al., 2019). A possible

mechanism is the transport of soil-air CH_4 from lower anaerobic soil horizons via aerenchyma tissue through stems, where it bypasses the oxygenated surface horizons, where the majority of CH_4 oxidation takes place (Teh et al., 2005).

Soil carbon dioxide (CO_2) emissions are the result of soil respiration: the production of CO_2 when soil organisms respire, and includes respiration of plant roots, the rhizosphere, microbes and fauna (Prentice et al, 2001). In Indonesia are controlled by soil moisture content (van Straaten et al., 2011; Swails et al. 2019) and temperature (Hassler et al., 2015). Riparian areas may have lower CO_2 emissions compared to well-drained sites, due to permanently high soil moisture content, especially during the wet season (van Straaten et al., 2011). Increased soil organic carbon and mineral nitrogen contents at riparian areas in oil palm plantations could, however, lead to increased soil CO_2 emissions.

Our present study focuses on GHG fluxes from stems (N_2O and CH_4) and the soil (N_2O, CH_4, and CO_2) in smallholder oil palm plantations on highly weathered Acrisol soils in riparian areas of Jambi, Indonesia. We conducted a year-round, monthly measurement, including a more intensive measurement following fertilization to quantify fertilizer-induced soil and stem GHG fluxes. We hypothesized that (1) riparian areas, serving as hotspots of biogeochemical processes, will have high N_2O, CH_4 and CO_2 fluxes as a consequence of high nutrient availability from fertilizer application and liming, and (2) tree stems are large contributors to the total N_2O and CH_4 emissions. Our study aimed to (1) quantify stem and soil GHG fluxes from smallholder oil palm plantations on riparian areas, and (2) to assess their seasonal and spatial controlling factors.

2.2 Materials and methods

2.2.1 Site description

This study was conducted in Jambi province, Indonesia (1º49'06"S, 103º19'35"E; elevation of 20 ± 9 m above sea level). The mean annual temperature is 26.7 ± 1.0 ºC and mean annual precipitation is 2235 ± 385 mm (1991 - 2011; climate station at Jambi Sultan Thana airport of the Meteorological, Climatological and Geophysical Agency). During our measurement year (2017 - 2018), annual rainfall in the study region was 2772 mm. The dry season (< 100 mm rainfall month[-1]) was from July to October 2017. Atmospheric nitrogen deposition from rainfall is between 12.9 ± 0.1 and 16.4 ± 2.6 kg N ha^{-1} yr^{-1} (Kurniawan et al., 2018). Our studied riparian areas of smallholder oil palm plantations were located alongside small rivers or streams, which were occasionally flooded during the rainy season (November – June). The

oil palm plantations displayed three spatial structures, distinctive of the common management practices: fertilized area (around 1-m radius from the tree base), inter-row (without direct fertilization), and frond-stacked area, where senesced palm fronds were piled up. The study sites have acidic clay Stagnosols (58 ± 4 % clay in the top 1-m depth) with soil characteristics ranges for pH of $4.3 - 5.5$, effective cation exchange capacity (ECEC) of $61 - 91$ mmol$_c$ kg^{-1}, and a base saturation (BS) of $19 - 75$ % (low values from the inter-rows and high values from the fertilized and limed areas around the palm base; Table A1). These soil characteristics showed the inherent spatial variation due to the management practices; hence, our field measurements were designed to encompass this variability (see section 2.2).

2.2.2 Experimental design

We selected four replicate plots of 50 x 50 m each in different smallholder oil palm plantations on riparian areas. The plantations were $10 - 20$ years old since conversion from forest, and had a planting density of 143 palms per hectare. The plots showed a flat topography, with a maximum elevation difference of only 2 m within plots. Fertilizers were applied two times per year, typical to smallholder management practices. Fertilizer sources were NPK-complete (i.e. Phonska, Mahkota), urea, triple superphosphate, muriate of potash and dolomite. The plots received on average 88 kg N ha^{-1} yr^{-1}, 38 kg P ha^{-1} yr^{-1} and 73 kg K ha^{-1} yr^{-1}. Two of the four farmers applied lime at a rate of ~200 kg dolomite ha^{-1} yr^{-1}, and two of the four farmers also applied ~75 kg K ha^{-1} yr^{-1} as muriate of potash.

Stem N$_2$O and CH$_4$ fluxes were measured from five trees per plot, which were selected based on two micro-topography classes (i.e. higher and lower positions within a plot). Due to physical limitation at one replicate plot (i.e. young palms with leaf axils still attached on the trunk), we only measured stem N$_2$O and CH$_4$ fluxes at three replicate plots. At 0.1 m distance from the base of each selected tree, we measured the soil-air GHG concentrations at 0.4-m depth. For the soil GHG flux measurements, each plot was stratified into two micro-topography classes and three management zones (both mentioned above) and accordingly, six chamber bases (2 micro-topography classes x 3 management zones) were installed permanently in each plot. Measurements of stem and soil GHG fluxes as well as soil-air GHG concentrations were conducted monthly from March 2017 to March 2018.

The monthly measurements may have missed the fertilizer-induced pulse of stem and soil GHG emission, and thus we conducted additional frequent measurements (10 sampling days) during 60 days following fertilizer application. For this follow-on study, we selected

two additional trees (one on each micro-topography class) in each of the three plots for stem GHG flux measurement. Adjacent to each tree, we established a chamber base and a soil gas sampling probe within the fertilized area of the tree base. We applied the same fertilizer forms, rates and methods as used by the smallholder farmers, ~0.7 kg urea, ~1.4 kg triple superphosphate and ~0.8 kg muriate of potash within the 1-m radius from the tree base. Measurements were conducted one day before and 1, 3, 5, 9, 14, 21, 29, 42, 60 days after fertilization, from January to March 2018.

2.2.3 Stem and soil GHG flux and soil-air GHG concentration measurements

Stem N_2O and CH_4 fluxes were measured using stem chambers, described in detail by Wen et al. (2017). Prior to stem chamber establishment, each tree was prepared by manually removing any remaining leaf axils to smoothen the stem surface. Then, parallel silicon strips (Otto Seal S110, Hermann Otto GmbH, Fridolfing, Germany) were applied 0.2-m apart around the stem to facilitate an airtight seal. The silicon strips were left on the tree throughout the measurement period in order to measure always at the same stem segment. Depending on the height of the oil palm stems in the three plots, measurements of stem GHG fluxes were at the stem heights between 0.6 m and 1.2 m from the ground, as we had to find stem segments that allow for logistical chamber installation. The stem chambers are removable and quick to assemble, and hence these were installed newly on each sampling day. These stem chambers were made of plastic foil (polyethylene terephthalate) with a Luer-lock gas sampling port, and wrapped around the stem on the pre-installed silicon rings (Figure A2). On top of the plastic foil, a polyethylene foam was placed, and all three (silicone strips, plastic foil, and foam) were tightened using lashing straps. The stem chamber was first completely evacuated, using a bicycle pump, and subsequently refilled with a known volume of ambient air for the exact calculation of stem GHG fluxes. Four gas samples, 23 ml each, were taken at 0, 20, 40 and 60 minutes after chamber completion and stored in pre-evacuated exetainers (Labco Limited, Lampeter, UK). To account for possible diurnal biases of stem GHG fluxes, we conducted the measurements among the three plots in random rotations such that across the measurement period all plots had random time of measurement during each sampling day. An additional experiment to measure stem flux as a function of height was unfortunately not possible, as the remaining oil palm leaf axils were too young to be cleared at a height above 1.2 m.

Soil GHG fluxes were measured simultaneously with the stem GHG fluxes, using the vented static chamber method described in our earlier studies (Hassler et al., 2015; Hassler et al., 2017). The chamber bases were permanently installed on each of the six sampling

locations per plot, mentioned above. During each measurement, we covered the chamber bases (0.05 m² area) with a vented, static polyethylene hood (total volume of 12 l). Four gas samples, 23 ml each, were taken at 1, 10, 19 and 28 minutes after chamber closure and injected into pre-evacuated exetainers.

Soil-air GHG concentrations were measured from the permanently installed stainless-steel probes with an inner diameter of 0.1 cm, equipped with a Luer-lock for withdrawing air samples (described in our earlier works; van Straaten et al., 2011; Koehler et al., 2012). After removing the pre-stored air within the tube, we took a gas sample of 23 mL and injected it into a pre-evacuated exetainer.

The exetainers were transported to the University of Gottingen, Germany every four months for analysis. These exetainers were tested to be leakproof (Hassler et al., 2015). The gas samples were analyzed for N_2O, CH_4 and CO_2 concentration using a gas chromatograph with an electron capture detector, flame ionization detector, an autosampler (SRI 8610C, SRI Instruments Europe GmbH, Bad Honnef, Germany) and using three concentrations of standard gases (Deuste Steininger GmbH, Mühlhausen, Germany). Hourly stem and soil GHG fluxes were calculated from the linear increase in GHG concentration over time of chamber closure, corrected by field-measured air temperature and pressure. Positive GHG fluxes indicate net emissions whereas negative fluxes indicate net uptake.

2.2.4 Annual and fertilizer-induced stem and soil GHG flux calculations

For annual stem GHG fluxes, we first interpolated the fluxes measured between 0.6- and 1.2-m stem height of each tree across the entire stem length, based on a calculated, best-fitting logarithmic relationship of stem GHG fluxes with height. This extrapolation showed that GHG emissions occurred up to a maximum height of ~ 3 m. The area for the whole stem emission was calculated at 0.2-m stem intervals based on a conical cylinder, as employed in our previous work (Wen, Corre, Rachow, Chen, & Veldkamp, 2017). We then assessed if there were statistical differences in stem GHG fluxes between the two micro-topography classes (see above), by using linear mix-effect models with micro-topography as fixed effect and trees and sampling days as random effects (see 2.6 for similar statistical analysis description). When statistical difference existed, we separated the two micro-topography classes (to which the trees belonged) and calculated the ground area-weighted stem GHG fluxes for each plot on each measurement day. The areal coverage of the micro-topography classes was based on detailed topographic survey conducted in each plot. For the annual stem

GHG fluxes for each replicate plot, we interpolated the values between measurement days using the trapezoid rule. The interpolation between measurement days of stem GHG fluxes was refined by taking into account the inundation phases (recorded whenever this occurred during a measurement day), based on the continuous measurements of groundwater level at the center of each plot (Orpheus Mini Water level Logger, OTT HydroMet, Loveland, US) and the rainfall data measured at maximally 20 km from the plots.

For annual soil GHG flux calculation, we first assessed the differences between the three spatial management zones and between the two micro-topography classes. When statistical difference existed, we separated between the three management zones for each of the two micro-topography classes to get to a ground area-weighted soil GHG flux for each plot on each measurement day. The areal coverages (used for the area-weighting) of the spatial management zone (fertilized, inter-row and frond-stacked areas) were determined in the field whereas the areal coverages of micro-topography classes were determined as described above. For the annual soil GHG fluxes for each replicate plot, we interpolated values between measurement days using the trapezoid rule. The interpolation between measurement days of soil GHG fluxes was again refined by the occurrence of inundation with reference to the groundwater level and rainfall measurements.

To calculate the fertilizer-induced stem and soil GHG fluxes at each plot, we estimated the total GHG fluxes during the entire period (60 days) following fertilizer application using the trapezoidal rule on day intervals between measured fluxes. This value was subtracted by the measured stem and soil GHG fluxes during the same period from the unfertilized trees. We calculated the emission factor as following: percentage (%) N_2O-N of N fertilizer yr^{-1} = (fertilized stem or soil N_2O fluxes − unfertilized stem or soil N_2O fluxes) × frequency of fertilization^{-1} × fertilized area (m^2 ha^{-1}) / N fertilization rate (kg N ha^{-1} yr^{-1} × 10^9 µg kg^{-1}) × 100, as employed in our previous work (Hassler et al., 2017).

2.2.5 Supporting measurements of controlling factors

Soil biochemical and physical characteristics were determined at the six sampling locations per plot (as mentioned above). At each sampling location, soil samples were collected in the top 0.1 m using a soil auger. Soil organic C and total N concentrations were determined from air-dried, sieved (2 mm) and ground samples, using a CN analyzer (Vario EL Cube, Elementar Analysis Systems GmbH, Hanau, Germany). The ECEC was measured by percolating unbuffered 1 mol L $^{-1}$ NH_4Cl on the air-dried, sieved soils, and exchangeable

cations (Ca, Mg, K, Na, Al, Fe and Mn) were measured using an inductively coupled plasma-atomic emission spectrometer (ICP-AES; iCAP 6300 Duo VIEW ICP Spectrometer, Thermo Fischer Scientific GmbH, Dreieich, Germany). Base saturation was calculated as percentage exchangeable base cations of the ECEC. Extractable P was determined using the Bray 2 method, typically used for highly weathered soils (Bray & Kurtz, 1945), and extracts were analyzed with the ICP-AES. For soil ^{15}N natural abundance signatures, soil samples were ground and then analyzed using isotope ratio mass spectrometry (Delta Plus, Finnigan MAT, Bremen, Germany). The soil bulk density and soil texture were measured from a soil pit dug next to the plot, using the core method (Blake & Hartge, 1986) and the pipette method (König & Fortmann, 1996), respectively.

Simultaneous to each GHG flux measurement, we measured the known controlling factors. Soil temperature was measured at 0.05-m depth close to the chamber base, and air temperature was measured at 1.2 m above the ground, both using a digital thermometer (GMH 3210, Greisinger Electronics GmbH, Regenstauf, Germany). Air pressure was measured using a digital barometer (GTD 1100, Greisinger Electronics GmbH, Regenstauf, Germany). Gravimetric soil moisture content was measured by oven-drying fresh soil samples at 105°C for at least 24 hours. Vapor pressure deficit (VPD) was calculated based on the relative humidity (continuously measured with a relative humidity probe; HMP45D, Vaisala, Helsinki, Finland) and air temperature (Allen, Pereira, Raes, & Smith, 1998).

Soil ammonium (NH_4^+) and nitrate (NO_3^-) were extracted in situ using prepared bottles of 0.5 mol L^{-1} K_2SO_4 solution to which fresh soil was added; soil collected at about 1 m from the chamber base in the top 0.05-m depth. Upon arrival at the field station, the bottles were shaken for 1 hour and filtered through K_2SO_4 pre-washed filter papers. Extracts were immediately frozen and transported to the University of Goettingen, Germany for analysis. Mineral N concentrations were determined using continuous flow injection colorimetry (SEAL Analytical AA3, SEAL Analytical GmbH, Norderstadt, Germany) by salicylate and dicloroisocyanuric acid reaction for NH_4+ (Autoanalyzer Method G-102-93), and by cadmium reduction method with NH_4Cl buffer for NO_3- (Autoanalyzer Method G-254-02).

2.2.6 Statistical analysis

Each parameter was tested for normal distribution (Shapiro-Wilk's test) and for equality of variance (Levene's test), and logarithmic or square root transformation was applied when these assumptions were not met. For time-series data (i.e. stem and soil GHG fluxes,

fertilizer-induced stem and soil GHG fluxes, soil-air GHG concentrations, and soil controlling factors), linear mixed-effect (LME) models were used to assess their differences among the three spatial management zones and between the two micro-topography classes with management zone or micro-topography as fixed effects, and replicate plot and measurement days as random effects. For stem GHG fluxes (located all on fertilized areas), the LME was conducted to test differences between micro-topography classes with plot and measurement days as random effects. The LME model included either a variance function that allows different variances of the response variable for the fixed effects and/or a first-order temporal autoregressive process that assumes a decreasing correlation between measurement days with increasing time distance (Crawley, 2007). We then selected the model with the best relative goodness of the model fit by using the Akaike information criterion. Tukey's HSD test was used to determine differences among fixed effects.

Spearman's rank correlation test was used to assess the temporal relationships of stem and soil GHG fluxes with the controlling factors (WFPS, soil temperature, mineral N content, soil-air GHG concentrations, VPD). For the monthly measured stem and soil GHG fluxes, correlation tests were conducted using the means of the three (stem) or four (soil) replicate plots on each measurement day (separately for each management zone) across 13 monthly measurements ($n = 13$). For the fertilizer-induced stem and soil GHG fluxes, we used the means of three replicate plots on each sampling day across 10 measurement days ($n = 10$). For correlation test between stem GHG fluxes and VPD, we used the three replicate plots (each represented by a mean of 5 trees) across five monthly measurements when VPD data were available ($n = 15$); for the correlation of stem fluxes with VPD during the fertilizer-induced stem GHG fluxes, we used the three replicate plots (each represented by a mean of 2 trees) across the 10 measurement days ($n = 30$). The spatial relationships of annual soil GHG fluxes with the soil biochemical characteristics (Table A1) were conducted on the values of the three management zones across four plots ($n = 12$), using Spearman's rank correlation test. For the soil CO_2 fluxes, we did a regression analysis with the WFPS using the average of the four replicate plots, separated by three management zones and two micro-topography classes, on each of the 13 monthly measurements ($n = 78$). Differences between fixed effects and correlation coefficients were considered statistically significant at $p \leq 0.05$, except for a few specified parameters where we clearly indicate marginal significance at $p \leq 0.09$. All statistical analyses were conducted using R 3.5.0 (R Core Team, 2018).

2.3 Results

2.3.1 Stem and soil greenhouse gas fluxes

The monthly measurements showed consistent stem and soil N_2O emissions during the whole year as well as elevated soil-air N_2O concentrations especially in the wet season (Figure 1a-c). Stem N_2O emissions were higher in the wet than in the dry season ($p < 0.01$; Table 1; Figure 1a) and higher during inundation events (e.g. Figure A1) than during unflooded conditions ($p < 0.01$; results not shown). Micro-topography did not influence the stem N_2O emissions across the measurement period ($p = 0.10$; results not shown). There was no difference in soil N_2O emissions between seasons ($p = 0.12$; Table 1) and micro-topography classes ($p = 0.10$; results not shown); however, the management zones distinctly differed with larger emissions from the fertilized area than the inter-row, particularly in the wet season ($p = 0.04$; Table 1; Figure 1b). Fertilizer application resulted in clear increases in stem and soil N_2O emissions as well as in soil mineral N content and soil-air N_2O concentrations (Figure 2a-e). Stem N_2O emissions peaked at 10 days after fertilization at low position within the plots and around 30 days at high position within the plots (Figure 2a), and were at most 240 times higher than during the unfertilized period (Figure 1a). Soil N_2O emissions after fertilizer application peaked at ~20 to 30 days, lasted for ~60 days (Figure 2b), and were at most 160 times higher than the unfertilized period (Figure 1b). The annual stem and soil N_2O emissions accounted for 2.8 ± 0.8 % and 97.2 ± 0.8 %, respectively, of the total (soil + stem) N_2O emission (Table 2). The N_2O emission factor from fertilizer (see section 2.4) was 3.9 ± 0.2 % (Table 2).

We measured consistent stem CH_4 emissions across the 13 monthly measurement period (Figure 3a). Stem CH_4 emissions were higher in the wet than in the dry season ($p < 0.01$; Table 1), higher during inundation events (e.g. Figure A1) than during unflooded conditions ($p < 0.01$; results not shown), and also higher at the low than the high positions within the plots ($p = 0.01$; results not shown). Thus, these conditions were taken into account in the temporal interpolation of fluxes for the annual flux estimates and for the spatial extrapolation of fluxes (see section 2.4). In the wet season, the soil was a net source of CH_4 and soil-air CH_4 concentrations were elevated; in the dry season, the soil served as a slight sink for atmospheric CH_4 and soil-air CH_4 concentrations were similar to atmospheric concentration (all $p < 0.01$; Table 1; Figure 3b,c). A distinct difference among the management zones was observed in the wet season, where soil CH_4 emissions were lower in the frond-stacked area than in the fertilized area and inter-rows ($p = 0.03$; Table 1). Also, soil CH_4 emissions were higher from the low than high positions within the plots in the wet season

($p < 0.01$; results not shown), and this was thus taken into account in the temporal interpolation and spatial extrapolation of fluxes for the annual CH_4 flux estimates (see section 2.4). Fertilizer application did not influence stem or soil CH_4 fluxes ($p > 0.09$). The annual stem CH_4 emissions accounted for 14.7 ± 5.7 % of the total (soil + stem) CH_4 flux, whereas the annual soil CH_4 fluxes accounted for 85.3 ± 5.7 % of the total CH_4 flux (Table 2).

Figure 1 Mean ($\pm$ SE, $n = 3$ sites (stem) or $n = 4$ sites (soil)) (a) stem and (b) soil N_2O fluxes and (c) soil-air N_2O concentrations at 0.4-m depth, measured from March 2017 to March 2018 in smallholder oil palm plantations on riparian areas in Jambi province, Indonesia. Gray shadings mark the dry season.
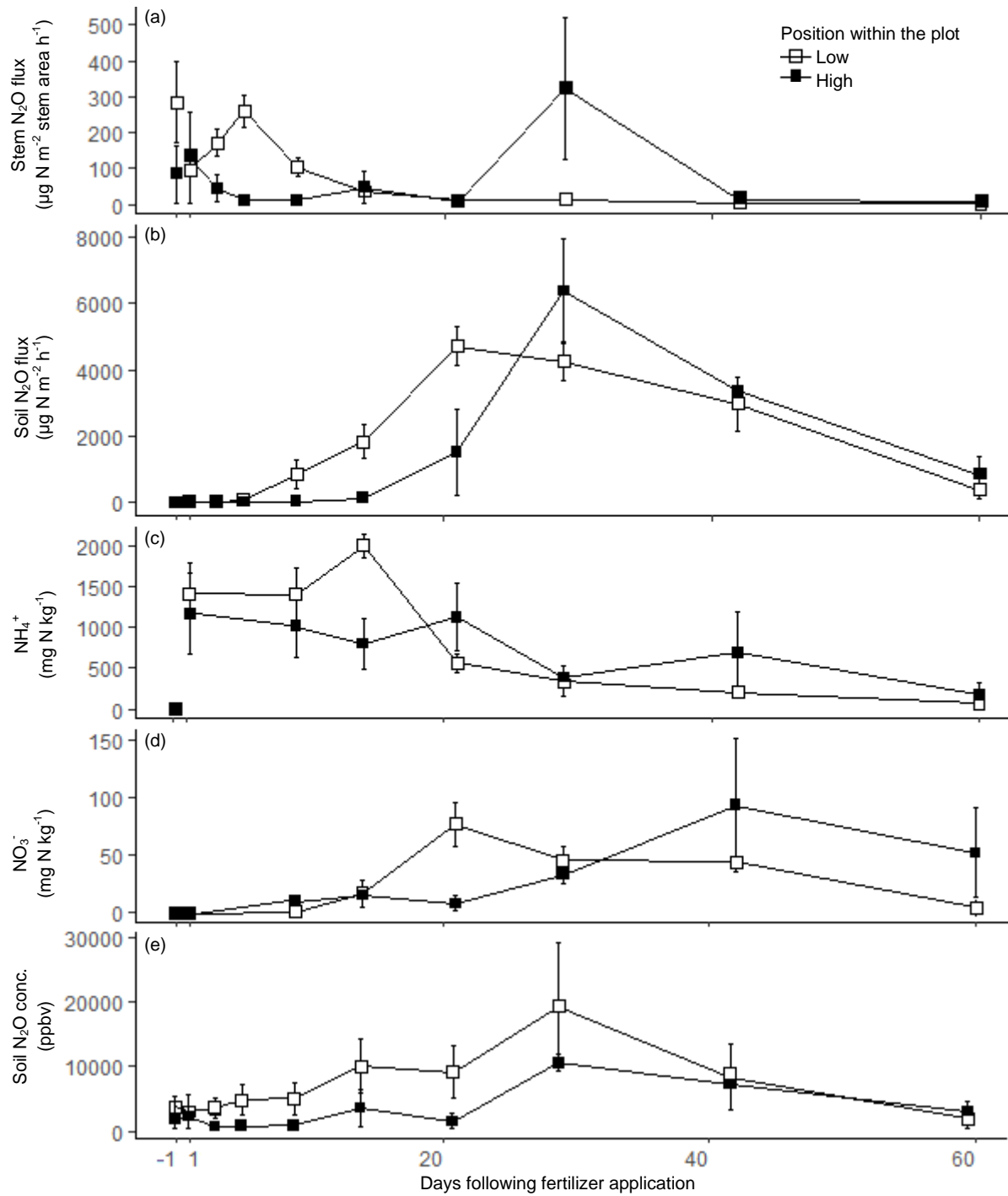
Figure 2 Mean (±SE, n = 3 sites) fertilizer-induced (a) stem and (b) soil N_2O fluxes, (c) soil NH_4^+ and (d) soil NO_3^- concentrations and (e) soil-air N_2O concentrations at 0.40-m depth during the 60 days following fertilization, using rates common to smallholder practices, measured from January to March 2018 in smallholder oil palm plantations on riparian areas in Jambi province, Indonesia.

Table 1 Mean ($\pm$SE, $n = 3$ sites (stem) or $n = 4$ sites (soil)) greenhouse gas (GHG) fluxes and their controlling soil factors (measured in the top 0.05-m depth) in smallholder oil palm plantations on riparian areas in Jambi province, Indonesia.

Season/ Management zone[a]	Stem GHG flux		Soil GHG flux			Controlling factors		
	N_2O (μg N m$^{-2}_{stem}$ h^{-1})	CH_4 (μg C m$^{-2}_{stem}$ h^{-1})	N_2O (μg N m^{-2} h^{-1})	CH_4 (μg C m^{-2} h^{-1})	CO_2 (mg C m^{-2} h^{-1})	Water-filled pore space (%)	NH_4^+ (mg N kg^{-1})	NO_3^- (mg N kg^{-1})
Dry season								
Fertilized	1.9 ± 0.6^B	3.1 ± 1.0^B	20.8 ± 11.2^{Aa}	-2.2 ± 2.4^{Aa}	161 ± 13^{Aa}	56.0 ± 3.7^{Bc}	14.4 ± 5.3^{Aa}	1.1 ± 0.7^{Aa}
Inter-row	-	-	3.0 ± 0.7^{Aa}	-10.5 ± 4.4^{Aa}	122 ± 12^{Ab}	86.4 ± 2.5^{Ba}	5.7 ± 0.5^{Ab}	0.1 ± 0.1^{Ab}
Frond-stacked	-	-	3.8 ± 1.1^{Aa}	0.1 ± 3.1^{Aa}	138 ± 10^{Aab}	70.2 ± 4.3^{Bb}	11.1 ± 1.9^{Aab}	0.3 ± 0.1^{Aab}
Wet season								
Fertilized	2.8 ± 0.5^A	27.6 ± 6.9^A	83.3 ± 58.2^{Aa}	77.6 ± 22.2^{Ba}	169 ± 12^{Aa}	66.7 ± 2.6^{Ac}	20.2 ± 7.4^{Aa}	0.8 ± 0.5^{Ba}
Inter-row	-	-	2.9 ± 0.7^{Ab}	52.5 ± 15.0^{Ba}	111 ± 10^{Ab}	92.2 ± 1.4^{Aa}	4.9 ± 0.4^{Ab}	0.1 ± 0.0^{Aa}
Frond-stacked	-	-	7.4 ± 2.5^{Aab}	19.4 ± 5.3^{Bb}	131 ± 8^{Aa}	80.3 ± 2.1^{Ab}	9.1 ± 1.6^{Aa}	0.2 ± 0.1^{Aa}

[a] For each column, different uppercase letters indicate significant differences between seasons for each management zone, and different lowercase letters indicate significant differences among management zones for each season (linear mixed-effects model with Tukey's HSD test at $p \le 0.05$).

Table 2 Annual stem, soil and total (stem + soil) (mean $\pm$ SE, $n = 3$ sites (stem) or $n = 4$ sites (soil)) greenhouse gas (GHG) fluxes, and fertilizer-induced (mean $\pm$ SE, $n = 3$ sites) GHG fluxes from smallholder oil palm plantations on riparian areas in Jambi province, Indonesia.

Annual GHG fluxes[a]	Monthly measurements			Fertilizer-induced measurements			Overall sum
	Stem	Soil	Total	Stem	Soil	Total	
N_2O (g N ha^{-1} yr^{-1})	12 ± 4	409 ± 90	421 ± 90	79 ± 8	3018 ± 305	3098 ± 306	3428 ± 318
CH_4 (g C ha^{-1} yr^{-1})	99 ± 46	605 ± 90	704 ± 101	0	0	0	704 ± 101
CO_2 (kg C ha^{-1} yr^{-1})	-	11002 ± 264	-	-	91 ± 13	-	11092 ± 264

[a] Temporal interpolation for monthly and fertilizer-induced GHG fluxes and spatial extrapolation into ground area are described in section 2.4.
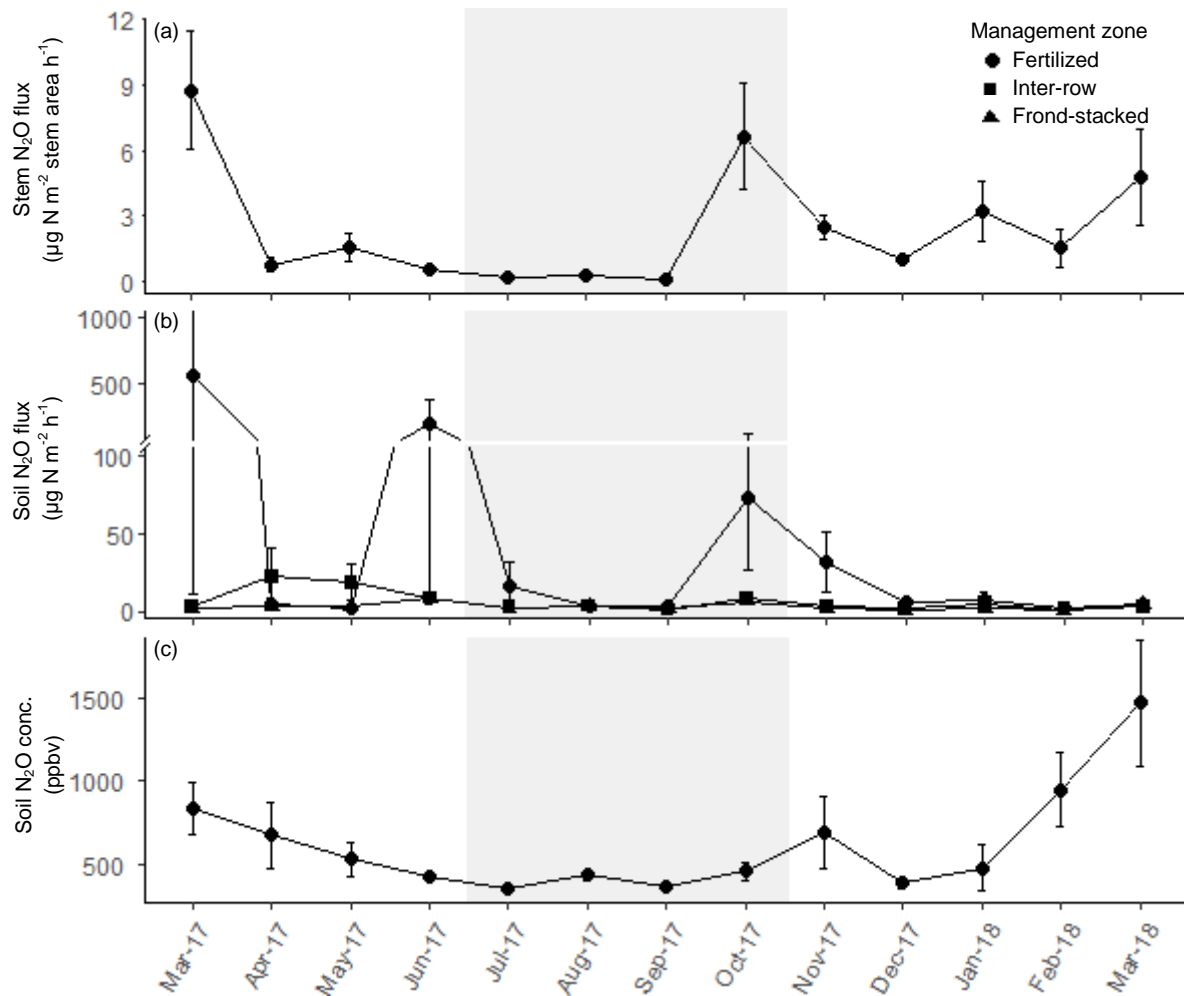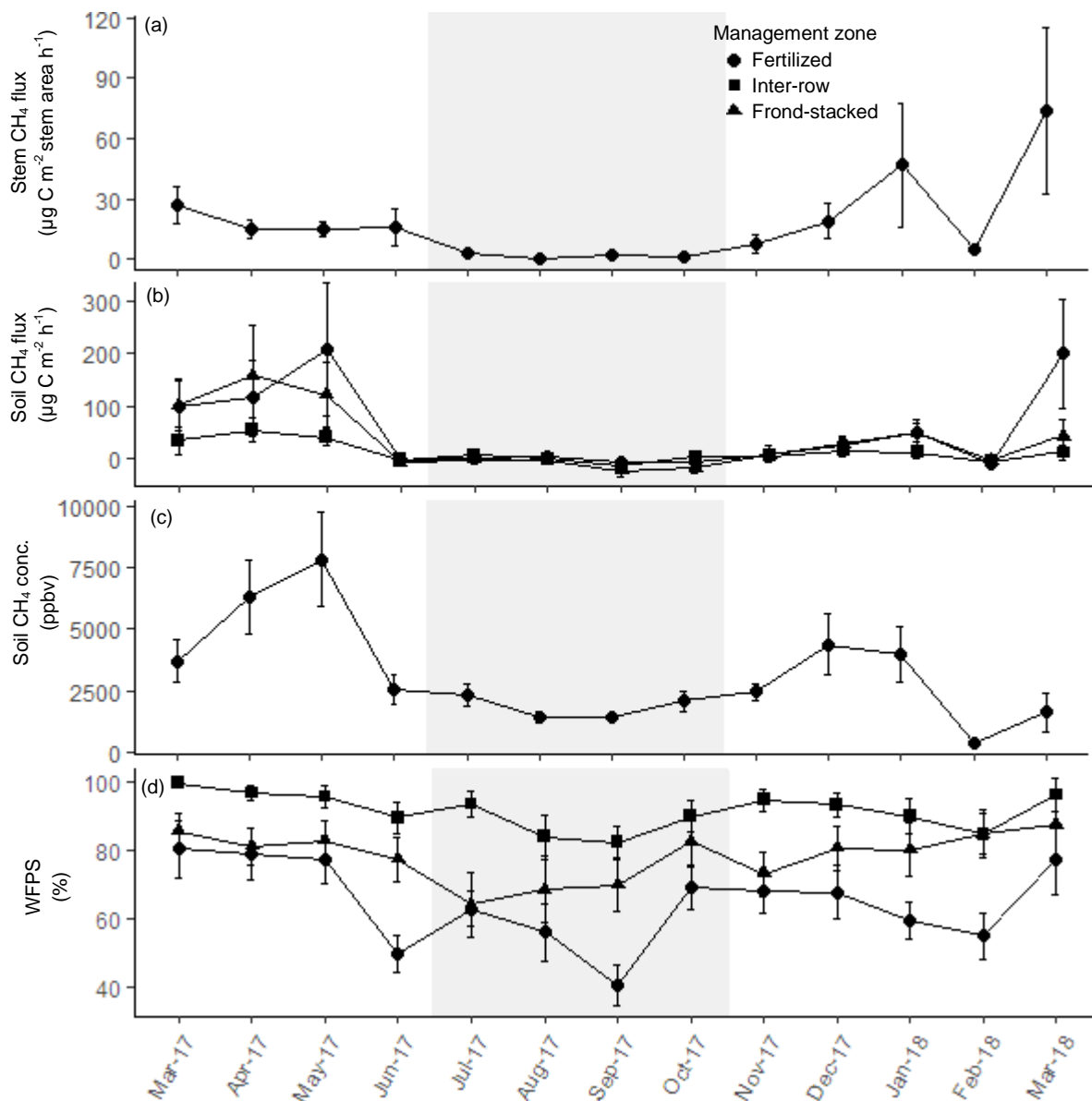
Figure 3 Mean (±SE, $n = 3$ sites (stem) or $n = 4$ sites (soil)) (a) stem and (b) soil CH_4 fluxes, (c) soil-air CH_4 concentrations at 0.4-m depth, and (d) water-filled pore space (WFPS, top 0.05-m depth), measured from March 2017 to March 2018 in smallholder oil palm plantations on riparian areas in Jambi province, Indonesia. Gray shadings mark the dry season.

The monthly measured soil CO_2 emissions did not differ between seasons ($p = 0.10$; Table 1). However, we observed a distinct difference among management zones, where soil CO_2 emissions were higher in the fertilized area than in the inter-row ($p = 0.03$; Table 1). There were no differences in soil CO_2 emissions between micro-topography classes ($p = 0.20$; results not shown). Fertilizer application increased soil CO_2 emissions, which peaked at ~ 4 days and lasted for ~ 8 days, but this fertilizer-induced soil CO_2 emission accounted for only 0.81 ± 0.00 % of the annual soil CO_2 emission (Table 2).

2.3.2 Controlling factors

Of the four soil controlling factors that were measured concurrently with the GHG fluxes (WFPS, extractable NH_4^+ and NO_3^-, and temperature), only the WFPS showed clear seasonal variation and was higher in the wet than in the dry season ($p < 0.01$; Table 1; Figure 3d). The WFPS was highest in the inter-row, followed by the frond-stacked area, and lowest in the fertilized area in both seasons ($p < 0.01$; Table 1). WFPS was higher at lower plot positions than at higher plot positions during both the monthly and fertilizer-induced measurements (both $p < 0.01$; results not shown). In the dry season, soil NH_4^+ and NO_3^- concentrations were higher in the fertilized area than in the unfertilized inter-row whereas the frond-stacked area was intermediate ($p = 0.01$; Table 1); in the wet season, NH_4^+ levels were lower in the inter-row than the two other zones ($p < 0.01$) while NO_3^- did not differ ($p = 0.78$; Table 1). NH_4^+ was consistently the dominant form of mineral N (Table 1) even after fertilization (Figure 2c,d). Following fertilization, NH_4^+ concentrations were highest during the first 15 days while the highest NO_3^- concentrations occurred after 20–40 days (Figure 2c,d). Soil-air N_2O concentrations peaked at around 30 days following fertilizer application and were 23-90 times higher than atmospheric concentrations (Figure 2e). The soil temperatures were higher in the fertilized than the frond-stacked areas ($p = 0.05$) in the wet season, whereas the inter-row did not differ from these two zones in both seasons ($p = 0.19$; results not shown).

Stem N_2O emissions, from monthly or fertilizer-induced measurements, were strongly correlated with WFPS and soil-air N_2O concentrations, and marginally correlated with VPD (Table 3). Stem CH_4 emissions were strongly correlated with soil-air CH_4 concentrations (fertilizer-induced measurements; Table 3) and only marginally correlated with WFPS and VPD (monthly measurements; Table 3). Soil N_2O emissions from the fertilizer-induced measurements were strongly correlated with soil NO_3^- contents (Table 3; Figure 2b,d); this correlation was not observed for the monthly measurements (Table 3). Soil CH_4 fluxes from the fertilized area and inter-row were positively correlated with WFPS; in the frond-stacked area this relationship was not detected (Table 3; Figure 3b,d). Soil CO_2 emissions exhibited a quadratic relationship with WFPS with the highest emissions occurring between 60 % and 80 % WFPS (Figure 4). The correlation between soil CO_2 emissions and soil temperature in the frond-stacked area (Table 3), likely reflects the effect of sampling time during the day rather than by a seasonal pattern, as temperature differences were limited (26.6 °C to 28.9 °C during the year-round measurements; results not shown).

Table 3 Spearman rank correlation coefficients to assess the temporal patterns of stem and soil greenhouse gas (GHG) fluxes with the controlling factors, water-filled pore space (WFPS), extractable NO_3^-, soil temperature (all measured within 0.05-m depth), soil-air concentration of GHG (measured at 0.4-m depth), and vapor pressure deficit (VPD) in the smallholder oil palm plantations on riparian areas in Jambi province, Indonesia.

	N_2O				CH_4			CO_2
	WFPS	Soil NO_3^-	Soil-air N_2O	VPD	WFPS	Soil-air CH_4	VPD	Soil temperature
Monthly measurements								
Stem	0.69***	0.12	0.72***	0.38	0.53*	0.46*	0.55*	-
Soil: Fertilized	0.24	0.47	0.07	-	0.71***	0.70**	-	0.14
Inter-row	0.25	0.03	-	-	0.78***	-	-	0.16
Frond-stacked	0.09	0.04	-	-	0.43	-	-	0.64**
Fertilizer-induced measurements								
Stem	0.47**	-	-0.14	0.44*	0.38	0.93***	0.37	-
Soil: Fertilized	-0.43	0.82**	0.81***	-	0.20	0.88***	-	-0.41

*** $p < 0.01$, ** $p = 0.01 - 0.05$, * $p > 0.05 - 0.08$; $n = 13$ for the monthly measured stem and soil GHG fluxes; $n = 10$ for the fertilizer-induced GHG fluxes; $n = 15$ (monthly measurements) or 30 (fertilizer-induced measurements) for stem GHG fluxes with VPD (see section 2.2.6).
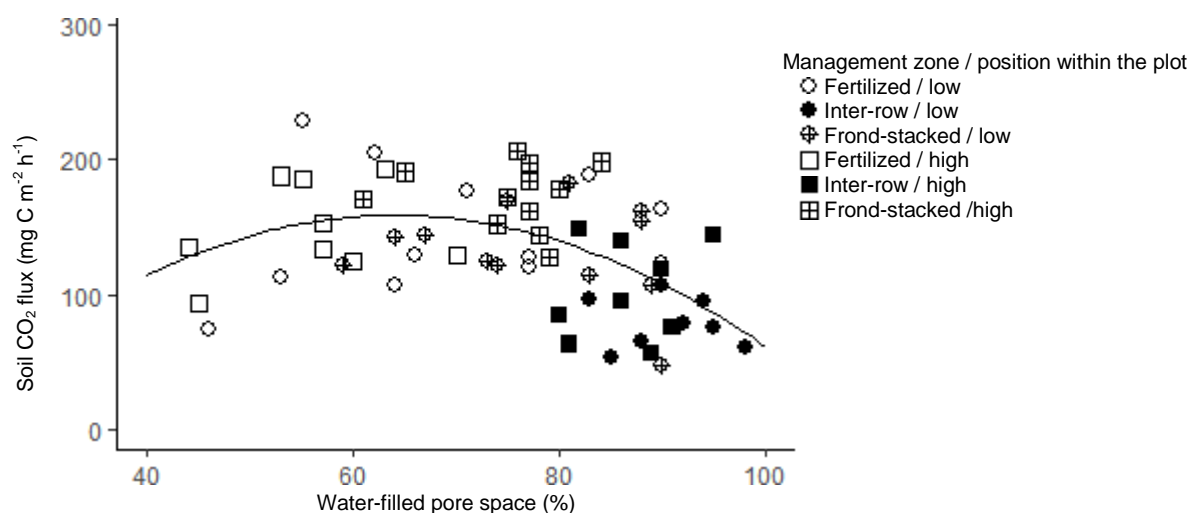
Figure 4 Soil CO_2 fluxes and water-filled pore space (top 0.05-m depth) in oil palm plantations on riparian areas in Jambi province, Indonesia. Each data point is the average of the four replicate plots, separated by three management zones and two micro-topography classes, on each of the 13 monthly measurements from March 2017 to March 2018. $y = -0.076\ x^2 + 9.8\ x - 155$ ($R^2 = 0.27$, $n = 3 \times 2 \times 13 = 78$, $p > 0.01$).

2.4 Discussion

2.4.1 Stem greenhouse gas fluxes

Stem N_2O and CH_4 flux measurements in a lowland, old-growth forest on well-drained soil in Panama revealed values between $51 - 759$ µg N m^{-2} h^{-1} and $66 - 76$ µg C m^{-2} h^{-1}, respectively (Welch et al., 2019). These are at most ~250 times (for stem N_2O emissions) and three times (for stem CH_4 emissions) higher than our present study (Table 1). Such high stem GHG

emissions are notable, given the combination of high N availability and high soil moisture content at our sites (i.e. fertilizer application and regular flooding; Table 1, Figures 2c,d, and 3d) should provide favorable conditions for N_2O production in the soil (Davidson et al., 2000), and consequently large stem N_2O fluxes (e.g. Wen et al., 2017). Stem CH_4 emissions measured in Amazonian floodplains range between $33 - 337000$ µg C m^{-2} h^{-1} (Pangala et al., 2017). Both these Panamanian and Amazonian studies reported stem GHG fluxes up to seven times higher than their soil N_2O and CH_4 emissions, whereas we have never observed higher stem than soil GHG emissions at our sites (Figures 1a,b, and 3a,b). Higher stem than soil N_2O and CH_4 emissions found at their sites may suggest a significant within-tree source of N_2O and CH_4 (Barba et al., 2019; Lenhart et al., 2019), which was not the case at our riparian sites.

Seasonal changes in precipitation quantities and the subsequent differences in WFPS (Table 1), as well as occasional inundation events (data not reported), clearly influenced stem N_2O and CH_4 emissions. The correlations of stem N_2O and CH_4 emissions with WFPS as well as their similarity in temporal patterns with soil N_2O and CH_4 emissions (Figures 1, 2, 3) suggest that these stem-emitted GHG might have, at least partly, originated from the soil. As the soil becomes increasingly anaerobic, the microorganisms' metabolic process changes from aerobic respiration to denitrification and eventually to methane production (Schlesinger and Bernhardt, 2013). The elevated soil-air N_2O and CH_4 concentrations might have stimulated diffusion and thus increased transportation within the stem and subsequent release into the atmosphere through stem surfaces. Transport of soil-borne GHG can take place both in gaseous form (e.g. Rusch & Rennenberg, 1998), via passive diffusion into the roots and transport via air-filled aerenchyma tissue, and in dissolved form (Koehler et al., 2012), after uptake of soil solution via the xylem sap flow (Pangala et al., 2013; Pitz & Megonigal, 2017). Our observed correlations between stem N_2O and CH_4 emissions and soil-air N_2O and CH_4 concentrations (Table 3) indicated this was also the main mechanism responsible for stem emissions of oil palms. In addition, the exponential decrease of stem N_2O and CH_4 emissions with stem height, supported the claim stem GHG was soil-borne (Díaz-Pinés et al., 2016; Wen et al., 2017). Furthermore, the observed correlations of stem N_2O and CH_4 emissions with the vapor pressure deficit (VPD; Table 3) suggest that an increasing VPD, which stimulates sap flow rates, might have led to increased transport of dissolved N_2O and CH_4 in soil water via xylem sap in the transpiration stream.

Differences in stem N_2O and CH_4 emissions from both micro-topography classes might be related to differences in WFPS. During the fertilizer-induced measurements (Figure 2), the higher WFPS at the lower positions (second level of control HIP; data not shown), has likely

caused an increased rate of nitrification of the applied N-fertilizer (Figure 2d) compared to higher positions with lower WFPS (Davidson et al., 2000). In turn, denitrification of the produced NO_3^- could have led to increased soil-air N_2O concentrations (Figure 2e), which caused the earlier peak in stem N_2O emissions at the lower positions (Figure 2a). During the monthly measurements, the higher WFPS at lower positions (data not shown) might have led to elevated stem CH_4 emissions (data not shown); increased WFPS has led to increased soil-air CH_4 concentrations (see previous paragraph), which in turn led to increased stem CH_4 emissions, as suggested by the correlations between stem CH_4 emissions and soil-air CH_4 concentrations and WFPS (Table 3).

The architecture of the oil palm stem and the fact that we measured at a stem height between $0.6 - 1.2$ m may have resulted in conservative stem N_2O and CH_4 flux estimates. Roots from the oil palm have highly developed aerenchyma tissue (Jourdan & Rey, 1997), known for transport of soil-borne N_2O and CH_4 through the plant (e.g. Rusch & Rennenberg, 1998). Furthermore, the oil palm stem does not contain heartwood, a non-conducting tissue for water (Corley & Tinker, 2015), and hence has a large capacity to transport gas and dissolved matter via transpiration stream. The combination of easy uptake of GHG via aerenchyma tissue and the easy pathway of diffusion from stem to the atmosphere, might have led to enhanced GHG emission at lower stem height. Recent studies (Díaz-Pinés et al., 2016; Pangala et al., 2017) reported stem N_2O and CH_4 emissions up to 66 % lower at 1.3 m than at 0.2 m stem height. Using the observed logarithmic relationship between stem N_2O and CH_4 emissions and stem height for upscaling (as described in section 2.2.4), the decrease in GHG emission over stem height was incorporated in the calculations. However, this method might have still led to underestimation at a stem height below 0.6 m, given the oil palm's conductive structure of sap-flux driven transport of dissolved GHG from the soil into the stem.

2.4.2 Soil greenhouse gas fluxes

Our findings suggest that riparian areas can be hotspots of soil N_2O emissions, as we measured 1) higher annual soil N_2O fluxes than values reported for smallholder oil palm plantations on well-drained, mineral soils ($0.23 - 1.1$ kg ha^{-1} yr^{-1}; Aini et al., 2015; Hassler et al., 2017; Ishizuka et al., 2005), and 2) a higher emission factor (EF) than the range of reported EF from oil palm plantations on well-drained, mineral soils ($0.2 - 3.1$ %; Aini et al., 2015; Hassler et al., 2017). This is in line with previous studies in the tropics, which also report enhanced N_2O emissions from riparian (Bowden et al., 1992; Kachenchart et al., 2012). Soil NO_3^- content was the main driver of temporal variation of soil N_2O fluxes following

fertilization (Table 3; Figure 2b,d). The earlier peak in soil N_2O emissions following fertilization at lower positions than at higher positions (Figure 2b), might have been the result of an increased rate of nitrification at the lower positions, due to a higher WFPS here (data not reported).Variation in soil N_2O fluxes (Table 1) between management zones can be explained by differences in soil NO_3^- content and WFPS (Table 1). In the fertilized area, high mineral N content (substrate of microbial N_2O production, first level of control in HIP; Table 1) and intermediate WFPS (second level of control in HIP; Table 1), both conducive for N_2O emissions (Davidson et al., 2000), led to high N_2O emissions (Table 1, Figure 1b). In contrast, the inter-row, having low mineral N content and high WFPS (Table 1) favors for reduction of N_2O to N_2, and thus resulted in low N_2O emissions (Davidson et al., 2000; Table 1). In the frond-stacked area, as a result of intermediate mineral N content and WFPS (Table 1; Figure 3d), an intermediate soil N_2O flux was found (Table 1, Figure 1b).

We measured net annual soil CH_4 emissions from riparian areas, which contradicted with the net annual CH_4 uptake reported from oil palm plantation systems on well-drained soils (0.52 to 3.78 kg ha^{-1} yr^{-1}; Hassler et al., 2015; Ishizuka et al., 2005). Annual net soil CH_4 emissions were also measured from forests located on tropical peatland landscapes (Bartlett et al., 1990; Smith et al., 2000), suggesting that the conditions of mineral soils on riparian areas can lead to the similar CH_4 production as on peatlands. During the dry season, the upper layers of the soil have a low WFPS and are well aerated; methanogenic archaea are probably dormant and the soil acts as CH_4 sink (Fiedler & Sommer, 2000). The occurrence of CH_4 production in combination with the diffusional limitation on the supply of CH_4 to methanotrophs at high WFPS, therewith partially offsetting CH_4 consumption, explains the strong net soil CH_4 emission during the wet season. Even though we found a strong correlation between soil CH_4 emissions and WFPS (Table 3), we found highest soil CH_4 emissions in the fertilized area in the wet season, which displayed the lowest WFPS (Table 2; Figure 3d). In this management zone, increased root respiration might have caused reduced O_2 availability, leading to increased CH_4 production (Butterbach-Bahl, Baggs, Dannenmann, Kiese, & Zechmeister-Boltenstern, 2013). The frond-stacked area showed in the lowest soil CH_4 emissions in the wet season as a result of intermediate WFPS and limited root respiration; whereas in the inter-row, intermediate soil CH_4 emissions might have been the result of a high WFPS and limited root respiration (Table 2; Figure 3b). Absent correlations between soil CH_4 emissions and soil mineral N content during both the annual and fertilizer-induced measurements, suggested that soil mineral N content did not control CH_4 production or consumption. An absent correlation between soil NO_3^- and CH_4 has been reported in

Panama before (Veldkamp et al., 2013); high soil moisture levels might overrule soil mineral N content as a controlling factor of soil CH_4 fluxes.

We measured annual soil CO_2 emissions which were comparable to the range of values reported from oil palm plantations from well-drained, mineral soils (9.22 – 10.3 Mg ha^{-1} yr^{-1}; Hassler et al., 2015; Ishizuka et al., 2005). This might be related to the quadratic response of soil CO_2 emissions with WFPS; which turned out to be the main controlling factor for soil CO_2 emissions (Table 1, Figure 4). The WFPS during our study was mainly above the optimum for CO_2 production (> 80 %; Table 1, Figure 4), whereas during the studies on well-drained sites, WFPS was mainly below the optimum for CO_2 production (< 60 %, Hassler et al., 2015). The quadratic response of soil CO_2 emissions to WFPS (Figure 4) is also found in other tropical regions around the world (e.g. Hassler et al., 2015; Matson et al., 2017). Variability in soil CO_2 emissions between the different management zones (Table 1; Figure 4) was related to differences in soil nutrient content. In the fertilized area, where the palms are located, high soil CO_2 emissions were probably largely contributed by root and root-exudate heterotrophic respiration (e.g. Goodrick et al., 2016), considering that SOC was low and the high ^{15}N values also suggested organic matter was highly decomposed (Table A1; Sotta, Corre, & Veldkamp, 2008). The inter-row, characterized by less vegetation and low root density (~ 4 – 5 m from the palm row), is receiving less organic C input (a high ^{15}N natural abundance suggests highly decomposed organic matter), which, therefore, resulted in the lowest soil CO_2 fluxes (Table 1). In the frond-stacked area, the high soil CO_2 emissions may have been the result of the nutrient-rich decomposing fronds; in the soil under the piled fronds, the high soil organic matter (SOM) content (Table A1) functioned as substrate for soil CO_2 production. Furthermore, a high base saturation and conversely low exchangeable Al (Table A1) are presumably resulting from the base cations released from decomposing fronds; the lowest ^{15}N natural abundance (Table A1) confirms the SOM is least decomposed here, which shows it receives the highest SOM input.

2.5 Conclusions

This study showed that both coverage of spatial variance in a certain landscape, as well as incorporation of all different components on an ecosystem scale (stem + soil fluxes), are important factors to take into account for landscape-scale GHG flux estimations. Incorporation of spatial variation and stem GHG fluxes in soil GHG flux measurements both led to significant increase of the total budget estimates, and therefore we conclude that neglecting these can result in significant underestimation.

Palm oil plantation systems on riparian areas showed elevated soil N_2O emissions, a higher emission factor of applied N-fertilizer, as well as net CH_4 emissions instead of CH_4 uptake compared to well-drained sites. This supported our hypothesis that riparian areas may indeed act as hotspots of GHG production and thus emission. Furthermore, the different management zones of oil palm plantations showed distinct differences in soil GHG fluxes. Both findings underline that spatial variability is an important factor to be considered in field-based GHG flux studies.

Stems were responsible for 2.8 ± 0.8 % (N_2O) to 14.7 ± 5.7 % (CH_4) of the total (stem + soil) GHG fluxes, supporting our second hypothesis that they can be important contributors to the total GHG fluxes. Correlations between stem GHG fluxes and soil-air GHG concentrations, VPD and WFPS, as well as similar trends between stem and soil GHG fluxes, suggested that stem-emitted N_2O and CH_4 most likely originated in the soil.

To improve estimates of oil palm stem N_2O and CH_4 emissions, we recommend measuring at stem heights below 0.6 m, to assess the spread of stem-emitted GHG over the height of the stem and thus being able to make more accurate stem GHG emission estimates. Furthermore, as the WFPS, the main controller of soil GHG fluxes at riparian sites, was constantly varying as a result of alternating dry and inundation periods, more-frequent measurements may help improve coverage of the high temporal variation in GHG fluxes it caused. Especially for the highly-fluctuating soil CH_4 fluxes, this might improve the accuracy of the soil GHG flux estimates.

Acknowledgements

Appendix

Table A1 Mean ($\pm$SE, $n = 4$) soil physical and biochemical characteristics in the top 10 cm in smallholder oil palm plantations on riparian areas in Jambi province, Indonesia.

Soil characteristics	Management zone		
	Fertilized area	Inter-row	Frond-stacked area
Bulk density (g cm^{-3})	0.9 ± 0.0^b	1.1 ± 0.0^a	0.7 ± 0.0^c
Soil organic C (g C kg^{-1})	35 ± 3^a	36 ± 2^a	54 ± 10^a
Total N (g N kg^{-1})	2.5 ± 0.2^a	3.0 ± 0.2^a	3.7 ± 0.4^a
C : N ratio	13.8 ± 0.6^a	12.2 ± 0.3^a	14.0 ± 0.7^a
Effective cation exchange capacity (mmol$_c$ kg^{-1})	95.9 ± 21.3^a	60.9 ± 2.8^a	89.7 ± 20.5^a
pH (1:4 H$_2$O)	5.5 ± 0.4^a	4.5 ± 0.1^b	4.7 ± 0.1^b
Base saturation (%)	74.5 ± 8.0^a	18.9 ± 5.3^b	47.9 ± 8.7^a
Exchangeable Al (mmol$_c$ kg^{-1})	14.7 ± 3.7^c	45.7 ± 3.9^a	31.7 ± 3.5^b
^{15}N natural abundance (‰)	6.4 ± 0.3^a	5.4 ± 0.3^{ab}	4.4 ± 0.5^b

For each parameter, different letters indicate significant differences between management zones (one-way ANOVA with Tukey's HSD at $p \leq 0.05$).

Figure A1 Stem GHG measurement during an inundation event.

Figure A2 A stem chamber attached to an oil palm stem.

References

Aini, F. K., Hergoualc'h, K., Smith, J. U., & Verchot, L. (2015). Nitrous oxide emissions along a gradient of tropical forest disturbance on mineral soils in Sumatra. *Agriculture, Ecosystems and Environment*, *214*, 107–117. https://doi.org/10.1016/j.agee.2015.08.022

Allen, R. G., Pereira, L. S., Raes, D., & Smith, M. (1998). Crop evapotranspiration - Guidelines for computing crop water requirements. *Irrigation and Drainage Paper No. 56, FAO*, 300. https://doi.org/10.1016/j.eja.2010.12.001

Barba, J., Bradford, M. A., Brewer, P. E., Bruhn, D., Covey, K., Haren, J., … Vargas, R. (2019). Methane emissions from tree stems: a new frontier in the global carbon cycle. *New Phytologist*, *222*(1), 18–28. https://doi.org/10.1111/nph.15582

Barba, J., Poyatos, R., & Vargas, R. (2019). Automated measurements of greenhouse gases fluxes from tree stems and soils: magnitudes, patterns and drivers. *Scientific Reports*, *9*(1). https://doi.org/10.1038/s41598-019-39663-8

Bartlett, K. B., Crill, P. M., Bonassi, J. A., Richey, J. E., & Harriss, R. C. (1990). Methane flux from the Amazon River floodplain: Emissions during rising water. *Journal of Geophysical Research*, *95*(D10), 16773. https://doi.org/10.1029/JD095iD10p16773

Blake, G., & Hartge, K. (1986). Bulk density. In *Methods of soil analysis part 1, physical and mineralogical methods* (pp. 363–375). Madison, WI.

Bowden, W. B., McDowell, W. H., Asbury, C. E., & Finley, A. M. (1992). Riparian nitrogen

dynamics in two geomorphologically distinct tropical rain forest watersheds: subsurface solute patterns. *Biogeochemistry*, *18*(2), 53–75. https://doi.org/10.1007/BF00002703

BPS (Badan Pusak Statistik): Statistical Oce of Jambi Province, available via https://jambi.bps.go.id/ (last access 01.04.2019), 2017.

Bray, R. H., & Kurtz, L. T. (1945). Determination of total, organic, and available forms of phosphorus in soils. *Soil Science*, *59*(1), 39–46. https://doi.org/10.1097/00010694-194501000-00006

Butterbach-Bahl, K., Baggs, E. M., Dannenmann, M., Kiese, R., & Zechmeister-Boltenstern, S. (2013). Nitrous oxide emissions from soils: how well do we understand the processes and their controls? *Philosophical Transactions of the Royal Society B: Biological Sciences*, *368*(1621), 20130122. https://doi.org/10.1098/rstb.2013.0122

Carlson, K. M., Curran, L. M., Asner, G. P., Pittman, A. M. D., Trigg, S. N., & Marion Adeney, J. (2013). Carbon emissions from forest conversion by Kalimantan oil palm plantations. *Nature Climate Change*, *3*(3), 283–287. https://doi.org/10.1038/nclimate1702

Corley, R., & Tinker, P. (2015). *The Oil Palm*. https://doi.org/10.1002/9781118953297

Corre, M. D., Sueta, J. P., & Veldkamp, E. (2014). Nitrogen-oxide emissions from tropical forest soils exposed to elevated nitrogen input strongly interact with rainfall quantity and seasonality. *Biogeochemistry*, *118*(1–3), 103–120. https://doi.org/10.1007/s10533-013-9908-3

Crawley, M. J. (2007). *The R Book*. https://doi.org/10.1002/9780470515075

Davidson, E. A., Keller, M., Erickson, H. E., Verchot, L. V., & Veldkamp, E. (2000). Testing a Conceptual Model of Soil Emissions of Nitrous and Nitric Oxides. *BioScience*, *50*(8), 667. https://doi.org/10.1641/0006-3568(2000)050

Díaz-Pinés, E., Heras, P., Gasche, R., Rubio, A., Rennenberg, H., Butterbach-Bahl, K., & Kiese, R. (2016). Nitrous oxide emissions from stems of ash (Fraxinus angustifolia Vahl) and European beech (Fagus sylvatica L.). *Plant and Soil*, *398*(1–2), 35–45. https://doi.org/10.1007/s11104-015-2629-8

Fiedler, S., & Sommer, M. (2000). Methane emissions, groundwater levels, and redox potentials of common wetland soils in a temperate-humid climate. *Global Biogeochemical Cycles*, *14*(4), 1081–1093.

Food and Agricultural Organization, *FAOSTAT Database*. Retrieved from http://faostat.fao.org *(last access 01.04.2019), 2019*.

Goodrick, I., Nelson, P. N., Nake, S., Webb, M. J., Bird, M. I., & Huth, N. (2016). Tree-scale spatial variability of soil carbon cycling in a mature oil palm plantation. *Soil Research*, *54*(4), 397–406. https://doi.org/10.1071/SR15211

Gregory, S. V, Swanson, F. J., McKee, W. A., & Cummins, K. W. (1991). An ecosystem perspective of riparian zones. *BioScience*, *41*(8), 540–550.

Haag, D., & Kaupenjohann, M. (2002). Landscape fate of nitrate fluxes and emissions in Central Europe. *Agriculture, Ecosystems & Environment*, *86*(1), 1–21. https://doi.org/10.1016/s0167-8809(00)00266-8

Hassler, E., Corre, M. D., Tjoa, A., Damris, M., Utami, S. R., & Veldkamp, E. (2015). Soil fertility controls soil-atmosphere carbon dioxide and methane fluxes in a tropical landscape converted from lowland forest to rubber and oil palm plantations. *Biogeosciences Discussions*, *12*(12), 9163–9207. https://doi.org/10.5194/bgd-12-9163-2015

Hassler, E., Corre, M. D., Kurniawan, S., & Veldkamp, E. (2017). Soil nitrogen oxide fluxes from lowland forests converted to smallholder rubber and oil palm plantations in Sumatra, Indonesia. *Biogeosciences*, *14*(11), 2781–2798. https://doi.org/10.5194/bg-14-2781-2017

Ishizuka, S., Iswandi, A., Nakajima, Y., Yonemura, S., Sudo, S., Tsuruta, H., & Murdiyarso, D. (2005). The variation of greenhouse gas emissions from soils of various land-use/cover types in Jambi province, Indonesia. *Nutrient Cycling in Agroecosystems*, *71*(1), 17–32. https://doi.org/10.1007/s10705-004-0382-0

Itoh, M., Ohte, N., Koba, K., Katsuyama, M., Hayamizu, K., & Tani, M. (2007). Hydrologic effects on methane dynamics in riparian wetlands in a temperate forest catchment. *Journal of Geophysical Research: Biogeosciences*, *112*(1), 1–14. https://doi.org/10.1029/2006JG000240

Jørgensen, B. B. (2006). Bacteria and Marine Biogeochemistry. In *Marine Geochemistry* (pp. 169–206). https://doi.org/10.1007/3-540-32144-6_5

Jourdan, C., & Rey, H. (1997). Architecture and development of the oil-palm (Elaeis guineensis Jacq.) root system. *Plant and Soil*, *189*(1), 33–48. https://doi.org/10.1023/A:1004290024473

Kachenchart, B., Jones, D. L., Gajaseni, N., Edwards-Jones, G., & Limsakul, A. (2012). Seasonal nitrous oxide emissions from different land uses and their controlling factors in a tropical riparian ecosystem. *Agriculture, Ecosystems and Environment*, *158*(3), 15–30. https://doi.org/10.1016/j.agee.2012.05.008

Koehler, B., Corre, M. D., Steger, K., Well, R., Zehe, E., Sueta, J. P., & Veldkamp, E. (2012). An in-depth look into a tropical lowland forest soil: Nitrogen-addition effects on the contents of N2O, CO2 and CH4 and N2O isotopic signatures down to 2-m depth. *Biogeochemistry*, *111*(1–3), 695–713. https://doi.org/10.1007/s10533-012-9711-6

Koehler, B., Corre, M. D., Veldkamp, E., Wullaert, H., & Wright, S. J. (2009). Immediate and long-term nitrogen oxide emissions from tropical forest soils exposed to elevated nitrogen input. *Global Change Biology*, *15*(8), 2049–2066. https://doi.org/10.1111/j.1365-2486.2008.01826.x

König, N., & Fortmann, H. (1996). Probenvorbereitungs-, Untersuchungs und Elementsbestiummungs-Methoden des Umweltanalytik-Labors der Niedersächsischen Forstlichen Versuchsanstalt. In *Berichtendes Forschungszentums Waldökosysteme.* (pp. 1–4). University of Göttingen.

Kotowska, M. M., Leuschner, C., Triadiati, T., Meriem, S., & Hertel, D. (2015). Quantifying above- and belowground biomass carbon loss with forest conversion in tropical lowlands of Sumatra (Indonesia). *Global Change Biology*, *21*(10), 3620–3634. https://doi.org/10.1111/gcb.12979

Kurniawan, S., Corre, M. D., Schulte-Bisping, H., van Straaten, O., Matson, A. L., Utami, S.

R., & Veldkamp, E. (2018). Conversion of tropical forests to smallholder rubber and oil palm plantations impacts nutrient leaching losses and nutrient retention efficiency in highly weathered soils. *Biogeosciences*, *15*(16), 5131–5154. https://doi.org/10.5194/bg-15-5131-2018

Lenhart, K., Behrendt, T., Greiner, S., Steinkamp, J., Well, R., Giesemann, A., & Keppler, F. (2019). Nitrous oxide effluxes from plants as a potentially important source to the atmosphere. *New Phytologist*, *221*(3), 1398–1408. https://doi.org/10.1111/nph.15455

Matson, A. L., Corre, M. D., Langs, K., & Veldkamp, E. (2017). Soil trace gas fluxes along orthogonal precipitation and soil fertility gradients in tropical lowland forests of Panama. *Biogeosciences*, *14*(14), 3509–3524. https://doi.org/10.5194/bg-14-3509-2017

Pangala, S. R., Enrich-Prast, A., Basso, L. S., Peixoto, R. B., Bastviken, D., Hornibrook, E. R. C., … Gauci, V. (2017). Large emissions from floodplain trees close the Amazon methane budget. *Nature*, *552*(7684), 230–234. https://doi.org/10.1038/nature24639

Pangala, S. R., Moore, S., Hornibrook, E. R. C., & Gauci, V. (2013). Trees are major conduits for methane egress from tropical forested wetlands. *New Phytologist*, *197*(2), 524–531. https://doi.org/10.1111/nph.12031

Pennock, D. ., & Corre, M. . (2001). Development and application of landform segmentation procedures. *Soil and Tillage Research*, *58*(3–4), 151–162. https://doi.org/10.1016/S0167-1987(00)00165-3

Pitz, S., & Megonigal, J. P. (2017). Temperate forest methane sink diminished by tree emissions. *New Phytologist*, *214*(4), 1432–1439. https://doi.org/10.1111/nph.14559

R Core Team (2018). *R: A Language and Environment for Statistical Computing. R Foundation for Statistical Computing, Vienna*. Retrieved from http://www.r-project.org

Rusch, H., & Rennenberg, H. (1998). Black alder (Alnus glutinosa (L.) Gaertn.) trees mediate methane and nitrous oxide emission from the soil to the atmosphere. *Plant and Soil*, *201*(1), 1–7. https://doi.org/10.1023/A:1004331521059

Smith, K. A., Ball, T., Conen, F., Dobbie, K. E., Massheder, J., & Rey, A. (2018). Exchange of greenhouse gases between soil and atmosphere: interactions of soil physical factors and biological processes. *European Journal of Soil Science*, *69*(1), 10–20. https://doi.org/10.1111/ejss.12539

Smith, L. K., Lewis, W. M., Chanton, J. P., Cronin, G., & Hamilton, S. K. (2000). Methane emissions from the Orinoco River floodplain, Venezuela. *Biogeochemistry*, *51*(2), 113–140. https://doi.org/10.1023/A:1006443429909

Sotta, E. D., Corre, M. D., & Veldkamp, E. (2008). Differing N status and N retention processes of soils under old-growth lowland forest in Eastern Amazonia, Caxiuanã, Brazil. *Soil Biology and Biochemistry*, *40*(3), 740–750. https://doi.org/10.1016/j.soilbio.2007.10.009

Sung, C. T. B. (2016). Availability, use, and removal of oil palm biomass in Indonesia. *International Council on Clean Transportation*, 1–39. https://doi.org/10.13140/RG.2.1.4697.4485

Swails, E., Hertanti, D., Hergoualc'h, K., Verchot, L., & Lawrence, D. (2019). The response of soil respiration to climatic drivers in undrained forest and drained oil palm plantations

in an Indonesian peatland. *Biogeochemistry*, *142*(1), 37–51. https://doi.org/10.1007/s10533-018-0519-x

Teh, Y. A., Silver, W. L., & Conrad, M. E. (2005). Oxygen effects on methane production and oxidation in humid tropical forest soils. *Global Change Biology*, *11*(8), 1283–1297. https://doi.org/10.1111/j.1365-2486.2005.00983.x

van Straaten, O., Veldkamp, E., & Corre, M. D. (2011). Simulated drought reduces soil CO 2 efflux and production in a tropical forest in Sulawesi, Indonesia. *Ecosphere*, *2*(10), art119. https://doi.org/10.1890/es11-00079.1

Veldkamp, E., Koehler, B., & Corre, M. D. (2013). Indications of nitrogen-limited methane uptake in tropical forest soils. *Biogeosciences*, *10*(8), 5367–5379. https://doi.org/10.5194/bg-10-5367-2013

Vidon, P., Marchese, S., Welsh, M., & McMillan, S. (2015). Short-term spatial and temporal variability in greenhouse gas fluxes in riparian zones. *Environmental Monitoring and Assessment*, *187*(8). https://doi.org/10.1007/s10661-015-4717-x

Welch, B., Gauci, V., & Sayer, E. J. (2019). Tree stem bases are sources of CH4 and N2O in a tropical forest on upland soil during the dry to wet season transition. *Global Change Biology*, *25*(1), 361–372. https://doi.org/10.1111/gcb.14498

Wen, Y., Corre, M. D., Rachow, C., Chen, L., & Veldkamp, E. (2017). Nitrous oxide emissions from stems of alder, beech and spruce in a temperate forest. *Plant and Soil*, *420*(1–2), 423–434. https://doi.org/10.1007/s11104-017-3416-5

Wolf, K., Flessa, H., & Veldkamp, E. (2012). Atmospheric methane uptake by tropical montane forest soils and the contribution of organic layers. *Biogeochemistry*, *111*(1–3), 469–483. https://doi.org/10.1007/s10533-011-9681-0

Yip, D. Z., Veach, A. M., Yang, Z. K., Cregger, M. A., & Schadt, C. W. (2018). Methanogenic Archaea dominate mature heartwood habitats of Eastern Cottonwood (Populus deltoides). *New Phytologist*. https://doi.org/10.1111/nph.15346

3 Soil and stem greenhouse gas fluxes on mineral soils in riparian areas are similar after conversion from forest to smallholder rubber plantations in Sumatra, Indonesia

Josephus Koks, Marife Corre, Olivier van Straaten, Alexander Knohl, Aiyen Tjoa, Edzo Veldkamp

Abstract

Forest-to-agriculture conversion in Sumatra, Indonesia is increasing at a rapid rate, leading to expansion to less-accessible, lower-located zones with high soil moisture content, known as riparian areas. Riparian areas are recognized as biogeochemical hotspots and can emit large quantities of greenhouse gas (GHG) emissions. In this study, we quantified soil and stem GHG fluxes from both forest and rubber plantations on mineral soils in riparian areas in Jambi Province, Indonesia, and assessed their controlling factors.

Over a one-year measurement period, we measured soil and stem GHG fluxes with both soil and stem chambers respectively, from four replicate plots per land-use type.

Soil N_2O emissions were low in both land uses. In soils in the forest, intermediate organic N content (7 – 11 mg N kg^{-1}) and high water-filled pore space (WFPS; >80 %), favored for reduction of N_2O to N_2, whereas in soils in the rubber plantation, low organic N content (4 – 5 mg N kg^{-1}) was limited for N_2O production. Net soil CH_4 emissions in the forest were the result of high soil CH_4 production due to anaerobic soil conditions caused by the high WFPS. In the rubber plantations, better-aerated soil, due to intermediate WFPS, resulted in a net soil CH_4 uptake. Soil CO_2 emissions were relatively low in both land uses due to a WFPS above the optimum for CO_2 production.

Stems contributed for $0.5 \pm 0.2 – 0.7 \pm 0.2$ % of total (soil + stem) N_2O fluxes and for $13.0 \pm 3.0 - 16.1 \pm 5.0$ % of the total CH_4 fluxes. Correlations between stem GHG emissions and soil-air GHG concentrations and vapor pressure deficit ($\rho = 0.49 – 0.70$; $p \leq 0.02$; $n = 24$) suggested transport of soil air within the tree in gaseous or in dissolved form as the main mechanism behind stem-emitted GHG.

Land-use change had a limited effect on GHG fluxes on riparian areas, which might have been a result of the strong, overruling effect that WFPS exerted on GHG fluxes.

Our study highlights that riparian areas are increased GHG emitters compared to well-drained sites, and that stems can be considerable contributors to GHG fluxes. Inadequate

coverage of these factors during GHG flux quantifications might lead to a significant underestimation.

3.1 Introduction

Forest conversion is widespread in Sumatra, Indonesia, where an estimated 70% of the original forest cover was converted to different land uses in 2010 (Margono et al., 2012; Carlson et al., 2013). Of the converted land uses, smallholder rubber cultivation constitutes as one of the most important cash crop systems, with a total plantation area of 3.7 million ha (BPS, 2017). Currently, the massive extent of this land-use change is leading to conversion of less-easily cultivable areas, such as riparian areas.

Riparian areas are the transitional zones between aquatic and terrestrial ecosystems (Gregory, Swanson, McKee, & Cummins, 1991). They intercept and retain nutrients and sediments from upland overland and subsurface runoff. Important ecological functions of riparian areas therefore include carbon (C) storage and removal of nitrogen (N) and phosphorus (P). Mechanisms of N and P removal include biotic uptake, physical adsorption and microbial denitrification (Décamps, Naiman, & McClain, 2009). Such important functions may be lost when natural riparian areas are converted to agriculture (e.g. Merritt & Cooper, 2000; Robertson & Rowling, 2000). Furthermore, riparian areas are also known to be strong greenhouse gas (GHG) emitters, due to increased denitrification and inhibited methane oxidation as a result of permanent high soil moisture content (Audet et al., 2014). Studies conducted on GHG fluxes from riparian areas in the tropics are sparse, even though tropical forests are known to be the single biggest natural source of N_2O (Bouwman, Van der Hoek, & Olivier, 1995). N_2O fluxes were found to be higher from different land uses on riparian areas, than on similar well-drained sites in Puerto Rico (Bowden, McDowell, Asbury, & Finley, 1992) and in Thailand (Kachenchart, Jones, Gajaseni, Edwards-Jones, & Limsakul, 2012). These studies have shown the capacity of riparian areas to be high GHG-emitters.

Conversion of tropical forests to agricultural land uses generally alters soil N-oxide fluxes by affecting soil N availability and aeration as a result of different management practices, which can add and export nutrients as well as compact or loosen the soil (Veldkamp, Purbopuspito, Corre, Brumme, & Murdiyarso, 2008). Converted agricultural land uses without fertilizer application generally experience long-term reductions of soil N-oxide fluxes or show comparable low-level N-oxide fluxes as those from former forests (Hassler, Corre, Kurniawan, & Veldkamp, 2017). Previous research on well-drained sites in our study

area has shown that rubber plantations display a lower soil N availability and fertility than forests (Allen, Corre, Tjoa, & Veldkamp, 2015). Given the limited knowledge on GHG production and consumption on riparian areas in the tropics, it is unclear how land-use change from forest to smallholder rubber plantation will affect GHG fluxes.

Nitrous oxide (N_2O) in tropical land-use systems can be produced by the processes of nitrification and denitrification (Firestone & Davidson, 1989). Seasonal variation is mainly controlled by the amount of soil available nitrogen and the soil water content; high available N leads to higher N_2O fluxes, whereas increasing water content stimulates denitrification and subsequent increased N_2O fluxes (Corre, Sueta, & Veldkamp, 2014; Koehler, Corre, Veldkamp, Wullaert, & Wright, 2009). In forest located on riparian areas, high N input and high soil water content might result in high N_2O fluxes, whereas in rubber plantations, the decrease in N availability after conversion to rubber plantations, might lead to reduced N_2O emissions.

Methane (CH_4) is another important soil GHG, which is consumed by methanotrophic bacteria during utilization as energy source, as well as produced by methanogenic archaea during anaerobic decomposition (Smith et al., 2018). The sum of both processes at the soil-atmosphere interface is therefore known as net soil CH_4 flux. Tropical lowland rainforests on upland mineral soils are usually sinks for CH_4 (e.g. Hassler et al., 2015), whereas wetlands are known to be sources of CH_4 (Kirschke et al., 2013; Z. Wang, Zeng, & Patrick, 1996). Seasonal variation in CH_4 fluxes is usually mainly controlled by soil water content and microbial composition (Verchot, Davidson, Cattânio, & Ackerman, 2000), while spatial variation is usually mainly explained by differences in soil texture: higher clay contents usually result in lower CH_4 uptake (Veldkamp, Koehler, & Corre, 2013). Soils on riparian areas might act as a methane source during anaerobic soil conditions, especially during Sumatra's long wet season (~ 7 – 8 months), and could therefore be a net annual CH_4 source.

The carbon dioxide (CO_2) flux coming from the soil, known as soil respiration, includes root, anaerobic and aerobic microbial respiration (Oertel, Matschullat, Zurba, Zimmermann, & Erasmi, 2016). Soil respiration often shows a quadratic response to soil moisture content, with optimal respiration conditions at a WFPS between 60 and 80 % (Hassler et al., 2015; Matson, Corre, Langs, & Veldkamp, 2017). The high soil moisture content at riparian areas may therefore lead to lower CO_2 emissions compared to well-drained sites, especially during the wet season. Moreover, conversion of riparian areas to rubber

smallholder plantation, known to reduce soil organic matter input (Kotowska, Leuschner, Triadiati, Meriem, & Hertel, 2015), might lead to reduced CO_2 emissions (Sauerbeck, 1993).

Tree stems, next to soils, have also recently been found to emit significant amounts of N_2O and CH_4 in tropical ecosystems (Pangala et al., 2017; Pangala, Moore, Hornibrook, & Gauci, 2013; Welch, Gauci, & Sayer, 2019). Possible mechanisms for stem GHG emissions are 1) transport of soil air via tree roots and stem to stem surface, through xylem sap and/or diffusion in aerenchyma tissue and lenticels (Pangala, Gowing, Hornibrook, & Gauci, 2014; Wen, Corre, Rachow, Chen, & Veldkamp, 2017) and 2) within-stem GHG production by methanogenic archaea residing in anaerobic pores within the stem (Wang et al., 2016; Yip, Veach, Yang, Cregger, & Schadt, 2018). Magnitudes, patterns, and drivers of these GHG fluxes remain poorly understood (Barba et al., 2019), and long-term, frequent measurement and spatial characterization of stem GHG fluxes is necessary. On well-drained soils in Panama, N_2O emissions from a tropical forest were around seven times higher from stems than from soils, and even though soils were net CH_4 consumers, stems showed net stem CH_4 emissions (Welch et al., 2019). Studies conducted on wet soils in the tropics also revealed the relative importance of stem-emitted GHG; in the Amazon floodplains, trees were found to contribute up to 65 % of the total GHG fluxes (Pangala et al., 2017), whereas from peatlands in Borneo, stem-emitted GHG contributed up to 85 % of the total GHG fluxes (Pangala et al., 2013). Variability among tree species and age influences the magnitude of the stem-emitted GHG fluxes (Pangala et al., 2013; Welch et al., 2019). Wood density, lenticel density, transpiration rates and sap flow rates may contribute to these species-level differences (Barba et al., 2019; Covey, Wood, Warren, Lee, & Bradford, 2012; Machacova, Papen, Kreuzwieser, & Rennenberg, 2013; Pihlatie, Ambus, Rinne, Pilegaard, & Vesala, 2005; Warner, Villarreal, McWilliams, Inamdar, & Vargas, 2017).

In this study, we present GHG fluxes from soils (N_2O, CH_4, and CO_2) and stems (N_2O and CH_4) in forest and smallholder rubber plantations on highly weathered Acrisol soils in riparian areas, measured during a year-long, monthly measurement campaign in Jambi, Indonesia. Our aims were to (1) quantify soil and stem GHG fluxes from forest and smallholder rubber plantation on riparian areas, (2) asses their controlling factors and (3) to determine the effect of land-use conversion from forest to smallholder rubber plantation on riparian area on the GHG fluxes. We hypothesized (1) that riparian areas, being hotspots of biogeochemical processes, will have high N_2O, CH_4 and CO_2 fluxes, (2) that tree stems are significantly contributing to the total N_2O and CH_4 fluxes, and (3) that reduced soil organic

carbon and soil mineral nitrogen content after the conversion of forest to rubber plantations on riparian areas will lead to reduced soil GHG production and thus lower soil GHG fluxes.

3.2 Material and methods

3.2.1 Study area and experimental design

Our study area is located in the lowlands (11 − 29 m above sea level) of Jambi province, Sumatra, Indonesia. The climate is humid tropical with a mean annual air temperature of 26.7 ± 1.0 ℃ and mean annual precipitation of 2235 ± 385 mm (data from Jambi Sultan Thaha Airport meteorological station). In the year we measured (2017-2018), the annual rainfall in the region was 2772 mm and the dry season (< 100 mm rainfall month^{-1}) lasted from July to October 2017. In forest and smallholder rubber plantations, we selected riparian study sites bordering small rivers and streams, known to be occasionally flooded during the wet season. On these sites, soil types were classified as acidic clay-loam Stagnosols (29 ± 2 % clay and 44 ± 2 % in the top 1-m depth).

For both land uses, we selected four 50 x 50 m replicate plots. The plots displayed variation in topography, ranging between 0.5 and 3.2 m on plot level. Accordingly, per plot, we installed a total of four to six soil chambers on both higher and lower positions within the plot to measure soil GHG fluxes. In the forest, where tree species differed from each other, we selected ten trees of the most common species per plot to measure stem GHG fluxes. In the rubber plantations, all trees belonged to the same species (*Hevea brasiliensis*) and were comparable in age (8 − 28 years old); therefore we considered six trees per plot sufficient. Trees were selected on higher and lower positions. At 0.1 m away from each tree, a soil gas probe was installed to measure soil-air GHG concentrations at 0.4-m depth. We collected GHG samples on a monthly base for 1 year from March 2017 to February 2018.

Additionally, we measured stem GHG emissions as a function of height to assess whether they showed trends with stem height. We installed stem chambers at three different heights (~120 m, ~240 m, ~360 m) per tree for a total of three trees per plot in both land uses, which we measured once in both seasons. Also, we assessed stem-emitted CH_4 after latex tapping through cutting the bark, a common management practice in rubber plantations (IRSG, 2010). Cutting might cause internal stress, known to enhance the emission of volatile organic compounds (Loreto, Barta, Brilli, & Nogues, 2006), and might have the same effect on CH_4 production. We measured stem CH_4 emissions at 1 hour before and 1, 3 and 5 hours after tapping. Furthermore, we assessed diurnal variation in stem GHG fluxes by measuring

stem GHG emissions from three rubber trees on a 2-hour interval for 26 hours. Due to access restrictions, we could not conduct the same experiment in the forest.

3.2.2 Soil and stem GHG flux measurement and auxiliary measurements

We measured soil GHG fluxes using static chambers, described in our earlier works (Corre et al., 2014; Hassler et al., 2015). Soil chambers were permanently installed at 0.02 m depth. The chambers were closed with a polyethylene lid during measurement, enclosing a volume of ~ 12 L air. To prevent pressure difference during measurement, we left a small ventilation channel open at the top of the chamber lid. At 1, 10, 19 and 28 minutes after chamber closure, we collected ~ 23 mL air samples using a syringe and stored them in pre-evacuated 12-mL exetainers (Labco Limited, Lampeter, UK).

Stem GHG fluxes were measured simultaneously with soil GHG fluxes using stem chambers, described in our earlier works (Wen et al., 2017). At diameter at breast height, we permanently installed two horizontal, parallel rings of silicon (Otto Seal S110, Hermann Otto GmbH, Fridolfing, Germany) 0.2 m from each other, to create an airtight seal and to ensure chambers were installed at the same height. During each measurement, we wrapped a nalophan plastic with pre-attached sampling port around the stem, and then by using a heat gun, we shrunk the plastic to fit closely around the silicone seal. We then attached foam bands around the silicon and used lashing straps adjust the airtightness of the chamber around the tree. At 0, 20, 40 and 60 minutes after closure, we collected ~23 mL air samples and stored it in pre-evacuated 12-mL exetainers.

Simultaneously to every stem GHG measurement, we collected a ~23 mL soil-air sample at 0.4-m depth from the pre-installed 0.1-cm diameter soil-air probes after removing 5 mL of dead air, as described in our earlier work (van Straaten, Veldkamp, & Corre, 2011). Samples were again stored in 12-mL exetainers.

The exetainers were stored in Indonesia for a maximum of 4 months and then brought to the University of Göttingen for analysis. Upon arrival in the laboratory, we measured the N_2O, CH_4 and CO_2 concentrations in the samples using a gas chromatograph with an electron capture detector and a flame ionization detector (SRI 8610C, SRI Instruments Europe GmbH, Bad Honnef, Germany) and by usage of 3 three different concentrations of standard gases (Deuste Steininger GmbH, Mühlhausen, Germany). We calculated the hourly soil and stem

GHG fluxes from the measured concentration difference over time, after correction with air temperature and pressure. For the permanently wet forest soils, GHG flux rates with signs of occurrence of CH_4 emissions through ebullition (e.g. Chanton & Whiting, 1995) were always carefully removed.

We measured soil factors known to control GHG fluxes simultaneously with GHG measurements. Soil and air temperature were measured close to the chambers with a digital thermometer (GMH 3210, Greisinger Electronics GmbH, Regenstauf, Germany). Air pressure was measured using a digital barometer (GTD 1100, Greisinger Electronics GmbH, Regenstauf, Germany). Water-filled pore space (WFPS) was measured by oven-drying around 100 grams of soil at 105 ℃ for at least 24 hours. Soil ammonium (NH_4^+) and nitrate (NO_3^-) were measured by adding ~ 100 grams of fresh soil to prepared bottles containing 150 mL 0.5 M K_2SO_4 solution. Soil was collected at representative chambers and trees and then pooled into two composite samples; one from higher and one from lower plot positions. The bottles containing the soil extracts were cooled until arrival in a field laboratory (maximum 4 hours later), shaken for 1 hour, filtered through K_2SO_4 pre-washed filter papers and then directly frozen. The frozen extracts were sent to Germany for measurement of NO_3^- and NH_4^+ concentrations using continuous flow injection colorimetry (SEAL Analytical AA3, SEAL Analytical GmbH, Norderstedt, Germany).

Soil biochemical and physical characteristics were determined from soil samples, collected with a soil auger in the top 0.1 m in 5 subplots per plot. We measured soil organic C and total N concentrations from air-dried, sieved (2 mm) and ground samples in a CN analyzer (Vario EL Cube, Elementar Analysis Systems GmbH, Hanau, Germany). We calculated the effective cation exchange capacity (ECEC) by measuring exchangeable cations (Ca, Mg, K, Na, Al, Fe and Mn) from air-dried, sieved soil samples after percolation with unbuffered 1 M L $^{-1}$ NH_4CL in an inductively coupled plasma-atomic emission spectrometer (ICP-AES; iCAP 6300 Duo VIEW ICP Spectrometer, Thermo Fischer Scientific GmbH, Dreieich, Germany). We measured ^{15}N natural abundance signatures from ground soil samples by using isotope ratio mass spectrometry (Delta Plus, Finnigan MAT, Bremen, Germany). We calculated base saturation as percentage exchangeable base cations of the ECEC. The soil texture was measured using the pipette method (König & Fortmann, 1996). The soil bulk density was measured from a soil pit dug next to the plot, using the core method (Blake & Hartge, 1986).

3.2.3 Annual flux rate calculations

Annual soil GHG fluxes were calculated on plot level by using the trapezoid rule between monthly measured soil GHG fluxes, after area-weighting the average GHG fluxes from the two micro-topography classes, if a significant difference existed. Per plot, the micro-topography was determined by measuring height differences between grid points placed at every 5 x 5 m in the plot, so that we were able to carefully calculate the amount of flooding in the plot. The interpolation between measurement days of soil GHG fluxes was further supported by determining the periods inundation took place (recorded whenever this occurred during a measurement day), based on the continuous measurements of groundwater level at the centre of each plot (Orpheus Mini Water level Logger, OTT HydroMet, Loveland, US) and the rainfall data measured at a maximum of 20 km from the plots.

Annual stem GHG emissions were calculated in two steps. First, for every tree, we interpolated the stem GHG emissions from 1.20 m stem height to the entire stem. We found the relationship between stem GHG emission and height to be best described by logarithmic formulas, which showed stem GHG emission occurred up to a stem height of ~ 3 m. Entire stem-based GHG emissions were then calculated using 0.2-m intervals based on a conical cylinder as described in our earlier study (Wen et al., 2017). Secondly, we used the trapezoid rule between plot averages of monthly measured stem GHG fluxes, using the same method as described for the soil GHG flux calculations. The interpolation between measurement days of stem GHG emissions was again further aided by information about the duration of inundation events with reference to groundwater level and rainfall data.

3.2.4. Statistical analysis

Linear mixed-effect (LME) models were used for time-series data (soil and stem GHG fluxes, soil-air GHG concentrations, and controlling factors) in order to determine differences in soil and stem GHG fluxes between land uses and between seasons and the two micro-topography classes for both land uses separately. In the LME we used land use or micro-topography as a fixed effect and replicate plot and measurement day as a random effect. Fixed parameters were first tested for normal distribution (Shapiro-Wilk's test) and equality of variance (Levene's test), and a logarithmic or square root transformation was applied when these assumptions were not met. Then, we added either a variance function that allows different variances of the response variable for the fixed effects and/or a first-order temporal autoregressive process that assumes a decreasing correlation between measurement days with

increasing time distance (Crawley, 2007). Finally, the Akaike information criterion was used to determine the best fitting LME. Tukey's HSD test was used to determine differences among fixed effects. For the annual soil and stem GHG fluxes, Levene's test was used on the calculated annual averages on plot level to determine differences between both land uses.

We used Spearman's rank correlation test to assess both temporal and spatial relationships of soil and stem GHG fluxes with soil factors subject to temporal variation (WFPS, soil temperature, soil mineral N content, soil-air GHG concentrations and VPD) as well as soil biochemical and physical characteristics subject to spatial variation (bulk density, soil organic C, total N content, C:N ratio, pH, ECEC, base saturation, Al content and ^{15}N natural abundance). For the relationship between soil and stem GHG fluxes and the soil factors (temporal variation), we used the means of the higher and lower positions from the 4 replicate plots per land use, on each measurement day across 12 monthly measurements ($n = 24$). For the correlation test between stem fluxes and VPD, we used the four replicate plots per land use, across five monthly measurements when VPD data were available ($n = 20$). For the correlation test between stem fluxes and DBH, we used the annual GHG emissions per tree ($n = 40$ in the forest, $n = 24$ in the rubber plantations). For the relationship between soil and stem GHG fluxes and the soil biochemical and physical characteristics (spatial variation) we used the mean annual soil and stem GHG fluxes of the higher and lower positions of every replicate plot per land use ($n = 8$). For the soil CO_2 fluxes, we conducted regression analysis for the parabolic relationship with the WFPS using the monthly plot means, as only limited correlations with soil factors were found.

We considered differences in fixed effects and correlation coefficients statistically significant at $p \leq 0.05$; except for specified parameters, where we indicated marginally significance at $p \leq 0.09$. We conducted all statistical analyses in R 3.5.0 (R Core Team, 2018).

3.3 Results

3.3.1 Soil characteristics

Bulk density increased after forest-to-rubber-plantation conversion, although only marginally significantly ($p = 0.08$; Table 1). Furthermore, conversion of forest to rubber plantation led to a loss of soil organic C and total N, a decrease in C:N ratio and effect cation exchange capacity (ECEC), but an increase in pH and ^{15}N natural abundance (Table 1). The water-filled pore space (WFPS) did not differ between forest and rubber plantations in both seasons, but mineral N content was higher in the forest than in the rubber plantations (Table 2).

Table 1 Means ($\pm$SE, $n = 4$) of soil biochemical and physical characteristics in the top 0.1 m in forest and smallholder rubber plantations on riparian areas in Jambi province, Indonesia.

Soil characteristics [a]	Land use	
	Forest	Rubber plantation
Bulk density (g cm^{-3})	0.7 ± 0.1^a	1.1 ± 0.1^a
Soil organic C (g C kg^{-1})	9.2 ± 2.6^a	2.4 ± 0.2^b
Total N (g N kg^{-1})	5.3 ± 1.3^a	2.0 ± 0.1^b
C:N ratio	16.4 ± 0.7^a	12.0 ± 0.5^b
pH (1:4 H_2O)	3.9 ± 0.1^b	4.4 ± 0.1^a
ECEC (mmol$_c$ kg^{-1})	87.9 ± 3.7^a	61.4 ± 2.2^b
Base saturation (%)	8.9 ± 2.0^a	17.5 ± 5.5^a
Al (mmol$_c$ kg^{-1})	66.0 ± 1.1^a	47.5 ± 3.3^a
^{15}N natural abundance (‰)	3.9 ± 0.2^b	5.5 ± 0.3^a
Clay content (0 – 1 m) (%)	30 ± 4^a	27 ± 2^a

[a] For each parameter, different letters indicate significant differences between land-use types (one-way ANOVA with Tukey's HSD at $p \leq 0.05$).

3.3.2 Soil and stem greenhouse gas emissions

We measured continuous soil and stem N_2O emissions, as well as elevated soil-air N_2O concentrations from both forest and rubber plantations (Fig. 1), throughout the year. Soil N_2O emissions did not differ between the forest and rubber plantations ($p \geq 0.41$; Table 2). Moreover, we did not detect any differences in soil N_2O emissions between dry and wet season in both land uses ($p \geq 0.15$; Table 2, Fig. 1a). Soil N_2O emissions were higher from lower than from higher positions in both forest and rubber plantations ($p \leq 0.03$; results not shown). In both land uses, annual stem N_2O emissions were only a small fraction of the annual soil N_2O emissions (> 5 %; Fig. 1a,b) and in the dry season, stem N_2O emissions were close to undetectable (though higher than zero; one-sample t-test at $p < 0.01$). Stem N_2O emissions were comparable between the land uses ($p > 0.38$; Fig. 1b). In the rubber plantations, stem N_2O emissions were higher in the wet season than in the dry season ($p < 0.01$; Table 2, Fig. 1b); this difference was only marginally significant in the forest ($p = 0.06$; Table 2). The highest stem N_2O emissions were measured at the higher positions in the forest, but at the lower positions in the rubber plantations ($p > 0.01$; results not shown). In both land uses, stem emissions were higher during inundation events ($p > 0.01$; results not shown). Stem N_2O emissions showed a clear decrease over stem height in both land uses (Fig. 2). In the forest, we did not detect differences in stem N_2O emissions between the different tree species ($p > 0.33$; Table A2) although some species seemed to be larger N_2O emitters; high

temporal and spatial variation might explain the absent significant differences. Diameter at breast height (DBH) correlated with stem N_2O emissions in the forest, where stems with a DBH between 0.2 and 0.4 m were emitting less N_2O than stems with a DBH > 0.4 m ($p <$ 0.01; Fig. A1a). In the rubber plantations, there was no difference detected between DBH classes ($p = 0.95$; results not shown). The increase in stem N_2O emissions over the course of the day in the rubber plantations was not significant (P = 0.23; Fig. 3), and diurnal variation was not considered during upscaling to annual stem N_2O fluxes (see section 2.2.3). Annual soil and stem N_2O emissions (Table 3) accounted for 99.5 ± 0.2 and 0.5 ± 0.2 % of the total (soil + stem) N_2O fluxes in the forest, and for 99.3 ± 0.2 % and 0.7 ± 0.2 % of the total N_2O fluxes in the rubber plantations.
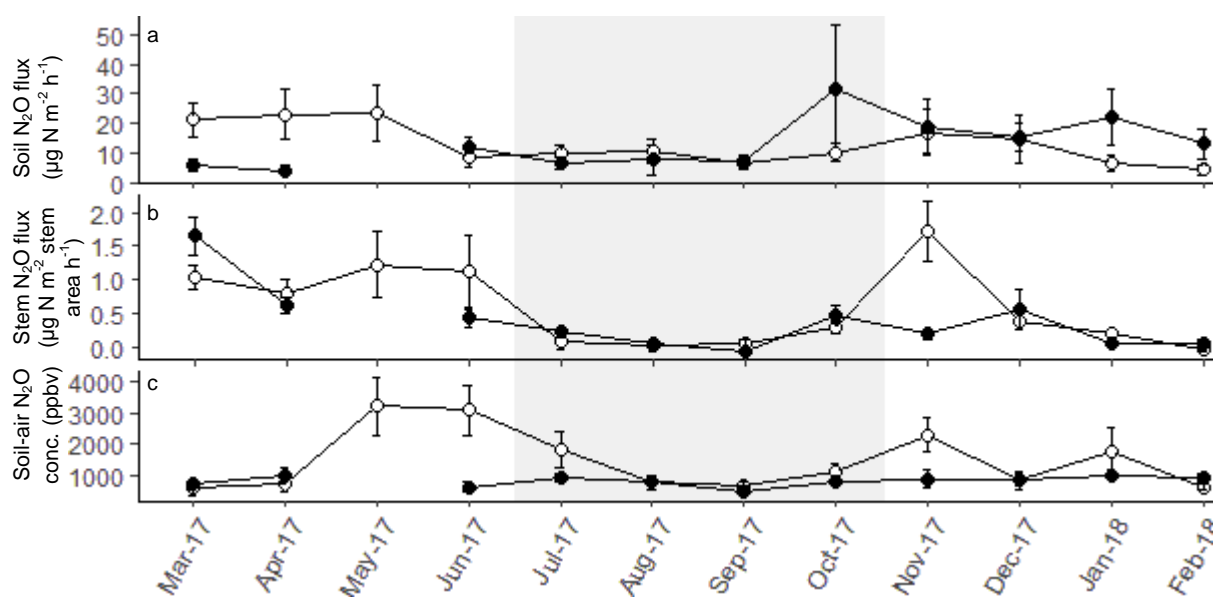
Figure 1 Mean (± SE, $n = 4$ sites) (a) soil and (b) stem N_2O fluxes and (c) soil-air N_2O concentrations at 0.4-m depth, measured from March 2017 to February 2018 in forest (⊖) and smallholder rubber plantations (⬤) on riparian areas in Jambi province, Indonesia. Gray shadings mark the dry season.

In both land uses, we measured alternating soil CH_4 uptake and emission in the dry season, whereas in the wet season we solely measured soil CH_4 emissions (Table 2, Fig. 4a). Soil CH_4 fluxes but did not differ between the land uses ($p = 0.15$) and were higher in the wet than in the dry season ($p \leq 0.04$). Micro-topography did not influence soil CH_4 emissions in the forest ($p = 0.30$; results not shown), but in the rubber plantations, soil CH_4 fluxes were higher from lower positions than from higher positions ($p < 0.01$; results not shown). Interpolation to annual soil CH_4 fluxes (see methods 2.2.3) showed net annual emission in the forest, but net annual uptake in the rubber plantations, although this difference was not significant ($p = 0.16$; Table 3). Stems in both the forest and rubber plantations were consistently emitting CH_4, and these emissions were higher in the wet than in the dry season

Table 2 Means (±SE, $n = 4$) of greenhouse gas fluxes (from soil and stem) and their controlling soil factors (measured in the top 0.05-m depth) in forest and smallholder rubber plantations on riparian areas in Jambi province, Indonesia.

Land use/ Season [a]	Soil flux			Stem flux		Controlling factors		
	N_2O (μg N m^{-2} h^{-1})	CH_4 (μg C m^{-2} h^{-1})	CO_2 (mg C m^{-2} h^{-1})	N_2O (μg N m^{-2} stem h^{-1})	CH_4 (μg C m^{-2} stem h^{-1})	Water-filled pore space (%)	NH_4^+ (mg N kg^{-1})	NO_3^- (mg N kg^{-1})
Forest								
Dry	12.9 ± 5.5^{Aa}	5.8 ± 24.7^{Ab}	137.5 ± 8.1^{Ba}	0.17 ± 0.04^{Ab†}	4.7 ± 2.3^{Ab}	81.6 ± 2.4^{Ab}	6.3 ± 0.6^{Ab}	0.48 ± 0.09^{Aa}
Wet	13.5 ± 2.4^{Aa}	99.8 ± 69.4^{Aa}	136.2 ± 7.2^{Aa}	0.50 ± 0.07^{Aa†}	23.4 ± 6.6^{Ba}	92.6 ± 1.2^{Aa}	10.6 ± 0.8^{Aa}	0.47 ± 0.10^{Aa}
Rubber plantation								
Dry	17.3 ± 6.3^{Aa}	5.17 ± 12.6^{Ab}	184.1 ± 13.1^{Ab}	0.10 ± 0.04^{Ab}	1.87 ± 0.59^{Ab}	73.8 ± 1.9^{Ab†}	4.0 ± 0.3^{Ba}	0.21 ± 0.03^{Ba}
Wet	19.1 ± 4.1^{Aa}	31.9 ± 15.6^{Aa}	143.5 ± 6.9^{Aa}	0.80 ± 0.12^{Aa}	43.2 ± 12.1^{Aa}	78.9 ± 1.4^{Aa†}	4.6 ± 0.3^{Ba}	0.17 ± 0.04^{Ba}

[a] For each column, different uppercase letters indicate significant differences between land uses and lowercase letters indicate significant differences between seasons for each land-use type (linear mixed-effects model with Tukey's HSD test at $p \leq 0.05$ or marginal significance at $^\dagger p \leq 0.09$).
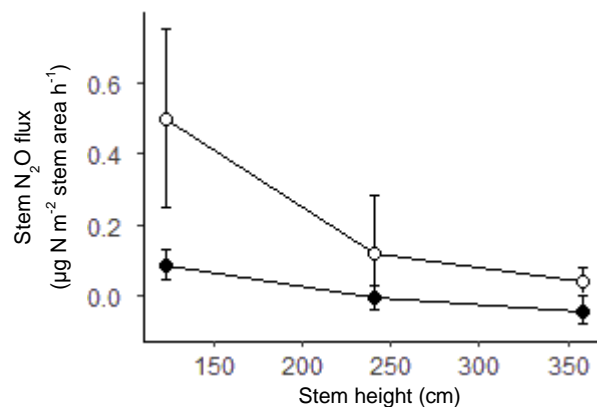
Figure 2 Mean (±SE, $n = 4$ sites) stem N_2O fluxes at three different stem heights during flooded conditions (water-filled pore space = 100 %) measured between March 2017 and February 2018 in forest (⊖) and smallholder rubber plantations (●).
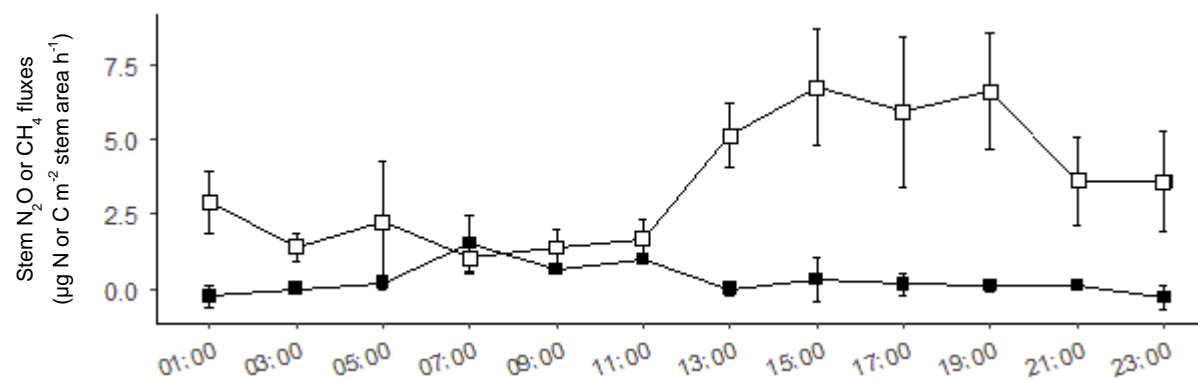
Figure 3 Mean stem (±SE, $n = 3$ trees) N_2O (⊟) and CH_4 (■) fluxes (μg N/C m^{-2} h^{-1}) measured in a smallholder rubber plantation on riparian area in December 2016, in Jambi province, Sumatra, Indonesia.

($p = 0.03$; Fig. 4b, Table 2). In the dry season, stem CH_4 emissions did not differ between land uses, but in the wet season, the rubber plantations showed higher stem CH_4 emissions than the forest ($p = 0.03$; Table 2). In both land uses, stem CH_4 emissions were higher at lower than at higher positions ($p < 0.01$; results not shown) and were higher during inundation events ($p < 0.01$; results not shown), with average increased emissions of 35 and 24 times the control levels for forest and rubber plantations respectively. Stem-emitted CH_4 decreased over stem height in both land uses (Fig. 5). Stem CH_4 emissions in the forest were highly variable among species, but again, did not differ from each other ($p \geq 0.18$; Table A2). In the forest, stems with a DBH > 0.8 m were emitting less CH_4 than stems with DBH ≤ 0.8 m ($p < 0.01$; Fig. A1b), whereas the rubber trees emitted more CH_4 from a DBH between 0.4 and 0.6 m than a DBH between 0.2 and 0.40 m ($p < 0.01$; Fig. A1b). We did not detect diurnal variation in stem CH_4 fluxes in the rubber plantations ($p = 0.35$; Fig. 3). Stem CH_4 emissions before and after tapping, did not differ ($p = 0.40$; results not shown) and thus did not respond to stress in the form of release of CH_4 as a volatile organic component and a stress effect was therefore not included for upscaling (see section 2.2.3). Total annual stem CH_4 emissions were comparable between forest and rubber plantations ($p = 0.36$; Table 3). Annual soil and stem CH_4 emissions (Table 3) accounted for 87.0 ± 3.0 % and 13.0 ± 3.0 % of the total (soil + stem) CH_4 fluxes in the forest, respectively, and for 83.9 ± 5.0 % and 16.1 ± 5.0 % of the total CH_4 fluxes in the rubber plantations, respectively.

Table 3 Annual soil, stem and total (soil + stem) (mean $\pm$ SE, $n = 4$ sites) N_2O and CH_4 fluxes and soil CO_2 fluxes from forest and smallholder rubber plantations on riparian areas in Jambi province, Indonesia. Extrapolations of soil and stem GHG fluxes to the ground area are described in Method 2.3.

Land use / Greenhouse gas[a]	Component		
	Soil	Stem	Total
Forest			
N_2O (kg N ha^{-1} yr^{-1})	1.1 ± 0.5^A	0.004 ± 0.001^A	1.1 ± 0.5^A
CH_4 (kg C ha^{-1} yr^{-1})	1.7 ± 1.2^A	0.15 ± 0.08^A	1.9 ± 1.2^A
CO_2 (Mg C ha^{-1} yr^{-1})	11.7 ± 0.5^A	-	-
Rubber plantation			
N_2O (kg N ha^{-1} yr^{-1})	0.8 ± 0.3^A	0.005 ± 0.001^A	0.8 ± 0.3^A
CH_4 (kg C ha^{-1} yr^{-1})	-0.5 ± 0.1^A	0.11 ± 0.04^A	-0.44 ± 0.1^A
CO_2 (Mg C ha^{-1} yr^{-1})	12.7 ± 1.3^A	-	-

[a] For each column, same uppercase letters indicate no differences in GHG between land uses (Levene's test at $p \leq 0.05$).

We did not observe a clear seasonal pattern in the monthly measured soil CO_2 emissions ($p = 0.25$; Table 2) in the forest, but soil CO_2 emissions were higher ($p < 0.01$; Table 2) in the dry season than in the wet season in the rubber plantations. Inundation events led to reduced soil CO_2 emissions ($p < 0.01$; data not shown). Micro-topography did not cause significant differences in soil CO_2 emissions in both the forest and rubber plantations ($p \geq 0.12$; results not shown).
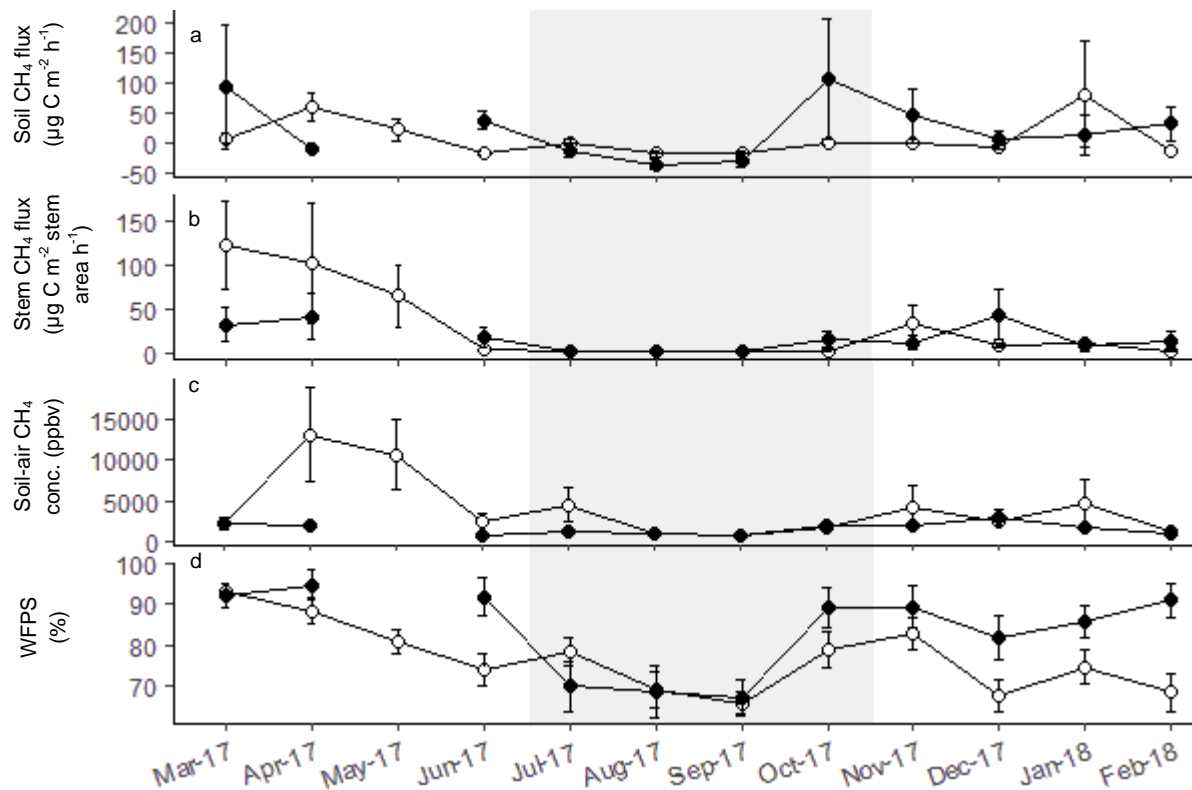
Figure 4 Mean ($\pm$SE, $n = 4$ sites) (a) soil and (b) stem CH_4 fluxes, (c) soil-air CH_4 concentrations at 0.4-m depth, and (d) water-filled pore space (WFPS, at 0.05-m depth), measured from March 2017 to February 2018 in forest (⊖) and smallholder rubber plantations (●) on riparian areas in Jambi province, Indonesia. Gray shadings mark the dry season.

3.3.3 Seasonally controlling factors

The WFPS was higher in the wet season than in the dry season in the forest ($p < 0.01$; Table 2); in the rubber plantations, this seasonal variation was marginally significant ($p = 0.09$; Table 2). WFPS was higher at lower positions than at higher positions in both land uses ($p \leq 0.04$; results not shown). Soil NH_4^+ content was higher in the wet season in the forest ($p = 0.04$; Table 2), but did not differ between seasons in the rubber plantations ($p = 0.68$; Table 2). Soil NO_3^- content did not differ between seasons in both land uses ($p \geq 0.64$; Table 2) and neither was there seasonal difference in soil temperature ($p \geq 0.10$; results not shown).

Figure 5 Mean (±SE, n = 4 sites) stem CH_4 emissions at three different stem heights during flooded conditions (water-filled pore space = 100 %) measured between March 2017 and February 2018 in forest (⊖) and smallholder rubber plantations (●) on riparian areas in Jambi province, Indonesia.

Soil N_2O emissions did not correlate with soil factors subject to temporal variation (WFPS, soil mineral N, soil temperature; $p \geq 0.21$; Table 4) in the forest. In the rubber plantations,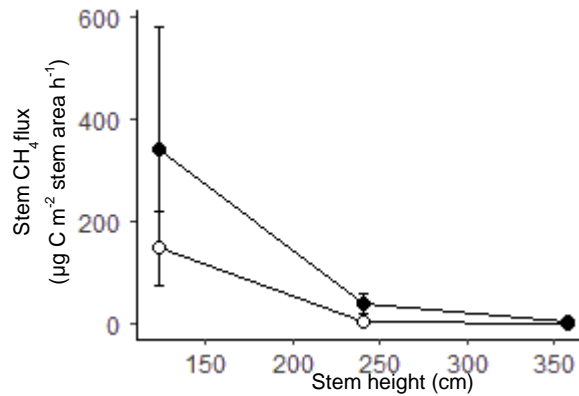 the soil N_2O emissions showed a strong correlation with the WFPS ($p < 0.01$; Table 4) but did not correlate with mineral N or soil temperature ($p \geq 0.16$; Table 4). In the forest, stem N_2O emissions strongly correlated with VPD ($p = 0.01$; Table 4), but did not show correlations with soil-air N_2O concentrations ($p = 0.37$; Table 4). Stem N_2O emissions in the rubber plantations were positively correlated with the soil-air N_2O concentrations ($p = 0.02$; Table 4), but not with the VPD ($p = 0.83$; Table 4). Furthermore, stem N_2O fluxes positively correlated with DBH in both land uses ($p < 0.04$; Table 4).

The WFPS was the most important controlling factor for both soil and stem CH_4 fluxes from both land uses as shown by the strong correlations (all $p < 0.01$; Table 4). Soil CH_4 emissions did not correlate with soil NH_4^+ and NO_3^- content in neither forest ($p \geq 0.67$; results not shown), nor rubber plantations ($p \geq 0.85$; results not shown). In the forest, stem CH_4 emissions did neither correlate with VPD ($p = 0.73$), nor with soil-air concentrations ($p = 0.37$; Table 4); in the rubber plantations stem CH_4 emissions did not correlate with VPD either ($p = 0.92$) but correlated with the soil-air concentrations ($p < 0.01$; Table 4). Stem CH_4 emissions positively correlated with DBH in the rubber plantations ($p = 0.07$; Table 4), but not in the forest ($p = 0.32$; Table 4).

In both land uses, soil CO_2 emissions were mainly controlled by the WFPS, following an exponential relationship (forest: $y = -0.11\ x^2 + 16\ x - 428$, $R^2 = 0.53$, $n = 24$, $p > 0.01$; rubber plantations: $y = -0.16\ x^2 + 23\ x - 643$, $R^2 = 0.45$, $n = 24$, $p > 0.01$; results not shown). Mineral N content did not correlate with soil CO_2 emissions, in both land uses ($\rho = -0.02 - -0.12$, $p \geq 0.73$; results not shown). In the rubber plantations, the correlation between soil CO_2

Table 4 Spearman rank correlation coefficients to assess the temporal patterns of soil and stem N_2O and CH_4 fluxes and soil CO_2 fluxes with the controlling factors, water-filled pore space (WFPS), extractable NO_3^-, soil temperature (all measured within 0.05-m depth), soil-air concentration of greenhouse gases (measured at 0.40-m depth), vapor pressure deficit (VPD) and diameter at breast height (DBH) in forest and smallholder rubber plantations on riparian areas in Jambi province, Indonesia. Correlation tests were conducted using the means for higher and lower positions of the four replicate plots on each measurement period across 12 monthly measurements ($n = 24$); for the correlation test between stem fluxes and VPD, we used the means of the trees per replicate plot and the five months when VPD data were available ($n = 20$); for the correlation test between stem fluxes and DBH, we used the annual GHG emissions per tree ($n = 40$ in the forest, $n = 24$ in the rubber plantations).

Land use / Green-house gas[a]	N_2O					CH_4				CO_2
	WFPS	Soil NO_3^-	Soil-air N_2O	VPD	DBH	WFPS	Soil-air CH_4	VPD	DBH	Soil temp.
Forest										
Soil	0.22	0.03	-0.26	-	-	0.74***	0.26	-	-	-0.08
Stem	-0.06	-0.50	0.22	0.58***	0.42**	0.82***	0.23	-0.09	-0.14	-
Rubber plantations										
Soil	0.70***	-0.16	0.34	-	-	0.68***	0.64***	-	-	0.55***
Stem	0.63***	-0.17	0.49**	-0.07	0.44**	0.75***	0.70***	-0.03	0.39*	-

* $p < 0.09$, ** $p < 0.05$, *** $p < 0.01$.

Table 5 Spearman rank correlation coefficients between annual soil N_2O, CH_4 and CO_2 fluxes and bulk density, soil organic carbon (SOC), total soil nitrogen (total N) and clay content ($n = 8$; 4 plots x 2 micro-topography positions) from forest and smallholder rubber plantations on riparian areas in Jambi province, Indonesia.

Controlling factor	Land use									
	Forest					Rubber plantations				
	Soil N_2O	Stem N_2O	Soil CH_4	Stem CH_4	Soil CO_2	Soil N_2O	Stem N_2O	Soil CH_4	Stem CH_4	Soil CO_2
Bulk density	-0.63*	0.00	-0.34	0.00	0.24	-0.54	-0.54	-0.39	-0.15	-0.73**
SOC	0.22	0.06	0.09	0.60	-0.54**	0.05	-0.16	-0.05	0.19	-0.98***
Total N	0.16	-0.17	-0.06	0.00	-0.27	0.18	0.19	-0.04	0.19	-0.93*
Clay content	-0.54	-0.33	-0.68*	0.00	0.00	-0.64*	-0.63*	-0.39	-0.04	-0.24

* $p < 0.09$, ** $p < 0.05$, *** $p < 0.01$.

emissions and soil temperature ($p < 0.01$; Table 4) rather reflects differences in sampling time during the day than a seasonal pattern, as temperature differences were limited (27.2 ± 0.1 and 28.1 ± 0.2 in the wet and dry season, respectively).

3.3.4 Spatially controlling factors

Soil and stem N_2O fluxes from both the forest and rubber plantations did not correlate with SOC, C:N ratio, total N, ECEC, BS or pH ($p > 0.11$; results not shown). In the forest, soil N_2O fluxes were negatively correlated with bulk density ($p = 0.09$; Table 5). In the rubber plantations, both soil and stem N_2O fluxes were marginally negatively correlated with clay content ($p = 0.09$; Table 5).

Soil CH_4 fluxes from both land uses did not correlate with bulk density, SOC, C:N ratio, total N, ECEC, BS and pH ($p > 0.17$; results not shown). In the forest, the soil CH_4 fluxes were negatively correlated with the clay content of the soil ($p = 0.06$; Table 5), whereas in the rubber plantations no further correlations were found ($p > 0.11$; Table 5, results not shown). Stem CH_4 emissions did not correlate with any of the sampled soil biochemical and physical characteristics ($p > 0.13$; Table 5, results not shown).

Soil CO_2 emissions negatively correlated with bulk density in the rubber plantations ($p < 0.01$; Table 5). The negative correlations between soil CO_2 emissions and soil organic carbon (SOC) in both land uses ($p < 0.04$; Table 5), as well as with total N in the rubber plantations ($p < 0.01$; Table 5), were driven by a correlation with micro-topography: at the lower positions, where SOC and total N were about twice as high (data not shown), soil CO_2 emissions were reduced as a result of high WFPS ($> 80\%$). Soil CO_2 emissions did not show any further correlations with any of the soil biochemical and physical characteristics ($p > 0.10$; Table 5, results not shown).

3.4 Discussion

3.4.1 Soil N_2O, CH_4, and CO_2 fluxes and their controlling factors

In line with our first hypothesis, soil N_2O fluxes from riparian areas were higher compared to the same land uses on well-drained soils. Soil N_2O fluxes from forest on riparian area were slightly higher than annual values reported from the same forest on well-drained Acrisol soils (10 µg N m^{-2} h^{-1}; Hassler, Corre, Kurniawan, & Veldkamp, 2017), similar to five lowland forest sites on Acrisol soils measured once (12 µg N m^{-2} h^{-1}; Ishizuka et al., 2005), but slightly lower than annual values reported from undisturbed forest on Ferralsols (20 µg N m^{-2} h^{-1} Aini,

Hergoualc'h, Smith, & Verchot, 2015), all measured in Jambi province. The mean soil N_2O fluxes from the rubber plantations on riparian areas (Table 2) were around two times higher than annual values measured from rubber plantations on well-drained Acrisol soils (8.6 µg N $m^{-2} h^{-1}$; Hassler et al., 2017) as well as from well-drained Ferralsol soils measured once (12 µg N $m^{-2} h^{-1}$; Aini et al., 2015), and much higher than annual values measured from well-drained sites on Ferralsol soils (1 µg N $m^{-2} h^{-1}$; Ishizuka et al., 2005), all measured in the same study area. Enhanced N_2O emissions from riparian sites in the tropics have been reported before (Bowden et al., 1992; Kachenchart et al., 2012).

In the forest, the absence of seasonal variation in soil N_2O fluxes might be related to the limited seasonal variation in WFPS and soil mineral N (Table 2): permanent near-anaerobic soil conditions in the forest (WFPS > 80 %; Table 2) could have stimulated further reduction of N_2O to N_2 by denitrifying bacteria (Davidson et al., 2000), which has led to low net N_2O emissions, and therefore absent correlations between soil N_2O emissions and both WFPS and mineral N content. In the rubber plantations, the strong correlation between soil N_2O emissions and WFPS ($P < 0.01$; Table 4) suggests the WFPS is the main controlling factor when it is around the optimum for N_2O production (60 - 80 %; Table 2; Davidson et al., 2000). The limited seasonal variation in soil NO_3^- content (Table 2) might explain the absent influence it has on the soil N_2O emissions. The significant effect of micro-topography on soil N_2O emissions might be related to an increased WFPS at lower positions compared to higher positions (results not shown).

Increased bulk density is known to reduce gas diffusivity and thereby enhance anaerobic soil conditions, which usually leads to soil N_2O production (Skiba, Hargreaves, Fowler, & Smith, 1992). In the forest, site-specific, increased bulk density probably led to increased anaerobic soil conditions, which further stimulated reduction of N_2O to N_2 and resulted in the negative correlation between bulk density and soil N_2O emissions (Table 5). The correlation between soil clay content and soil N_2O fluxes is usually positive (Matson, Vitousek, Livingston, & Swanberg, 1990; Sotta, Corre, & Veldkamp, 2008), caused by higher N availability of finer-textured soils, which stimulates soil N_2O emissions. The negative correlation we found in the rubber plantations (Table 5) might have been driven by the negative correlation with WFPS: lower positions with increased clay contents (compared to higher positions; data not reported), had higher WFPS, which stimulated soil N_2O emissions.

In line with our first hypothesis, we measured low soil CH_4 uptake (rubber plantations; Table 3) or even soil CH_4 emissions (forest; Table 3). Soil CH_4 uptake was reported from

well-drained Acrisol soils in the same lowland forest (-1.6 µg C m^{-2} h^{-1}; Hassler et al., 2015) and from logged, old-growth forest on well-drained Acrisol soils in the same area (-21.3 – 4.2 µg C m^{-2} h^{-1}; Ishizuka, Tsuruta, & Murdiyarso, 2002), as well as from rubber plantations on well-drained sites in the same study area (-6 – -10 µg C m^{-2} h^{-1}; Hassler et al., 2015; Ishizuka et al., 2005). The calculated net annual soil CH_4 uptake (Table 3) from the riparian sites is only half as much as from the well-drained sites in the same study area (-0.93 kg C ha^{-1} $year^{-1}$; Hassler et al., 2015).

The WFPS turned out to be the strongest controlling factor on the soil CH_4 fluxes in both land uses (Table 4; Fig. 5a,d); high soil moisture levels can overrule soil mineral N content as the main controlling factor of soil CH_4 fluxes (Koehler et al., 2012). Furthermore, low soil mineral N content might have caused N limitation on methanotrophic activity (Veldkamp et al., 2013) which may have contributed to decreased CH_4 uptake and thus higher net CH_4 emissions. In the rubber plantations, inhibited soil CH_4 uptake or increased soil CH_4 emission at lower positions was the result of increased WFPS (compared to higher positions; results not shown). In the forest, the limited difference in WFPS between lower and higher positions did not lead to differences in soil CH_4 emissions (results not shown).

The negative correlation between soil CH_4 emissions and soil clay content in the forest (Table 5) was found in tropical forests before (summarized by Veldkamp et al., 2013); higher clay content decreases the contribution of larger pores to the porosity of the soil, resulting in decreased soil-air diffusivity and thus CH_4 emissions.

In contrast to our first hypothesis, reported soil CO_2 emissions from riparian sites did not differ from soil CO_2 emissions from the same land uses on well-drained soils. Soil CO_2 emissions reported from lowland forest on well-drained Acrisol soils in the same study area were slightly higher (186 µg C m^{-2} h^{-1}; Hassler et al., 2015, 162 µg C m^{-2} h^{-1}; Ishizuka et al., 2005) than in forest on riparian area (Table 2), whereas soil CO_2 emissions from rubber plantations on well-drained Acrisol soils were slightly lower (75 mg C m^{-2} h^{-1}; Ishizuka et al., 2002) or slightly higher in the wet season (183 mg C m^{-2} h^{-1}; similar in dry season; Hassler et al., 2015) than from rubber plantations on riparian sites (Table 2).

The curvilinear relationship found between soil CO_2 fluxes and WFPS (results not shown), was also reported from other regions in the world (e.g. van Straaten et al., 2011), and shows that soil CO_2 emissions are highest at a WFPS between 50 and 55 %. In both land uses, WFPS was above 55 % (often ≥ 70 %; Table 2, Fig. 4d), which led to moderate soil CO_2

emissions, comparable to well-drained sites (WFPS > 55 %; Hassler et al., 2015). In the forest, the permanently high WFPS might have therefore limited seasonal variation in soil CO_2 emissions, whereas, in the rubber plantations, higher soil CO_2 emissions in the dry season were likely the result of a lower WFPS (Table 2), closer to the optimum for CO_2 production. Soil NO_3^- content, similar between both seasons (Table 2), might have been too low to stimulate soil respiration and subsequent soil CO_2 emissions (e.g. Niu et al., 2010).

The reduced CO_2 emissions in the rubber plantations, as a result of site-specific, decreased bulk density (Table 5), might have been the result of limited gas diffusion coherent to soil compaction (Jensen, McQueen, & Shepherd, 1996). The strong negative correlations between soil CO_2 emissions and SOC and total N concentrations reflected the correlation with WFPS as explained in section 3.3.4.

3.4.2 Stem N_2O and CH_4 emissions and their controlling factors

The mean N_2O emissions we measured from forest and rubber tree stems at riparian areas (Table 2) were lower than those reported from tropical forest stems during the wet season on well-drained soils in Panama ($51 - 759$ µg m^{-2} h^{-1}; Welch, Gauci, & Sayer, 2019). Also, the mean stem CH_4 fluxes from forest and rubber plantations (Table 2) were lower than those reported from stems on well-drained tropical forest in Panama during a four-month campaign at the dry-wet interphase ($66 - 76$ µg C m^{-2} h^{-1}; Welch et al., 2019), as well as annual values from tree stems in Amazonian floodplain forest ($33 - 337000$ µg C m^{-2} h^{-1}; Pangala et al., 2017), and on the lower end of the range reported from a two-week measuring campaign on forested wetlands on peat in Borneo ($17 - 185$ µg C m^{-2} h^{-1}; Pangala et al., 2015).

In both land uses, the correlations of stem N_2O and CH_4 emissions with WFPS (Table 4) as well as their similarity in temporal patterns with soil N_2O and CH_4 emissions (Fig. 1, 5) and the strong increase during inundation events (data not shown) suggest that these stem-emitted GHG might have, at least partly, originated in the soil. When the soil becomes increasingly anaerobic, the metabolic process from soil microorganisms changes from aerobic respiration to denitrification and then methane production (Schlesinger and Bernhardt, 2013). Resulting elevated N_2O and CH_4 concentrations in soil pores, lead to enhanced gas diffusion and thus increased transport (via solution in xylem sap or via air-filled aerenchyma tissue) within the stem and subsequent release into the atmosphere through stem surfaces (e.g. Wen et al., 2017). In the forest, the positive correlation between stem N_2O emissions and the vapor pressure deficit (VPD; Table 4) supports this claim, as an increasing VPD, known to stimulate

sap flow rates (e.g. Yin et al., 2004), might have caused transport of more dissolved N_2O in soil water, which in turn led to increased N_2O emissions at stem surface. In the rubber plantations, the correlation between both stem N_2O and CH_4 emissions and corresponding soil-air N_2O and CH_4 concentrations (Table 4) further supports the claim stem-emitted GHG were soil-borne (Maier, Machacova, Lang, Svobodova, & Urban, 2018; Wen et al., 2017). Furthermore, the exponential decrease in stem N_2O and CH_4 emissions with stem height in both the land uses (Fig. 2; Fig. 5), suggested stem-emitted GHG were coming from the soil.

In contrast to our second hypothesis, stem N_2O emissions turned out to be negligible for the total (soil + stem) N_2O flux. In the forest, the low stem N_2O emissions, their limited seasonal variation (Table 2), and their subsequent absent correlations with WFPS and N content (Table 4), could be the result of the permanent near-anaerobic soil conditions (mechanism described in paragraph 4.1), given the soil is the source of the stem-emitted N_2O (e.g. Wen et al., 2017). The fact that higher positions showed increased stem N_2O emissions compared to lower positions (results not shown), suggests near-anaerobic conditions (high WFPS) in the lower positions were limiting for stem N_2O emissions, likely as a result of the same mechanism that controlled the soil N_2O emissions (described in 3.4.1). Also in the rubber plantations, the WFPS appeared to be the main controlling factor for stem N_2O emissions, given by 1) the strong correlations they showed with each other (Table 4, Fig. 3), 2) the direct effect of inundation (results not shown) on the soil N_2O emissions, and 3) the higher N_2O emissions coming from lower positions with an optimum WFPS for soil N_2O production.

In line with our second hypothesis, stem CH_4 emissions contributed significantly to the total (soil + stem) GHG fluxes. In both the forest and the rubber plantations, the strong seasonal variation in stem CH_4 emissions (Table 2), the strong correlations with WFPS (Table 4; Fig. 4), and the strong increases during inundation events (results not shown), suggest that soil moisture content is the main controlling factor of stem CH_4 emissions. Transport of soil-air CH_4 is suggested as the mechanism behind stem CH_4 emissions because of the higher stem CH_4 emissions from lower compared to higher positions. The high WFPS at lower positions (results not shown) has led to higher soil CH_4 production, which in turn resulted in increased stem CH_4 emissions.

Higher stem CH_4 emissions from the rubber plantations than from the forest during the wet season (Table 1) might have been the result of differences in tree age and species, factors known to influence stem GHG emissions (Welch et al., 2019; Pangala, Moore, Hornibrook, &

Gauci, 2013). Species may differ in wood density and presence of aerenchyma tissue and lenticels, which is known to control the quantity of stem-emitted GHG (Barba et al., 2019). Furthermore, older and bigger trees have larger and deeper root systems and can therefore access deeper, anaerobic soil layers (Pierret et al., 2016), which are known to have high soil-air GHG concentrations (Koehler et al., 2012). However, as we did not measure species-specific factors as wood density, presence of lenticels and rooting depth, we are not able to determine the cause of the difference in stem-emitted GHG in the wet season, or the similarity in the dry season, between the both land uses.

In the forest, the increase in stem-emitted N_2O with increasing stem diameter at breast height (DBH; Table 4, Fig. A1a), simultaneous to a decrease in stem-emitted CH_4 with increasing stem DBH (Fig. A1b), suggests different mechanisms are responsible for both stem-emitted GHG. A decrease in stem CH_4 emissions with increasing diameter was also reported from tropical forested wetlands on Borneo, Indonesia (Pangala et al., 2013) and was attributed to an increase of wood specific density during the lifespan of a tree, as this might negatively influence within-stem CH_4 production (e.g. less space for methanogenic archaea to reside). Furthermore, stem CH_4 emissions did not show a correlation with VPD (Table 4) and did not show a diurnal pattern in stem CH_4 emissions (Fig. 3). This suggested a limited influence of changes in sap flow, suggesting within-stem CH_4 production was a significant, additional source of stem CH_4 emissions. Stem N_2O emissions, on the contrary, did correlate with VPD (Table 4) and, though not significantly different during measurement, showed a diurnal pattern (Fig. 3), suggesting transport of soil-air as the main stem GHG-emitting mechanism. The positive correlation between stem N_2O emissions and soil clay content in the rubber plantations might have also been driven by the correlation with WFPS (see section 3.4.1), given the soil is indeed the source of stem N_2O emissions.

3.4.3 Effects of land-use conversion

In contrast with our third hypothesis, the conversion of forest to rubber plantations did not lead to significant changes in soil and stem GHG fluxes. This partly contradicted with studies conducted on well-drained sites, which reported comparable soil N_2O emissions, but reduced soil CH_4 uptake and decreased soil CO_2 emissions after conversion from forest to rubber plantations (Aini et al., 2015; Hassler et al., 2015; Hassler et al., 2017).

The strong influence of WFPS on riparian land uses might be a stronger controller of soil GHG fluxes than the spatial variability in soil characteristics, especially in N-limited

land-use systems (Hassler et al., 2017). Furthermore, N-oxide emissions generally account for only a small fraction of soil available N, and with the low initial mineral N content, changes in the N-cycle after land-use conversion might have simply been too low to be detected (e.g. Hassler et al., 2017). Higher ^{15}N natural abundance signatures in the rubber plantations compared to the forest (Table 1) showed that soil organic matter (SOM) was more decomposed, indicating a reduced return of organic matter to the soil (Craine et al., 2015; Tiessen, Karamanos, Stewart, & Selles, 1984). The reduction in SOC (Table 1) did not lead to changes in soil GHG fluxes. Given the low soil mineral N content, rubber plantations were probably N-limited and the SOC content did therefore not directly influence GHG fluxes. Site-specific increase in bulk density negatively controlled soil N_2O emissions in the forest, probably through increased anaerobic conditions. Because of the decrease in WPFS after the conversion to rubber plantations (Table 2), here it might not have had the same effect as it had in the forest (see section 3.4.1). However, the increased bulk density did result in reduced CO_2 emissions, as suggested by the strong negative correlation in the rubber plantations, which is absent in the forest (Table 5). Soil clay content did not differ between forest and rubber plantations (Table 1), and the differences in soil clay content did mainly reflect spatial variability within the plots, rather than between land uses and were thus not related to land-use conversion.

Even though differences in tree species may result in differences in quantities of stem-emitted GHG (Pangala et al., 2013), the conversion of the different forest species to a *Hevea brasiliensis* monoculture did not significantly change net stem N_2O and CH_4 emissions between both land uses (Table 3; see section 3.4.2).

3.5 Conclusions

This study was one of the first to determine soil and stem GHG fluxes from riparian sites in the tropics. The results indicate that riparian areas emit increased quantities of soil GHG compared to well-drained sites and that stems can be considerable contributors to GHG fluxes, especially during and after inundation periods. Soils from forest and rubber plantations on riparian areas emitted almost double rates of N_2O and showed reduced CH_4 uptake (rubber plantations) or even net CH_4 emissions (forest), but soil CO_2 emissions from riparian sites were lower compared to those from well-drained sites. Stems contributed up to $0.5 - 0.7$ % of the total (soil + stem) N_2O emissions and up to $13.0 - 16.1$ % of the total CH_4 fluxes. These percentages might be conservative because we measured only at a height of ~ 1.2 m, though it turned out that stem GHG emissions decrease exponentially over height. Therefore, we

recommend measuring stem GHG emissions at various heights, starting from the stem base, to obtain more detailed information about the relationship between stem GHG emissions and height.

The conversion of forest to rubber plantations exerted limited effects on soil and stem GHG fluxes. The effect of changes in soil characteristics after the conversion from forest to rubber plantations on the GHG fluxes might have been overruled by the strong influence of the high WFPS. Although our study showed that the conversion from forest to rubber plantations did not lead to differences in soil GHG fluxes, it should be kept in mind that GHG production and consumption is only one component in the carbon and nitrogen cycles, and that conversion is known to have a strong impact on other components (e.g. carbon storage, Allen et al., 2015; or nitrogen leaching, Kurniawan et al., 2018). We assume the limited effect of land-use change was specific for the conversion from forest to rubber plantations, because of the specific site conditions (WFPS above the optimum for N_2O production in the forest; low mineral N content in the rubber plantations), and might not represent the effect of land-use conversion to other land-use types on riparian areas in the tropics.

Until now, large GHG contributions from riparian areas, as well as GHG contributions from stems, have rarely been taken into account in soil GHG studies in the tropics. Our study suggested that this can lead to significant underestimation of total GHG fluxes and shows that current protocols for GHG-flux measurements require improvement to capture both the effect of landscape-scale variability on GHG fluxes, as well as contributions from stems, in order to obtain the most accurate soil GHG flux budget.

Acknowledgements

Appendix

Table A1 Age and mean (±SE, $n = 4$) tree density, tree height, basal area, diameter at breast height (DBH) of lowland forest and rubber plantations (with ≥ 0.10-m diameter at breast height) on riparian areas in Jambi province, Sumatra, Indonesia.

Land use	Age range (years)	Tree density (n ha^{-1})	Tree height (m)	Basal area (m² ha^{-1})	DBH (m)	Main species
Forest	Not determined	550	39.4	7.5	0.19	*Elaeocarpus serratus; Macaranga conifera; Pternandra caerulenscens*
Rubber plantation	8 - 27	560	23.2	3.3	0.17	*Hevea brasiliensis*

Table A2 Means (±SE, $n = 4$) of stem greenhouse gas fluxes from different tree species in forest on riparian areas in Jambi province, Indonesia.

Species	Stem GHG fluxes	
	N$_2$O (μg N m^{-2} stem h^{-1})	CH$_4$ (μg C m^{-2} stem h^{-1})
Elaeocarpus serratus	0.14 ± 0.00[A]	5.12 ± 1.44[A]
Macaranga conifera	0.41 ± 0.11[A]	3.13 ± 0.77[A]
Pternandra caerulenscens	0.42 ± 0.09[A]	0.00 ± 0.15[A]

[a] For each column, same uppercase letters indicate no differences in stem GHG between species (linear mixed-effects model with Tukey's HSD test at $p \leq 0.05$).
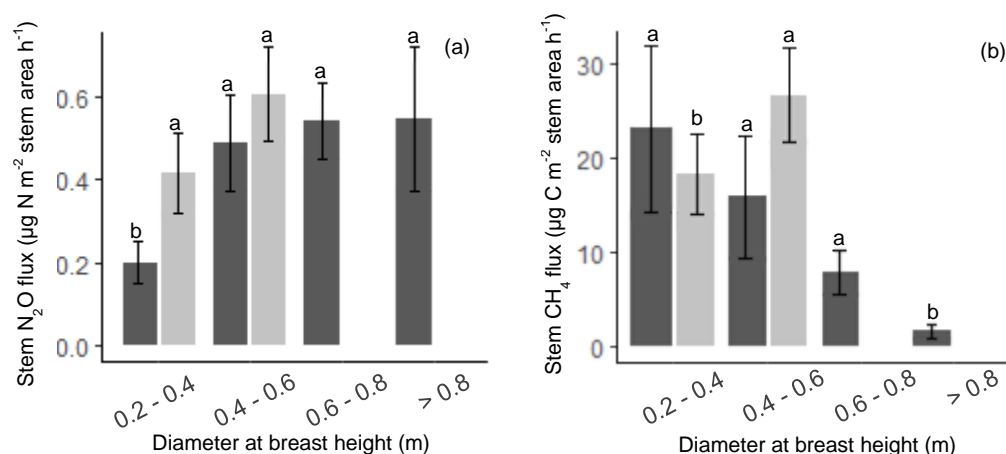
Figure A1 Mean (±SE, $n = 4$ sites) stem (a) N$_2$O and (b) CH$_4$ emissions from stem segments, separated by different classes of diameter at breast height (DBH), measured between March 2017 and February 2018 in forest (dark gray) and smallholder rubber plantations (light gray) on riparian areas in Jambi province, Indonesia. Different lowercase letters indicate significant differences in stem (a) N$_2$O and (b) CH$_4$ emissions between different DBH classes per land use.

References

Aini, F. K., Hergoualc'h, K., Smith, J. U., & Verchot, L. (2015). Nitrous oxide emissions along a gradient of tropical forest disturbance on mineral soils in Sumatra. *Agriculture, Ecosystems and Environment*, *214*, 107–117. https://doi.org/10.1016/j.agee.2015.08.022

Allen, K., Corre, Ma. D., Tjoa, A., & Veldkamp, E. (2015). Soil Nitrogen-Cycling Responses to Conversion of Lowland Forests to Oil Palm and Rubber Plantations in Sumatra, Indonesia. *PLOS ONE*, *10*(7), e0133325. https://doi.org/10.1371/journal.pone.0133325

Audet, J., Hoffmann, C. C., Andersen, P. M., Baattrup-Pedersen, A., Johansen, J. R., Larsen, S. E., … Elsgaard, L. (2014). Nitrous oxide fluxes in undisturbed riparian wetlands located in agricultural catchments: Emission, uptake and controlling factors. *Soil Biology and Biochemistry*, *68*, 291–299. https://doi.org/10.1016/j.soilbio.2013.10.011

Barba, J., Bradford, M. A., Brewer, P. E., Bruhn, D., Covey, K., Haren, J., … Vargas, R. (2019). Methane emissions from tree stems: a new frontier in the global carbon cycle. *New Phytologist*, *222*(1), 18–28. https://doi.org/10.1111/nph.15582

Blake, G., & Hartge, K. (1986). Bulk density. In *Methods of soil analysis part 1, physical and mineralogical methods* (pp. 363–375). Madison, WI.

Bouwman, A. F., Van der Hoek, K. W., & Olivier, J. G. J. (1995). Uncertainties in the global source distribution of nitrous oxide. *Journal of Geophysical Research*, *100*(D2), 2785. https://doi.org/10.1029/94JD02946

Bowden, W. B., McDowell, W. H., Asbury, C. E., & Finley, A. M. (1992). Riparian nitrogen dynamics in two geomorphologically distinct tropical rain forest watersheds: subsurface solute patterns. *Biogeochemistry*, *18*(2), 53–75. https://doi.org/10.1007/BF00002703

BPS (Badan Pusak Statistik): Statistical Oce of Jambi Province, available via https://jambi.bps.go.id/ (last access 01.04.2019), 2017. (n.d.).

Carlson, K. M., Curran, L. M., Asner, G. P., Pittman, A. M. D., Trigg, S. N., & Marion Adeney, J. (2013). Carbon emissions from forest conversion by Kalimantan oil palm plantations. *Nature Climate Change*, *3*(3), 283–287. https://doi.org/10.1038/nclimate1702

Chanton, J. P., & Whiting, G. J. (1995). Trace gas exchange in freshwater and coastal marine environments: Ebullition and transport by plants. In *Biogenic Trace Gases: Measuring Emissions from Soil and Water* (pp. 98–125).

Corre, M. D., Sueta, J. P., & Veldkamp, E. (2014). Nitrogen-oxide emissions from tropical forest soils exposed to elevated nitrogen input strongly interact with rainfall quantity and seasonality. *Biogeochemistry*, *118*(1–3), 103–120. https://doi.org/10.1007/s10533-013-9908-3

Covey, K. R., Wood, S. A., Warren, R. J., Lee, X., & Bradford, M. A. (2012). Elevated methane concentrations in trees of an upland forest. *Geophysical Research Letters*, *39*(15), 1–6. https://doi.org/10.1029/2012GL052361

Craine, J. M., Brookshire, E. N. J., Cramer, M. D., Hasselquist, N. J., Koba, K., Marin-Spiotta, E., & Wang, L. (2015). Ecological interpretations of nitrogen isotope ratios of terrestrial plants and soils. *Plant and Soil*, *396*(1–2), 1–26.

https://doi.org/10.1007/s11104-015-2542-1

Crawley, M. J. (2007). *The R Book*. https://doi.org/10.1002/9780470515075

Davidson, E. A., Keller, M., Erickson, H. E., Verchot, L. V., & Veldkamp, E. (2000). Testing a Conceptual Model of Soil Emissions of Nitrous and Nitric Oxides. *BioScience*, *50*(8), 667. https://doi.org/10.1641/0006-3568(2000)050

Décamps, H., Naiman, R. J., & McClain, M. E. (2009). Riparian Zones. In *Encyclopedia of Inland Waters* (pp. 396–403). https://doi.org/10.1016/B978-012370626-3.00053-3

Firestone, M. K., & Davidson, E. A. (1989). Microbiological Basis of NO and N2O Production and Consumption in Soil. *Exchange of Trace Gases between Terrestrial Ecosystems and the Atmosphere*, 7–21.

Gregory, S. V, Swanson, F. J., McKee, W. A., & Cummins, K. W. (1991). An ecosystem perspective of riparian zones. *BioScience*, *41*(8), 540–550.

Hassler, E., Corre, M. D., Tjoa, A., Damris, M., Utami, S. R., & Veldkamp, E. (2015). Soil fertility controls soil-atmosphere carbon dioxide and methane fluxes in a tropical landscape converted from lowland forest to rubber and oil palm plantations. *Biogeosciences Discussions*, *12*(12), 9163–9207. https://doi.org/10.5194/bgd-12-9163-2015

Hassler, E., Corre, M. D., Kurniawan, S., & Veldkamp, E. (2017). Soil nitrogen oxide fluxes from lowland forests converted to smallholder rubber and oil palm plantations in Sumatra, Indonesia. *Biogeosciences*, *14*(11), 2781–2798. https://doi.org/10.5194/bg-14-2781-2017

IRSG (2010). *Rubber statistical bulletin*. The International Rubber Study Group, Singapore, p1-55.

Ishizuka, S., Iswandi, A., Nakajima, Y., Yonemura, S., Sudo, S., Tsuruta, H., & Murdiyarso, D. (2005). The variation of greenhouse gas emissions from soils of various land-use/cover types in Jambi province, Indonesia. *Nutrient Cycling in Agroecosystems*, *71*(1), 17–32. https://doi.org/10.1007/s10705-004-0382-0

Ishizuka, S., Tsuruta, H., & Murdiyarso, D. (2002). An intensive field study on CO 2 , CH 4 , and N 2 O emissions from soils at four land-use types in Sumatra, Indonesia. *Global Biogeochemical Cycles*, *16*(3), 22-1-22–11. https://doi.org/10.1029/2001GB001614

Jensen, L. S., McQueen, D. J., & Shepherd, T. G. (1996). Effects of soil compaction on N-mineralization and microbial-C and -N. I. Field measurements. *Soil and Tillage Research*, *38*(3–4), 175–188. https://doi.org/10.1016/S0167-1987(96)01033-1

Jørgensen, B. B. (2006). Bacteria and Marine Biogeochemistry. In *Marine Geochemistry* (pp. 169–206). https://doi.org/10.1007/3-540-32144-6_5

Kachenchart, B., Jones, D. L., Gajaseni, N., Edwards-Jones, G., & Limsakul, A. (2012). Seasonal nitrous oxide emissions from different land uses and their controlling factors in a tropical riparian ecosystem. *Agriculture, Ecosystems and Environment*, *158*(3), 15–30. https://doi.org/10.1016/j.agee.2012.05.008

Kirschke, S., Bousquet, P., Ciais, P., Marielle Saunois, J., Canadell, osep G., Dlugokencky, E. J., … Zeng, G. (2013). Three decades of global methane sources and sinks. *Nature*

Geoscience, *6*(10), 813–823. https://doi.org/10.1038/ngeo1955

Koehler, B., Corre, M. D., Steger, K., Well, R., Zehe, E., Sueta, J. P., & Veldkamp, E. (2012). An in-depth look into a tropical lowland forest soil: Nitrogen-addition effects on the contents of N2O, CO2 and CH4 and N2O isotopic signatures down to 2-m depth. *Biogeochemistry*, *111*(1–3), 695–713. https://doi.org/10.1007/s10533-012-9711-6

Koehler, B., Corre, M. D., Veldkamp, E., Wullaert, H., & Wright, S. J. (2009). Immediate and long-term nitrogen oxide emissions from tropical forest soils exposed to elevated nitrogen input. *Global Change Biology*, *15*(8), 2049–2066. https://doi.org/10.1111/j.1365-2486.2008.01826.x

König, N., & Fortmann, H. (1996). Probenvorbereitungs-, Untersuchungs und Elementsbestimmungs-Methoden des Umweltanalytik-Labors der Niedersächsischen Forstlichen Versuchsanstalt. In *Berichtendes Forschungszentums Waldökosysteme.* (pp. 1–4). University of Göttingen.

Kotowska, M. M., Leuschner, C., Triadiati, T., Meriem, S., & Hertel, D. (2015). Quantifying above- and belowground biomass carbon loss with forest conversion in tropical lowlands of Sumatra (Indonesia). *Global Change Biology*, *21*(10), 3620–3634. https://doi.org/10.1111/gcb.12979

Kurniawan, S., Corre, M. D., Schulte-Bisping, H., van Straaten, O., Matson, A. L., Utami, S. R., & Veldkamp, E. (2018). Conversion of tropical forests to smallholder rubber and oil palm plantations impacts nutrient leaching losses and nutrient retention efficiency in highly weathered soils. *Biogeosciences*, *15*(16), 5131–5154. https://doi.org/10.5194/bg-15-5131-2018

Loreto, F., Barta, C., Brilli, F., & Nogues, I. (2006). On the induction of volatile organic compound emissions by plants as consequence of wounding or fluctuations of light and temperature. *Plant, Cell and Environment*, *29*(9), 1820–1828. https://doi.org/10.1111/j.1365-3040.2006.01561.x

Machacova, K., Papen, H., Kreuzwieser, J., & Rennenberg, H. (2013). Inundation strongly stimulates nitrous oxide emissions from stems of the upland tree Fagus sylvatica and the riparian tree Alnus glutinosa. *Plant and Soil*, *364*(1–2), 287–301. https://doi.org/10.1007/s11104-012-1359-4

Maier, M., Machacova, K., Lang, F., Svobodova, K., & Urban, O. (2018). Combining soil and tree-stem flux measurements and soil gas profiles to understand CH4 pathways in Fagus sylvatica forests. *Journal of Plant Nutrition and Soil Science*, *181*(1), 31–35. https://doi.org/10.1002/jpln.201600405

Margono, B. A., Turubanova, S., Zhuravleva, I., Potapov, P., Tyukavina, A., Baccini, A., … Hansen, M. C. (2012). Mapping and monitoring deforestation and forest degradation in Sumatra (Indonesia) using Landsat time series data sets from 1990 to 2010. *Environmental Research Letters*, *7*(3). https://doi.org/10.1088/1748-9326/7/3/034010

Matson, A. L., Corre, M. D., Langs, K., & Veldkamp, E. (2017). Soil trace gas fluxes along orthogonal precipitation and soil fertility gradients in tropical lowland forests of Panama. *Biogeosciences*, *14*(14), 3509–3524. https://doi.org/10.5194/bg-14-3509-2017

Matson, P. A., Vitousek, P. M., Livingston, G. P., & Swanberg, N. A. (1990). Sources of variation in nitrous oxide flux from Amazonian ecosystems. *Journal of Geophysical*

Research, *95*(D10), 16789. https://doi.org/10.1029/JD095iD10p16789

Merritt, D. M., & Cooper, D. J. (2000). Riparian vegetation and channel change in response to river regulation: a comparative study of regulated and unregulated streams in the Green River Basin, USA. *Regulated Rivers: Research & Management*, *16*(6), 543–564. https://doi.org/10.1002/1099-1646(200011/12)16:6<543::AID-RRR590>3.0.CO;2-N

Niu, S., Wu, M., Han, Y., Xia, J., Zhang, Z., Yang, H., & Wan, S. (2010). Nitrogen effects on net ecosystem carbon exchange in a temperate steppe. *Global Change Biology*, *16*(1), 144–155. https://doi.org/10.1111/j.1365-2486.2009.01894.x

Oertel, C., Matschullat, J., Zurba, K., Zimmermann, F., & Erasmi, S. (2016). Greenhouse gas emissions from soils—A review. *Geochemistry*, *76*(3), 327–352. https://doi.org/10.1016/j.chemer.2016.04.002

Pangala, S. R., Enrich-Prast, A., Basso, L. S., Peixoto, R. B., Bastviken, D., Hornibrook, E. R. C., … Gauci, V. (2017). Large emissions from floodplain trees close the Amazon methane budget. *Nature*, *552*(7684), 230–234. https://doi.org/10.1038/nature24639

Pangala, S. R., Gowing, D. J., Hornibrook, E. R. C., & Gauci, V. (2014). Controls on methane emissions from Alnus glutinosa saplings. *New Phytologist*, *201*(3), 887–896. https://doi.org/10.1111/nph.12561

Pangala, S. R., Moore, S., Hornibrook, E. R. C., & Gauci, V. (2013). Trees are major conduits for methane egress from tropical forested wetlands. *New Phytologist*, *197*(2), 524–531. https://doi.org/10.1111/nph.12031

Pierret, A., Maeght, J.-L., Clément, C., Montoroi, J.-P., Hartmann, C., & Gonkhamdee, S. (2016). Understanding deep roots and their functions in ecosystems: an advocacy for more unconventional research. *Annals of Botany*, *118*(4), 621–635. https://doi.org/10.1093/aob/mcw130

Pihlatie, M., Ambus, P., Rinne, J., Pilegaard, K., & Vesala, T. (2005). Plant-mediated nitrous oxide emissions from beech (Fagus sylvatica) leaves. *New Phytologist*, *168*(1), 93–98. https://doi.org/10.1111/j.1469-8137.2005.01542.x

R Core Team (2018). R: A Language and Environment for Statistical Computing. R Foundation for Statistical Computing, Vienna. *Retrieved from http://www.r-project.org*

Robertson, A. I., & Rowling, R. W. (2000). Effects of livestock on riparian zone vegetation in an Australian dryland river. *Regulated Rivers: Research & Management*, *16*(5), 527–541. https://doi.org/10.1002/1099-1646(200009/10)16:5

Sauerbeck, D. R. (1993). CO2-emissions from agriculture: Sources and mitigation potentials. *Water, Air, & Soil Pollution*, *70*(1–4), 381–388. https://doi.org/https://link.springer.com/article/10.1023%2FA%3A1012617516477

Skiba, U., Hargreaves, K. J., Fowler, D., & Smith, K. A. (1992). Fluxes of nitric and nitrous oxides from agricultural soils in a cool temperate climate. *Atmospheric Environment. Part A. General Topics*, *26*(14), 2477–2488. https://doi.org/10.1016/0960-1686(92)90100-Y

Smith, K. A., Ball, T., Conen, F., Dobbie, K. E., Massheder, J., & Rey, A. (2018). Exchange of greenhouse gases between soil and atmosphere: interactions of soil physical factors and biological processes. *European Journal of Soil Science*, *69*(1), 10–20.

https://doi.org/10.1111/ejss.12539

Sotta, E. D., Corre, M. D., & Veldkamp, E. (2008). Differing N status and N retention processes of soils under old-growth lowland forest in Eastern Amazonia, Caxiuanã, Brazil. *Soil Biology and Biochemistry*, *40*(3), 740–750. https://doi.org/10.1016/j.soilbio.2007.10.009

Steinkamp, R., Butterbach-Bahl, K., & Papen, H. (2001). Methane oxidation by soils of an N limited and N fertilized spruce forest in the Black Forest, Germany. *Soil Biology and Biochemistry*, *33*(2), 145–153. https://doi.org/10.1016/S0038-0717(00)00124-3

Tiessen, H., Karamanos, R. E., Stewart, J. W. B., & Selles, F. (1984). Natural Nitrogen-15 Abundance As an Indicator of Soil Organic Matter Transformations in Native and Cultivated Soils. *Soil Science Society of America Journal*, *48*(2), 312–315. https://doi.org/10.2136/sssaj1984.03615995004800020017x

van Straaten, O., Veldkamp, E., & Corre, M. D. (2011). Simulated drought reduces soil CO 2 efflux and production in a tropical forest in Sulawesi, Indonesia. *Ecosphere*, *2*(10), art119. https://doi.org/10.1890/es11-00079.1

Veldkamp, E., Koehler, B., & Corre, M. D. (2013). Indications of nitrogen-limited methane uptake in tropical forest soils. *Biogeosciences*, *10*(8), 5367–5379. https://doi.org/10.5194/bg-10-5367-2013

Veldkamp, Edzo, Purbopuspito, J., Corre, M. D., Brumme, R., & Murdiyarso, D. (2008). Land use change effects on trace gas fluxes in the forest margins of Central Sulawesi, Indonesia. *Journal of Geophysical Research: Biogeosciences*, *113*(G2), n/a-n/a. https://doi.org/10.1029/2007JG000522

Verchot, L. V., Davidson, E. A., Cattânio, J. H., & Ackerman, I. L. (2000). Land-use change and biogeochemical controls of methane fluxes in soils of eastern Amazonia. *Ecosystems*, *3*(1), 41–56. https://doi.org/10.1007/s100210000009

Wang, Z. P., Gu, Q., Deng, F. D., Huang, J. H., Megonigal, J. P., Yu, Q., … Han, X. G. (2016). Methane emissions from the trunks of living trees on upland soils. *The New Phytologist*, *211*(2), 429–439. https://doi.org/10.1111/nph.13909

Wang, Z., Zeng, D., & Patrick, W. H. J. (1996). Methane Emissions from Natural Wetlands. *Environmental Monitoring and Assessment*, *42*, 143–161.

Warner, D. L., Villarreal, S., McWilliams, K., Inamdar, S., & Vargas, R. (2017). Carbon Dioxide and Methane Fluxes From Tree Stems, Coarse Woody Debris, and Soils in an Upland Temperate Forest. *Ecosystems*, *20*(6), 1205–1216. https://doi.org/10.1007/s10021-016-0106-8

Welch, B., Gauci, V., & Sayer, E. J. (2019). Tree stem bases are sources of CH4 and N2O in a tropical forest on upland soil during the dry to wet season transition. *Global Change Biology*, *25*(1), 361–372. https://doi.org/10.1111/gcb.14498

Wen, Y., Corre, M. D., Rachow, C., Chen, L., & Veldkamp, E. (2017). Nitrous oxide emissions from stems of alder, beech and spruce in a temperate forest. *Plant and Soil*, *420*(1–2), 423–434. https://doi.org/10.1007/s11104-017-3416-5

Yin, G., Zhou, G., Morris, J., Huang, Z., Chu, G., & Zhou, G. (2004). Sap flow response of Eucaylyptus (Eucalyptus urophylla) to environmental stress in South China. *Journal of*

Zhejiang University-SCIENCE A, 5(10), 1218–1225. https://doi.org/10.1631/jzus.2004.1218

Yip, D. Z., Veach, A. M., Yang, Z. K., Cregger, M. A., & Schadt, C. W. (2018). Methanogenic Archaea dominate mature heartwood habitats of Eastern Cottonwood (Populus deltoides). *New Phytologist*. https://doi.org/10.1111/nph.15346

4 Variation in annual precipitation results in inter-annual variability in greenhouse gas fluxes from forest converted to smallholder oil palm and rubber plantations on mineral soils in Sumatra, Indonesia

Josephus Koks, Marife Corre, Alexander Knohl, Aiyen Tjoa, Edzo Veldkamp

Summary

Sumatra, Indonesia, is a hotspot for land-use conversion, but information on inter-annual variation in soil greenhouse gas (GHG) fluxes related to this conversion is sparse. In Jambi province, Indonesia, we measured one year of soil N_2O, CH_4 and CO_2 fluxes from forest, oil palm and rubber plantations across two landscapes (clay and loam Acrisol soils) with soil chambers in 2017 and compared these with measurements at the same locations from 2013. In general, annual soil N_2O and CO_2 fluxes were lower in 2017 than in 2013 for most land uses across both landscapes, whereas CH_4 fluxes did not show differences between years. The data suggested that the main driver of these differences was decreased soil moisture content in 2017, as a result of less precipitation. This showed that differences in annual precipitation quantities can lead to different annual soil-emitted GHG fluxes.

Keywords: inter-annual variation; soil trace gasses; N_2O; CH_4; CO_2

Highlights

- Inter-annual variation in soil N_2O, CH_4, and CO_2 (hereafter greenhouse gasses; GHG) fluxes was determined from forest and smallholder oil palm and rubber plantations in Jambi province, Indonesia.
- Long-term studies improve our understanding of the links between soil GHG fluxes and their controlling factors, especially relevant for relatively new land-use systems.
- A decreased amount of precipitation and the subsequent decreased water-filled pore space (WFPS) was the main cause of decreased annual soil GHG fluxes (mainly CO_2) in the second measurement year.
- The occurrence of inter-annual variation in soil GHG fluxes in all three land uses highlighted its importance for long-term GHG flux measurements.

4.1 Introduction

Even though oil palm and rubber plantations currently cover large areas in Sumatra, Indonesia (BPS, 2017), long-term studies quantifying greenhouse gas (GHG) fluxes from these land

uses are sparse. The few extended studies on soil GHG fluxes from oil palm and rubber plantations on mineral soils in Sumatra (Aini, Hergoualc'h, Smith, & Verchot, 2015; Hassler et al., 2015; Hassler et al., 2017) cover a maximum measurement period of 13 months and do not account for inter-annual variation. Long-term studies improve our understanding of the links between soil GHG fluxes and their controlling factors (e.g. Meehl, Branstator, & Washington, 1993). Several studies in the tropics showed that GHG fluxes are strongly influenced by soil moisture content, which varies seasonally and inter-annually as a result of rainfall quantity, suggesting considerable inter-annual variation in GHG fluxes (e.g. Corre, Sueta, & Veldkamp, 2014; Veldkamp, Koehler, & Corre, 2013).

This paper aims to (1) quantify the inter-annual variability in GHG fluxes between two measurement years from smallholder oil palm and rubber plantations after conversion from forest, in Sumatra, Indonesia, and to (2) assess the relative importance of the various climatic and site management factors that drive the reported variability. We hypothesized that 2013s high precipitation quantities (above annual average) led to relatively high GHG fluxes, and that average precipitation quantities in 2017 will therefore result in lower GHG fluxes.

4.2 Materials and methods

This study was conducted in Jambi province, Indonesia, with a mean annual temperature of $26.7 \pm 1.0 \degree C$ and mean annual precipitation of 2235 ± 385 mm. In 2013, annual rainfall in the study region was 3418-3475 mm, whereas, in 2017, annual rainfall was 2772 mm.

We selected two different landscapes, with the same highly weathered Acrisol soil type, but different soil textures: loam and clay. Within each landscape, we selected three land uses: as a reference land use either forest (on the loam Acrisol) or forest infused with rubber trees (hereafter 'forest rubber'; on the clay Acrisol), and as conversion land uses smallholder oil palm and rubber monoculture plantations. Smallholder oil palm plantations received between $48 - 88$ kg N yr^{-1} in both measured years; rubber plantations were unfertilized.

We used the same methods as in 2013 (Hassler et al., 2015; Hassler et al., 2017). In each landscape, for each land use, we selected four 50 m x 50 m replicate plots with four randomly-selected 5 m x 5 m subplots, where we installed one chamber base (0.05 m^2 area) for GHG flux measurement. During each measurement, we covered the chamber bases with vented static polyethylene hoods (total volume of ~12 L). Four gas samples of 23 mL each were taken at 1, 10, 19 and 28 minutes after closure and then injected into pre-evacuated exetainers (Labco Limited, Lampeter, UK). Simultaneously, soil water content (24h oven-dried at 105 ºC, expressed as water-filled pore space using 2.65 g cm^{-3} as particle density and

the measured bulk density) and NH_4^+ and NO_3^- concentrations (0.5 M K_2SO_4 extraction) were determined from one pooled soil sample per plot. Measurements were conducted on monthly (loam Acrisol) or bi-monthly base (clay Acrisol) from March 2017 to February 2018.

In Göttingen, Germany, concentrations of N_2O, CH_4 and CO_2 in the air samples were analyzed using a gas chromatograph with an electron capture detector, flame ionization detector, an autosampler (SRI 8610C, SRI Instruments Europe GmbH, Bad Honnef, Germany) and using three standard gas concentrations (Deuste Steininger GmbH, Mühlhausen, Germany). Mineral N concentrations were determined using continuous flow injection colorimetry (SEAL Analytical AA3, SEAL Analytical GmbH, Norderstadt, Germany).

Hourly soil GHG fluxes were calculated from the linear increase in gas concentration over time after chamber closure, corrected by field-measured air temperature and pressure. Annual GHG fluxes were calculated by interpolating the monthly-averaged GHG flux values on plot level between measurement days, by using the trapezoid rule (Hassler et al., 2015).

We first tested the data for normal distribution (Shapiro-Wilk test) and then assessed differences in annual soil GHG fluxes between years with either paired t-tests (normal distribution) or Wilcoxon signed-ranked test (no normal distribution) on annual soil GHG fluxes on plot level ($n = 8$). Spearman's rank correlation test was used to assess the temporal relationships of soil GHG fluxes with the controlling factors (WFPS, soil temperature, mineral N content) for each landscape and land use, by using the mean on each measurement day across 6 or 12 (bi-) monthly measurements ($n = 6$ or $n = 12$). Differences were considered statistically significant at $p \leq 0.05$ and marginally significant at $p \leq 0.09$. All statistical analyses were conducted using R 3.5.0 (R Core Team, 2018).

4.3 Results

In the clay Acrisol landscape, the annual soil N_2O fluxes in the oil palm plantations were lower in 2017 ($p = 0.02$; Table 1), whereas no difference was detected in the other land uses ($p \geq 0.10$; Table 1); annual soil CH_4 uptake (negative flux) did not differ in any of the land uses ($p \geq 0.37$; Table 1); annual soil CO_2 fluxes were lower in 2017 in both forest rubber ($p = 0.05$; Table 1) and rubber plantations ($p = 0.07$; Table 1) but not in oil palm plantations ($p = 0.86$). In the loam Acrisol landscape, the annual soil N_2O fluxes were lower in the rubber plantations in 2017 ($p = 0.07$; Table 1), but comparable in both other land uses ($p \geq 0.17$; Table 1); annual soil CH_4 uptake was lower in the oil palm plantations in 2017 ($p = 0.01$; Table 1), but did not differ in the forest and rubber plantations ($p \geq 0.47$; Table 1); and annual

soil CO_2 fluxes were lower in 2017 in both the forest and the oil palm plantations ($p \leq 0.02$; Table 1), but not in the rubber plantations ($p = 0.88$; Table 1).

Table 1 Means ($\pm$SE, $n = 4$) of annual greenhouse gas fluxes from soils in forest and smallholder oil palm and rubber plantations on well-drained, mineral soils, as measured in 2012/2013 (Hassler et al., 2015; Hassler et al., 2017) and 2017/2018, in Jambi province, Sumatra, Indonesia.

Landscape/ Land use[a]	Greenhouse gas (unit) / measurement period					
	N_2O (kg N ha^{-1} yr^{-1})		CH_4 (kg C ha^{-1} yr^{-1})		CO_2 (Mg C ha^{-1} yr^{-1})	
	2012/2013	2017/2018	2012/2013	2017/2018	2012/2013	2017/2018
Clay Acrisol soil						
Forest rubber	0.62 ± 0.14^A	0.24 ± 0.09^A	-1.85 ± 0.59^A	-2.30 ± 0.55^A	16.1 ± 0.7^A	14.1 ± 0.9^B
Rubber	0.46 ± 0.21^A	0.19 ± 0.06^A	-0.29 ± 0.12^A	-0.32 ± 0.16^A	$16.1 \pm 1.4^{\dagger A}$	$11.7 \pm 0.8^{\dagger B}$
Oil Palm	1.01 ± 0.25^A	0.22 ± 0.09^B	-0.52 ± 0.26^A	-0.86 ± 0.14^A	9.2 ± 0.6^A	9.5 ± 1.1^A
Loam Acrisol soil						
Forest	0.88 ± 0.15^A	1.24 ± 0.39^A	-0.18 ± 1.55^A	-1.84 ± 0.50^A	16.2 ± 1.2^A	12.6 ± 1.1^B
Rubber	$0.69 \pm 0.17^{\dagger A}$	$0.18 \pm 0.02^{\dagger B}$	-0.93 ± 0.35^A	-0.82 ± 0.24^A	16.5 ± 1.3^A	10.5 ± 1.4^A
Oil Palm	1.13 ± 0.53^A	0.30 ± 0.09^A	-1.38 ± 0.31^A	-0.49 ± 0.31^B	10.3 ± 0.9^A	6.0 ± 0.39^B

[a]Different uppercase letters indicate significant differences in soil GHG fluxes per land use and per landscape between the two measured years (paired t-tests or Wilcoxon test at $p \leq 0.05$ and marginally significant at $^{\dagger}p \leq 0.09$)

In the clay Acrisol landscape, the annual mean WFPS in the oil palm plantations was lower in 2017 ($p = 0.02$; Table 2), whereas in the other land uses there was no difference detected ($p \geq 0.20$; Table 2). In the loam Acrisol landscape, the annual mean WFPS was lower in 2017 in all land uses ($p \leq 0.02$; Table 2). On average, across all landscapes and land uses, WFPS was reduced with 28 ± 2 %, whereas soil NH_4^+ and NO_3^- content and soil temperature did not differ between the two measured years ($p \geq 0.11$; Table 2).

Table 2 Mean ($\pm$SE, $n = 4$ sites) controlling soil factors (measured in the top 0.05-m depth) in forest and smallholder oil palm and rubber plantations on well-drained, mineral soils, as measured in 2012/2013 (Hassler et al., 2015; Hassler et al., 2017) and 2017/2018, in Jambi province, Sumatra, Indonesia.

Landscape/ Land use[a]	Controlling soil factor / measurement period					
	Water-filled pore space (%)		NO_3^- (mg N kg^{-1})		Soil temperature (ºC)	
	2012/2013	2017/2018	2012/2013	2017/2018	2012/2013	2017/2018
Clay Acrisol soil						
Forest rubber	86 ± 5^A	58 ± 2^B	0.2 ± 0.0^A	0.5 ± 0.2^A	26.0 ± 0.3^A	26.4 ± 0.2^A
Rubber	61 ± 7^A	47 ± 3^A	0.1 ± 0.0^A	0.1 ± 0.0^A	27.1 ± 0.2^A	27.8 ± 0.2^A
Oil Palm	73 ± 6^A	56 ± 5^A	1.3 ± 0.9^A	0.2 ± 0.0^A	27.2 ± 0.3^A	27.6 ± 0.3^A
Loam Acrisol soil						
Forest	63 ± 3^A	47 ± 2^B	0.6 ± 0.1^A	0.9 ± 0.1^A	26.0 ± 0.1^A	26.2 ± 0.1^A
Rubber	72 ± 5^A	51 ± 4^B	0.1 ± 0.0^A	0.1 ± 0.0^A	27.4 ± 0.2^A	26.8 ± 0.2^A
Oil Palm	58 ± 6^A	38 ± 4^B	0.8 ± 0.5^A	0.8 ± 0.2^A	27.4 ± 0.2^A	26.7 ± 0.2^A

[a]Different uppercase letters indicate significant differences in controlling soil factors from the same land uses in the same landscapes between the measured years (paired t-tests or Wilcoxon test at $p \leq 0.05$).

The correlation coefficients between the soil N_2O and CO_2 emissions and the controlling factors are rather consistent between the two years (Table A1) and do not show a clear shift. However, the correlation coefficients between soil CH_4 fluxes and the controlling factors showed that the WFPS was a weaker controlling factor: five significant positive correlations were found across landscapes and land uses in 2013, whereas only two of these positive correlations were found in 2017 (Table A1).

4.4 Discussion

Though not pronounced in all landscapes and land uses, an inter-annual trend in soil GHG fluxes was partly detectable: most soil CO_2 fluxes and few soil N_2O emissions decreased between 2013 and 2017 across landscapes and land uses, whereas CH_4 fluxes did not show major changes(Table 1). The WFPS was the only soil factor considerably lower in 2017, showing a significant decrease in four of the six measured landscape / land-use combinations (Table 2), which is in line with the decreased quantity of precipitation in 2017 (see section 4.2). This (partly) confirmed our hypothesis that reduced precipitation quantities in 2017 would lead to decreased soil GHG fluxes. Differences in temperature between the two measured years were too limited to influence GHG fluxes (Table 2) and management practices did not differ between both measured years (see section 4.2).

A mean annual WFPS of around 60 – 80 % (Table 2), as measured in 2013, is known to lead to the highest proportion of N_2O on the total gaseous N created during denitrification processes (Davidson, Keller, Erickson, Verchot, & Veldkamp, 2000). The lower mean annual WFPS in 2017 (below 60%; Table 2) might have resulted in a lower total amount of N_2O produced during denitrification processes in 2017, and therefore lower soil N_2O fluxes in some of the landscape / land use combinations. Two significant correlations between the soil N_2O fluxes and WFPS in two of the six landscape / land use combinations in 2017, compared to no correlations of this kind in 2013, suggested that the WFPS might have indeed been a more limiting factor in 2017 than it was in 2013. This decrease thus resulted in lower soil N_2O emissions.

The reduced average annual soil CH_4 uptake in the oil palm plantations on the loam Acrisol soils (Table 1) might have been the result of N limitation on soil CH_4 production (e.g. Hassler et al., 2015), as the plot that received the highest amount of N-fertilizer ($\sim$ 88 kg N yr^{-1}) showed a net emission of 0.25 kg C ha^{-1} yr^{-1}. The decrease in amount of significant correlations found between soil CH_4 fluxes and the WFPS between 2013 and 2017 in the

different landscape / land-use combinations (five in 2013 compared to two in 2017; Table A1), showed that WFPS was a stronger controller of soil CH_4 fluxes in 2013 and had a less pronounced effect on the soil CH_4 fluxes in 2017. As the WFPS is often known to be the strongest controlling factor of soil CH_4 fluxes (e.g. Hassler et al., 2015) and there was no significant change in the other controlling factors between the two measured years, one would expect the lower WFPS in 2017 to result in lower soil CH_4 fluxes (meaning more CH_4 uptake). The soil CH_4 uptake seems indeed higher in 2017 in most of the landscape / land use combinations, but the difference is not significant as a result of the high spatial variation (high standard error; Table 1).

The mean annual WFPS, as found in 2013, coincides with the range of WFPS percentages (~60 – 80 %) found to result into the highest CO_2 production (e.g. Hassler et al., 2015; Sotta et al., 2007). The lower mean annual WFPS, as found in 2017, might have led to drought stress, resulting in decreased total root respiration and therefore lower soil CO_2 fluxes. The only significant correlation found between the soil CO_2 fluxes and the controlling factors, is one with the WFPS in the oil palm plantation in the loam Acrisol soil in 2017 (Table A1). This correlation is the result of two specific data points, which were measured during precipitation events after fertilizer application and can therefore be disregarded.

In this study, only two different years with a time-gap of four years were compared. This showed us that inter-annual variability in soil GHG fluxes did occur, but the data was not sufficient to determine the relative importance of this inter-annual variability on the long-term soil GHG flux budget of these land uses. Long-term, multiple-year measurements of soil GHG fluxes are recommended to determine the inter-annual variability on the long run.

4.5 Conclusion

This study showed the occurrence of inter-annually variability in soil GHG fluxes in both forest, as well as in oil palm and rubber plantation systems, in Jambi province, Indonesia. A decrease in WFPS resulted in decreased soil CO_2 emissions in most of the landscape / land-use combinations and reduced soil N_2O emissions in a minority of the landscape / land-use combinations. Soil CH_4 fluxes did not differ between the two measured years. To which extend inter-annual variation in soil GHG fluxes influences the soil GHG budget on a multiple-year timescale cannot be concluded from this study. However, its occurrence highlights the importance of long-term measurements for more precise soil GHG flux budget estimations in the tropics.

Acknowledgements

Appendix

Table A1 Pearson or Spearman's rank correlation coefficients (clay: $n = 12$ (2013), $n = 6$ (2017); loam: $n = 12$ (2013 and 2017)) for the temporal patterns of soil N_2O, CH_4 and CO_2 fluxes with water-filled pore space (WFPS), NO_3^- and soil temperature (all measured within 0.05-m depth) in forest converted to smallholder oil palm and rubber plantations on well-drained areas in Jambi province, Indonesia.

Land use	Variable	WFPS		NO_3^-		Soil temp.	
		2013	2017	2013	2017	2013	2017
Clay Acrisol soil							
Forest rubber	Soil N_2O flux	-0.02	0.06	0.15	-0.09	0.11	0.11
	Soil CH_4 flux	0.74***	0.83**	-0.19	0.10	0.49	-0.14
	Soil CO_2 flux	0.21	0.00	0.61**	-0.39	0.38	-0.15
Rubber	Soil N_2O flux	0.03	0.65	0.44	-0.25	0.47	0.67
	Soil CH_4 flux	0.84***	-0.28	-0.52*	0.34	-0.14	-0.08
	Soil CO_2 flux	-0.39	0.09	0.14	0.09	0.49	0.73*
Oil palm	Soil N_2O flux	0.07	0.80*	0.14	-0.04	-0.08	-0.81**
	Soil CH_4 flux	0.69***	0.61	0.13	0.31	-0.09	-0.28
	Soil CO_2 flux	-0.37	-0.02	0.24	-0.65	0.82***	0.71
Loam Acrisol soil							
Forest rubber	Soil N_2O flux	0.25	0.52*	0.32	-0.60*	-0.19	-0.41
	Soil CH_4 flux	0.32	0.41	-0.24	-0.17	0.19	0.47
	Soil CO_2 flux	0.05	0.37	0.23	-0.55*	0.58**	0.16
Rubber	Soil N_2O flux	0.20	0.00	0.10	0.60**	0.43	0.40
	Soil CH_4 flux	0.84***	0.26	-0.11	-0.33	-0.07	-0.73***
	Soil CO_2 flux	-0.54*	0.09	-0.07	0.03	0.16	0.94***
Oil palm	Soil N_2O flux	0.30	0.16	0.57*	0.48	-0.77***	-0.15
	Soil CH_4 flux	0.86***	0.67**	0.17	-0.46	0.16	-0.10
	Soil CO_2 flux	-0.29	0.74***	0.36	-0.31	0.57*	0.19

*$p < 0.09$, **$p < 0.05$, ***$p < 0.01$.

References

Aini, F. K., Hergoualc'h, K., Smith, J. U., & Verchot, L. (2015). Nitrous oxide emissions along a gradient of tropical forest disturbance on mineral soils in Sumatra. *Agriculture, Ecosystems and Environment*, *214*, 107–117. https://doi.org/10.1016/j.agee.2015.08.022

BPS (Badan Pusak Statistik): Statistical Oce of Jambi Province, *available via https://jambi.bps.go.id/ (last access 01.04.2019)*, 2017.

Corre, M. D., Sueta, J. P., & Veldkamp, E. (2014). Nitrogen-oxide emissions from tropical forest soils exposed to elevated nitrogen input strongly interact with rainfall quantity and seasonality. *Biogeochemistry*, *118*(1–3), 103–120. https://doi.org/10.1007/s10533-013-9908-3

Davidson, E. A., Keller, M., Erickson, H. E., Verchot, L. V., & Veldkamp, E. (2000). Testing a Conceptual Model of Soil Emissions of Nitrous and Nitric Oxides. *BioScience*, *50*(8), 667. https://doi.org/10.1641/0006-3568(2000)050

Hassler, E., Corre, M. D., Tjoa, A., Damris, M., Utami, S. R., & Veldkamp, E. (2015). Soil fertility controls soil-atmosphere carbon dioxide and methane fluxes in a tropical landscape converted from lowland forest to rubber and oil palm plantations. *Biogeosciences Discussions*, *12*(12), 9163–9207. https://doi.org/10.5194/bgd-12-9163-2015

Hassler, E., Corre, M. D., Kurniawan, S., & Veldkamp, E. (2017). Soil nitrogen oxide fluxes from lowland forests converted to smallholder rubber and oil palm plantations in Sumatra, Indonesia. *Biogeosciences*, *14*(11), 2781–2798. https://doi.org/10.5194/bg-14-2781-2017

Meehl, G. A., Branstator, G. W., & Washington, W. M. (1993). Tropical Pacific Interannual Variability and CO 2 Climate Change. *Journal of Climate*, *6*(1), 42–63. https://doi.org/10.1175/1520-0442(1993)006<0042:TPIVAC>2.0.CO;2

R Core Team (2018). R: A Language and Environment for Statistical Computing. R Foundation for Statistical Computing, Vienna. *Retrieved from http://www.r-project.org*

Smith, K. A., Dobbie, K. E., Ball, B. C., Bakken, L. R., Sitaula, B. K., Hansen, S., … Orlanski, P. (2000). Oxidation of atmospheric methane in Northern European soils, comparison with other ecosystems, and uncertainties in the global terrestrial sink. *Global Change Biology*, *6*(7), 791–803. https://doi.org/10.1046/j.1365-2486.2000.00356.x

Sotta, E. D., Veldkamp, E., Schwendenmann, L., Guimaraes, B. R., Paixao, R. K., RUIVO, M. de L. P., … Meir, P. (2007). Effects of an induced drought on soil carbon dioxide (CO2) efflux and soil CO2 production in an Eastern Amazonian rainforest, Brazil.

Global Change Biology, *13*(10), 2218–2229. https://doi.org/10.1111/j.1365-2486.2007.01416.x

Veldkamp, E., Koehler, B., & Corre, M. D. (2013). Indications of nitrogen-limited methane uptake in tropical forest soils. *Biogeosciences*, *10*(8), 5367–5379. https://doi.org/10.5194/bg-10-5367-2013

5 Synthesis

5.1 Quantification of annual greenhouse gas fluxes

We quantified annual soil N_2O, CH_4 and CO_2 fluxes (hereafter summarized as GHG) from forest, and smallholder oil palm and rubber plantations on well-drained, mineral loam and clay Acrisol soils, as well as on loam/clay Stagnosol soils on riparian areas (Table 1).

Table 1 Annual soil (mean ± SE, $n = 4$ sites) N_2O, CH_4 and CO_2 fluxes from forest and smallholder oil palm and rubber plantations on riparian areas in Jambi province, Indonesia, measured in 2017/2018.

Land use[a]	Hydrological conditions					
	Well-drained			Riparian		
	N_2O	CH_4	CO_2	N_2O	CH_4	CO_2
	(kg N ha^{-1} yr^{-1})	(kg C ha^{-1} yr^{-1})	(Mg C ha^{-1} yr^{-1})	(kg N ha^{-1} yr^{-1})	(kg C ha^{-1} yr^{-1})	(Mg C ha^{-1} yr^{-1})
	Loam Acrisol / Stagnosol soil					
Forest	1.24 ± 0.39^{Aa}	-1.84 ± 0.50^{Aa}	12.6 ± 1.1^{Ab}	1.0 ± 0.0^{b}	2.6 ± 1.0^{a}	11.7 ± 0.5^{a}
Oil palm	0.30 ± 0.09^{Ab}	-0.49 ± 0.31^{Aa}	6.0 ± 0.39^{Ba}	3.3 ± 0.3^{a}	0.6 ± 0.0^{a}	11.1 ± 0.3^{a}
Rubber	0.18 ± 0.02^{Ab}	-0.82 ± 0.24^{Aa}	10.5 ± 1.4^{Ab}	0.7 ± 0.1^{b}	-0.6 ± 0.1^{a}	12.7 ± 1.3^{a}
	Clay Acrisol soil					
Forest[b]	0.24 ± 0.09^{Ba}	-2.30 ± 0.55^{Aa}	14.1 ± 0.9^{Aa}			
Oil palm	0.22 ± 0.09^{Aa}	-0.86 ± 0.14^{Ab}	9.5 ± 1.1^{Ab}			
Rubber	0.19 ± 0.06^{Aa}	-0.32 ± 0.16^{Ab}	11.7 ± 0.8^{Aab}			

[a] For each column, different uppercase letters indicate significant differences between landscapes and lowercase letters indicate significant differences between land-use types ((Levene's test at $p \leq 0.05$). [b] Forest infused with rubber trees.

5.2 Landscape-scale variability in greenhouse gasses on loam Acrisol soils: well-drained versus riparian

Soil N_2O emissions from forest and smallholder rubber plantations, both unfertilized land-use types with relatively low mineral N availability, were comparable between well-drained and riparian sites. Oil palm plantations, a fertilized land-use type characterized by high available mineral N, showed 3 – 16 times higher soil N_2O emissions at riparian sites than at well-drained sites, as well as an emission factor of 3.9 % compared to 0.9 – 3.3 % (Aini et al., 2016; Hassler et al., 2017). Our study showed that, provided there is sufficient available organic N (substrate of microbial N_2O production, first level of control in hole-in-pipe model, HIP; Davidson et al., 2000) and an intermediate WFPS (second level of control in HIP; optimum between 60 – 80 %), soil N_2O fluxes coming from riparian areas might be enhanced compared to well-drained soils. However, a WFPS above 80 % (as in the forest) can inhibit these enhanced soil N_2O fluxes by subsequent further reduction of N_2O into N_2 (Davidson et

al., 2000), whereas low mineral N availability (as in the rubber plantations) will not lead to enhanced soil N_2O fluxes because of the lack of substrate.

The forest and oil palm plantations on riparian sites, having a relatively high WFPS (> 60 %), turned both out to be net soil CH_4 emitters, whereas on the well-drained sites in the same land uses we measured almost constant soil CH_4 uptake. In the forest, a net annual soil CH_4 emission of 2.6 kg C ha^{-1} yr^{-1} from riparian sites opposed a net annual soil CH_4 uptake of 1.8 or 0.2 kg C ha^{-1} yr^{-1} from well-drained sites (this study; Hassler et al., 2017, respectively). This suggests that when over 40 or 7 % of the forest is located on riparian sites, CH_4 uptake and emission balance each other out, and the forest might turn from a net CH_4 sink into a net CH_4 source. The possible occurrence of CH_4 production in combination with the diffusional limitation on the supply of CH_4 to methanotrophs at high WFPS in the upper soil layers, therewith partially offsetting CH_4 consumption, explains the strong net soil CH_4 emissions from both riparian land uses (Smith et al., 2000). In the rubber plantations, with intermediate WFPS (~ 70 %), soil CH_4 uptake remained larger than soil emission, which resulted in a net annual CH_4 uptake. Our study showed that as a result of high WFPS at riparian sites, soil CH_4 production might be increased, whereas soil CH_4 uptake might be reduced. The resulting net CH_4 emissions suggest that riparian areas are enhanced soil CH_4 emitters.

In all land uses, soil CO_2 emissions were comparable between well-drained and riparian sites. The WFPS was the most important factor that controlled soil CO_2 emissions, following a curvilinear relationship. This curvilinear relationship is also found in other regions in the world and shows the highest soil CO_2 emissions at a WFPS between 50 and 60 % (Matson et al., 1990; Sotta et al., 2008; van Straaten et al., 2011). WFPS was below the optimum of 50 % in the well-drained sites, whereas it was above the optimum of 60 % in riparian sites. This might have been one of the main reasons why soil CO_2 emissions were comparable though hydrological circumstances were not. Variation in temperature was too limited to influence the soil CO_2 emissions, and soil mineral N was too low to significantly control CO_2 emissions (except for in the fertilized zone in the oil palm). Our study showed that, even though the WFPS might be an important controlling factor of soil CO_2 emissions, an increase does not necessarily lead to increased soil CO_2 emissions.

5.3 Inter-annual variation in greenhouse gas emissions

We determined inter-annual variation in GHG fluxes as a result of inter-annual differences in GHG-flux drivers as precipitation (Basso et al., 2016), temperature (Hashimoto et al., 2011)

or management practices (Herbst et al., 2013) by comparing soil GHG fluxes from well-drained soils between 2013 and 2017. We found soil CO_2 emissions decreased in 67 % of the measured plots, and soil N_2O emissions and CH_4 uptake decreased in 17 % of the plots. At the same time, there was no increase in any of the measured GHG fluxes. In 2017, there was 20 % less precipitation, and subsequently, the average WFPS was on average 28 ± 2 % lower across landscapes and land uses. Strong correlation coefficients between the soil GHG fluxes and the WFPS showed that the WFPS was the main factor controlling the soil GHG fluxes in both years. This, in turn, suggested that the decrease in WFPS, as a result of the decrease in annual precipitation, led to the decreases in soil GHG fluxes. Differences in temperature were too limited to influence the GHG fluxes and management practices did not differ between both measured years.

5.4 Mechanisms behind stem-emitted GHG

Several findings in this study suggested that the transport of soil air, entering the tree from the roots and being released at the stem surface, was the main mechanism behind the stem N_2O and CH_4 (summarized as GHG in this paragraph) emissions in our study area. The amount of stem-emitted GHG decreased with stem height following a logarithmic relationship in all three land uses, which suggested stem-emitted GHG entered the tree from the roots, below the soil surface (e.g. Wen et al., 2017). Furthermore, we found several strong correlations between soil-air GHG concentrations at 0.4-m depth and stem GHG emissions at diameter at breast height (DBH, ~1.2 m above the soil surface), suggesting it was the soil air which was emitted at the stem surface. Also, in all three land uses, several strong correlations between stem-emitted GHG and the vapor pressure deficit (VPD), known to stimulate sap flow rates, suggested that an increased rate of sap flow stimulated stem GHG emissions. Additionally, many strong correlations between the stem GHG emissions and the WFPS suggested that changing soil processes, as a result of increased soil moisture content, also directly influenced the stem GHG emissions. As we did not examine production of GHG within the stem (for instance, by methanogenic archaea residing in anaerobic pores within the stem; e.g Yip et al., 2018), we cannot exclude or quantify contributions of this mechanism to the total stem GHG emissions. In the forest, the decreasing stem CH_4 emissions from stems with an increasing DBH were probably the result of decreased within-stem CH_4 production after increasing wood density with tree age. This suggested that stem-emitted CH_4 might be partly produced within stems and that the stem-emitted CH_4 at stem surface could be the net result of both soil-transported and within-stem produced CH_4.

5.5 Contributions from tree stems

We measured consistent N_2O emissions from stems in all three land uses. They were low compared to soil N_2O fluxes, especially in the dry season, but significantly higher than zero (one-sample t-test at $P < 0.01$). In the forest and rubber plantations, stem N_2O emissions accounted for less than 1 % of the total (soil + stem) emitted N_2O (Table 2). Stem N_2O emissions might have been generally low, as a result of low soil mineral N availability. In the oil palm plantations, stem N_2O emissions accounted for 2.8 % (Table 2). The fact that stem N_2O emissions accounted for a higher percentage than in the other land uses, might be related to the high soil mineral N content in the oil palm plantations after fertilization, as stem N_2O emissions clearly increased following fertilization. Furthermore, we measured continuous stem CH_4 emissions, even simultaneously with soil CH_4 uptake. Stem CH_4 emissions accounted for $13 - 16$ % across land uses, which was a significant contribution to the total CH_4 fluxes (Table 2). The higher contributions of stem CH_4 emissions to the total CH_4 fluxes compared to contributions of stem N_2O emissions to the total N_2O fluxes, could be related to difference in uptake processes (in gas or dissolved form) for both GHG, or additional production of CH_4 within the stem (e.g. Yip et al., 2018; see section 5.4).

The stem GHG fluxes in our study area were small compared to other stem GHG fluxes reported from forest ecosystems in the tropics. A study conducted in forest on well-drained, mineral soil in Panama reported stem N_2O flux values of up to ~750 times the values we found (Welch et al., 2019). From a forest on mineral soil on floodplains in the Amazonas, CH_4 flux values of up to ~15000 times the values we found were reported (Pangala et al., 2017). And from a forest on organic peat soils on Borneo, CH_4 flux values of up to ~8 times the values we found were reported (Pangala et al., 2013). Although for the last study, the higher average fluxes can be explained by the permanent wet conditions and the high organic C content of the soil (optimal for CH_4 production; Smith et al., 2000), the high flux differences with the other two studies must have more complex reasons. Both studies measured stem emissions at a lower height ($0.2 - 1.4$ m), whereas we only measured at diameter at breast height (1.4 m). As stem GHG emissions are known to decrease with height (Pangala et al., 2017; Wen et al., 2017), our measurements, therefore, might be conservative. Our relatively low stem GHG fluxes could also be the result of differences in tree architecture between measured tree species. Amount of lenticels, presence of aerenchyma tissue and wood density are characteristics known to influence quantities of stem-emitted GHG (e.g. Barba et al., 2019). Furthermore, clayey soils ($27 - 58$ % clay) in our study area might have inhibited

diffusion of soil-air GHG (e.g. Veldkamp et al., 2013), compared to more sandy soils in the other studies (percentage clay not reported), as their soil GHG were also increased compared to the GHG fluxes we measured. Another reason for the larger quantities of stem-emitted GHG in the other studies might be a significant source of within-stem GHG production (e.g. Yip et al., 2018), which was not present at our sites (see section 5.4).

Table 2 Annual stem GHG gas emissions (mean ± SE, $n = 4$ sites) and the percentage of the total (soil + stem) they account for, from forest and smallholder oil palm and rubber plantations on riparian areas in Jambi province, Indonesia.

Land use[a]	Stem emissions (kg C ha^{-1} yr^{-1})		Percentage total fluxes (soil + stem)	
	N$_2$O	CH$_4$	N$_2$O	CH$_4$
Forest	0.004 ± 0.001[b]	0.150 ± 0.084[a]	0.5 ± 0.2	13.0 ± 3.0
Oil Palm	0.017 ± 0.007[a]	0.099 ± 0.046[a]	2.8 ± 0.8	14.7 ± 5.7
Rubber	0.005 ± 0.001[b]	0.110 ± 0.039[a]	0.7 ± 0.2	16.1 ± 5.0

[a] For each column, different lowercase letters indicate significant differences between land- use types (Levene's test at $p \leq 0.05$).

5.6 Effect of land-use change on GHG fluxes from riparian areas

The most pronounced changes in soil characteristics after the conversion from forest to the plantation types on riparian areas included a decrease in soil organic carbon (SOC), total nitrogen and effective cation exchange capacity (ECEC), as well as an increase in bulk density.

Soil N$_2$O emissions were similar between the forest and the rubber plantations, but higher in the oil palm plantations. A decrease in soil mineral N, as a result of decreased N input through reduced litter input, did not lead to different soil and stem N$_2$O emissions between the forest and rubber plantations on riparian areas: the initial amount of mineral N was relatively low, and frequent flooding events might have led to frequent conversion and therefore loss of recently mineralised nitrogen. The increase in soil N$_2$O emissions in the oil palm plantations could be explained by an increased amount of mineral nitrogen as a result of management practices (see 5.2). The amount of applied N-fertilizer that was converted into gaseous N (emission factor) was higher at the riparian sites than at well-drained sites, suggesting land-use change in riparian areas can have a more pronounced influence on N$_2$O production than it has at well-drained sites. Significant correlations between soil N$_2$O emissions and the soil characteristics were limited to negative ones with bulk density and clay content. Increased bulk density and clay content both lead to reduced soil gas diffusivity and

therewith increased anaerobic soil conditions, which in turn can lead to further reduction of N_2O to N_2. The resulted net decrease in produced N_2O can therefore explain these negative correlations. The increase in bulk density after the conversion from forest to plantation might have therefore prevented from even higher soil N_2O emissions.

Soil CH_4 fluxes did not significantly differ after the conversion from forest to plantations on the riparian areas. The riparian forest systems showed significantly higher annual soil moisture content, which stimulated CH_4 production, and resulted in the highest hourly soil CH_4 fluxes. The bulk density and clay content were significantly higher in the oil palm plantations than in the other land-use types, which led to anoxic field conditions and also resulted in high soil CH_4 production and therefore high hourly soil CH_4 fluxes. The rubber plantation systems, with intermediate WFSP and bulk density, showed the lowest hourly soil CH_4 fluxes. However, due to the strong effect of spatial variability within plots, rather than the effect of land-use conversion, annual soil CH_4 fluxes did not differ significantly between the three different land-use types. A negative correlation between soil CH_4 fluxes clay content was the only correlation found, and could be explained by increased anaerobic soil conditions and subsequent increased CH_4 production. The strong effect of the fluctuating soil moisture content in these landscape components probably overruled the effect of bulk density, soil total N or aluminium content on the soil CH_4 fluxes, known to be of influence on well-drained sites.

Soil CO_2 emissions did not change after forest conversion either. Even though SOC content decreased after the conversion to plantations, concentrations were still relatively high in these riparian land uses and therefore not limiting for soil respiration. The decrease in SOC might have therefore had a limited effect on the total soil CO_2 emissions in the plantations. Furthermore, also here, the effect of the strongly varying soil moisture content was likely the strongest controlling factor, as suggested by the strong quadratic relationships that were found between soil CO_2 emissions and soil moisture content in all three land uses. Significant correlations between soil CO_2 emissions and the soil characteristics were limited to a negative one with soil organic carbon (SOC) and a positive one with pH. The negative correlation with SOC was driven by the effect of micro-topography, as lower plot positions were characterized by higher SOC content and showed decreased, and thus the lowest, soil CO_2 emissions during inundation events. The positive correlation with pH was mainly driven by outlaying data points from the fertilized area of the oil palm plantations, which showed a combination of the highest pH due to frequent liming and the highest CO_2 emissions due to root respiration.

The strong correlations between the soil N_2O, CH_4 and CO_2 fluxes (hereafter summarized as GHG; Table 1) and the temporal variation in soil moisture content, as well as similarity between GHG flux patterns and soil moisture content, showed that soil moisture content was the most important controlling factor of almost all three measured GHG fluxes on all three land uses (except for the soil N_2O emissions in the oil palm plantations). The soil moisture content thereby potentially overruled GHG-controlling factors as a result of differences in soil characteristics after land-use conversion. In summary, the effect of land-use change on soil and stem GHG fluxes on riparian areas might have been limited because of the strong effect of temporal variation in soil moisture content on all three GHG fluxes.

5.7 Outlook

This study highlighted the fact that GHG flux estimates of tropical land-use systems on ecosystem-scale could be more accurate than they currently are. Significant underestimation in soil GHG fluxes that might result from the exclusion of GHG fluxes coming from minor landscape components like riparian areas, was most pronounced for soil CH_4 fluxes in the forest: calculations revealed that if 7 % of the tropical rainforest is located on riparian sites, the system can change from a net CH_4 sink into a net CH_4 source. This study is one of the first to address the importance of soil GHG fluxes from riparian areas in the tropics, which leaves most tropical ecosystems with riparian components currently unquantified, therewith revealing a major data gap. Quantification of soil GHG fluxes from the most common tropical land-use types (i.e. cash crop plantation systems such as coffee and cacao) located on riparian areas, can serve as an attempt to fill this gap and obtain this much-needed information for improved predictions in atmospheric GHG concentrations in the tropics. Year-long studies are known to cover temporal variation in soil GHG fluxes well, but our study also revealed that inter-annual variation in controlling factors, such as precipitation, can lead to significant differences in annual fluxes. Ideally, research on soil GHG fluxes should, therefore, cover multiple years to account for this variation. Furthermore, we found that stem GHG emissions contributed to up to 16 % of total (soil + stem) GHG fluxes in our land uses. Stems are thus important contributors to total GHG fluxes. As stem GHG contributions are currently largely unqualified in the majority of tropical ecosystems, additional research is urgently needed. Not only will this lead to better insights of total GHG fluxes from other tropical land-use types, but it might also help clarify underlying mechanisms and lead to better understanding of controlling factors, enabling us to make more accurate stem GHG flux calculations. Our study revealed that that the effect of land-use change on soil GHG emissions can be more

pronounced at riparian areas than it is at well-drained areas. For instance, there was a higher increase in soil N_2O emissions after conversion of forest to oil palm plantation on riparian areas than on well-drained areas. This shows that spatial variability should be considered while measuring the effect of land-use change. Furthermore, this shows that from an environmental point of view, it is recommended to carefully consider crop type and concurrent management practices while cultivating crops on riparian areas, as they can have a significant different environmental impact in terms of GHG emissions. As our study has shown the various spatial and temporal effects on GHG emissions, upscaling of these data to total GHG budgets from land-use systems or regions might provide valuable climatic data. Our study showed that riparian areas emit higher quantities of GHG, but the relative contribution of these increased emissions to the total emitted GHG budget remains unclear. For instance, establishing the total area of oil palm plantation located on riparian and well-drained area can help us to determine the total soil GHG flux contributions coming from both landscape components and find out their relative importance to the total soil GHG budget. More accurate knowledge on the total GHG flux budgets coming from these important land-use systems in the tropics would provide us a better understanding of the effects of land-use change on atmospheric conditions in this region.

References

Barba, J., Bradford, M. A., Brewer, P. E., Bruhn, D., Covey, K., Haren, J., … Vargas, R. (2019). Methane emissions from tree stems: a new frontier in the global carbon cycle. *New Phytologist*, *222*(1), 18–28. https://doi.org/10.1111/nph.15582

Basso, L. S., Gatti, L. V., Gloor, M., Miller, J. B., Domingues, L. G., Correia, C. S. C., & Borges, V. F. (2016). Seasonality and interannual variability of CH 4 fluxes from the eastern Amazon Basin inferred from atmospheric mole fraction profiles. *Journal of Geophysical Research: Atmospheres*, *121*(1), 168–184. https://doi.org/10.1002/2015JD023874

Davidson, E. A., Keller, M., Erickson, H. E., Verchot, L. V., & Veldkamp, E. (2000). Testing a Conceptual Model of Soil Emissions of Nitrous and Nitric Oxides. *BioScience*, *50*(8), 667. https://doi.org/10.1641/0006-3568(2000)050

Fiedler, S., & Sommer, M. (2000). Methane emissions, groundwater levels, and redox potentials of common wetland soils in a temperate-humid climate. *Global Biogeochemical Cycles*, *14*(4), 1081–1093.

Hashimoto, S., Morishita, T., Sakata, T., & Ishizuka, S. (2011). Increasing trends of soil greenhouse gas fluxes in Japanese forests from 1980 to 2009. *Scientific Reports*, *1*, 9–12. https://doi.org/10.1038/srep00116

Hassler, E., Corre, M. D., Tjoa, A., Damris, M., Utami, S. R., & Veldkamp, E. (2015). Soil fertility controls soil-atmosphere carbon dioxide and methane fluxes in a tropical

landscape converted from lowland forest to rubber and oil palm plantations. *Biogeosciences Discussions*, *12*(12), 9163–9207.

Hassler, E., Corre, M. D., Kurniawan, S., & Veldkamp, E. (2017). Soil nitrogen oxide fluxes from lowland forests converted to smallholder rubber and oil palm plantations in Sumatra, Indonesia. *Biogeosciences*, *14*(11), 2781–2798.

Herbst, M., Friborg, T., Schelde, K., Jensen, R., Ringgaard, R., Vasquez, V., … Soegaard, H. (2013). Climate and site management as driving factors for the atmospheric greenhouse gas exchange of a restored wetland. *Biogeosciences*, *10*(1), 39–52. https://doi.org/10.5194/bg-10-39-2013

Koehler, B., Corre, M. D., Steger, K., Well, R., Zehe, E., Sueta, J. P., & Veldkamp, E. (2012). An in-depth look into a tropical lowland forest soil: Nitrogen-addition effects on the contents of N2O, CO2 and CH4 and N2O isotopic signatures down to 2-m depth. *Biogeochemistry*, *111*(1–3), 695–713. https://doi.org/10.1007/s10533-012-9711-6

Matson, P. A., Vitousek, P. M., Livingston, G. P., & Swanberg, N. A. (1990). Sources of variation in nitrous oxide flux from Amazonian ecosystems. *Journal of Geophysical Research*, *95*(D10), 16789. https://doi.org/10.1029/JD095iD10p16789

Pangala, S. R., Enrich-Prast, A., Basso, L. S., Peixoto, R. B., Bastviken, D., Hornibrook, E. R. C., … Gauci, V. (2017). Large emissions from floodplain trees close the Amazon methane budget. *Nature*, *552*(7684), 230–234. https://doi.org/10.1038/nature24639

Pangala, S. R., Moore, S., Hornibrook, E. R. C., & Gauci, V. (2013). Trees are major conduits for methane egress from tropical forested wetlands. *New Phytologist*, *197*(2), 524–531.

Schlesinger, W. H., & Bernhardt, E. S. (2013). *Biogeochemistry: An Analysis of Global Change*. https://doi.org/10.1016/C2010-0-66291-2

Smith, L. K., Lewis, W. M., Chanton, J. P., Cronin, G., & Hamilton, S. K. (2000). Methane emissions from the Orinoco River floodplain, Venezuela. *Biogeochemistry*, *51*(2), 113–140. https://doi.org/10.1023/A:1006443429909

Sotta, E. D., Corre, M. D., & Veldkamp, E. (2008). Differing N status and N retention processes of soils under old-growth lowland forest in Eastern Amazonia, Caxiuanã, Brazil. *Soil Biology and Biochemistry*, *40*(3), 740–750. https://doi.org/10.1016/j.soilbio.2007.10.009

van Straaten, O., Veldkamp, E., & Corre, M. D. (2011). Simulated drought reduces soil CO 2 efflux and production in a tropical forest in Sulawesi, Indonesia. *Ecosphere*, *2*(10), art119. https://doi.org/10.1890/es11-00079.1

Veldkamp, E., Koehler, B., & Corre, M. D. (2013). Indications of nitrogen-limited methane uptake in tropical forest soils. *Biogeosciences*, *10*(8), 5367–5379. https://doi.org/10.5194/bg-10-5367-2013

Welch, B., Gauci, V., & Sayer, E. J. (2019). Tree stem bases are sources of CH4 and N2O in a tropical forest on upland soil during the dry to wet season transition. *Global Change Biology*, *25*(1), 361–372. https://doi.org/10.1111/gcb.14498

Wen, Y., Corre, M. D., Rachow, C., Chen, L., & Veldkamp, E. (2017). Nitrous oxide emissions from stems of alder, beech and spruce in a temperate forest. *Plant and Soil*, *420*(1–2), 423–434. https://doi.org/10.1007/s11104-017-3416-5

Yip, D. Z., Veach, A. M., Yang, Z. K., Cregger, M. A., & Schadt, C. W. (2018). Methanogenic Archaea dominate mature heartwood habitats of Eastern Cottonwood (Populus deltoides). *New Phytologist*. https://doi.org/10.1111/nph.15346

Acknowledgements

First of all I'd like to thank my supervisors Prof. Dr. Edzo Veldkamp and Dr. Marife Corre for their support during my PhD. Not only did they help me to significantly improve my scientific writing and speaking, also did they teach me valuable life lessons.

I'd like to thank the DFG, who financed my PhD through the 'CRC-990' framework and therewith made this PhD possible in the first place.

Very special thanks go to Greta Formaglio, who was not only a very pleasant colleague, but also turned out to be an amazing friend. I really am not sure I would have managed it to this point without your help. Thank you!

It goes without saying that I very much appreciated the great help of my motived, always-laughing and strong assistants Nando, Somad, Madan and Happy. I don't know how I could have ever collected almost 15.000 greenhouse gas samples without your help!

Furthermore I'd like to thank my fellow (post-) doctoral researchers Marcus, Oliver, Rhodine, Leonie, Evelyn, Amanda, Raphael, Yuan, Jie, Guantao, Guadong, Dan and Xenia for their valuable feedbacks and help – special thanks go off course to my buddy Najeeb!

Also, I'd like to thank Dr. Barbara Wick, Yvonne Hein and Prof. Dr. Stefan Scheu for their reliable project management, as well as their personal involvement in completing my PhD.

I much appreciated the laboratory and technical assistance provided by Martina, Kerstin and Dirk, and I'd like to thank Andrea in particular, as her help reached far beyond the lab!

Another 'thank you' goes to Isabelle, Clara, Kyra, Pierre-Andre, Johannes, Florian, Rico, Joyson, Jenny, Fenna, Daniel, Nadjia, Dirk, Miriam, Kathrin, Britta, Nina, Valyntina, Anton, Alena, Katja, Fabian, Carina, Rahmi and all my other colleagues who made my time in Jambi unforgettable.

Also, I'd kindly like to thank Ibu Aiyen, Mega, Rizky, Yuking and Ozy for their great assistance in Jambi.

Last, but not least, I'd like to thank my sister Michelle, my brother Niels, and my parents, for the uncountable Skype calls, their multiple visits to both Jambi and Göttingen, and for their unlimited amount of support, especially in the times I didn't believe I'd be able to finish this PhD.

DECLARATION OF ORIGINALITY AND CERTIFICATE OF AUTHORSHIP

I, Josephus Adrianus Koks, hereby declare that I am the sole author of this dissertation entitled "Tropical forest conversion to rubber and oil palm plantations: landscape-scale and inter-annual variability of soil greenhouse gas (GHG) fluxes and the contribution of tree-stem emissions to the soil GHG budget in Jambi province, Sumatra, Indonesia", and that all references and data sources have been appropriately acknowledged. I furthermore declare that this work has not been submitted elsewhere in any form as part of another dissertation procedure. I certify that the manuscripts presented in chapters 2, 3 and 4 have been written by me as first author.

Göttingen, September 2019   _____

                                                    (Josephus Adrianus Koks)